FIRST EDITION

Intraoral Welding of Titanium Implants

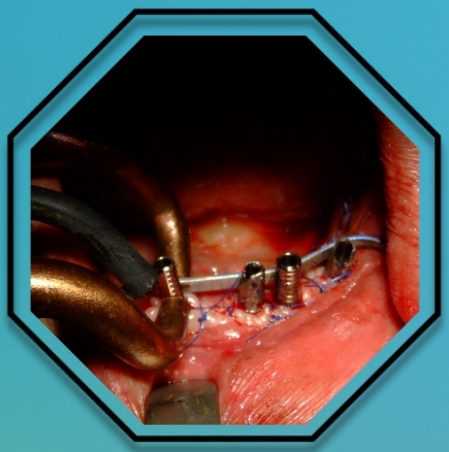

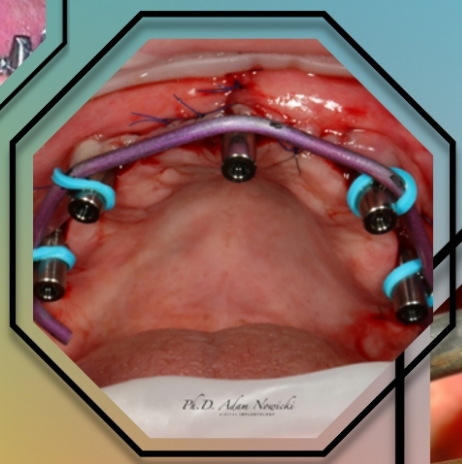

Grigore Lăzărescu
Marco Bellina
Adam Aleksander Nowicki
Elizabet-Zahra Sareh
Gabriel Kevorkian

Grigore Lăzărescu

Marco Bellina **Adam Aleksander Nowicki**
Elizabet-Zahra Sareh **Gabriel Kevorkian**

SUDURA INTRAORALĂ A IMPLANTURILOR DIN TITAN

Intraoral Welding *of* Titanium Implants

ISBN: 978-973-0-42335-8

București

2025

INTRAORAL WELDING OF TITANIUM IMPLANTS

Grigore Lăzărescu, MD, DDS, PhD
Graduate of Carol Davila University of Medicine and Pharmacy, Bucharest – Faculty of Dentistry
Major in Prosthodontics and Implantology
Associated Professor, University of Medicine and Pharmacy of Craiova – Faculty of Dentistry
Former Lecturer, Carol Davila University of Medicine and Pharmacy, Bucharest – Faculty of Dentistry
Private Practice – Bucharest, Romania

Marco Bellina, MD, DDS
Graduate of Alma Mater Studiorum – University of Bologna
Major in Prosthodontics and Implantology
Private Practice – Milan, Italy

Adam Aleksander Nowicki, MD, DDS, PhD
Graduate of Pomorska Akademia Medyczna, Szczecin
Major in Restorative Dentistry, Microsurgery and Occlusion
Clinical Implantologist – Szczecin, Poland

Elizabet-Zahra Sareh, MD, BEng
Graduate of Carol Davila University of Medicine and Pharmacy, Bucharest – Faculty of Dentistry
Graduate of University POLITEHNICA of Bucharest – Faculty of Electronics, Telecommunications and Information Technology
University of Agronomic Sciences and Veterinary Medicine of Bucharest – Faculty of Biology
Analyst Programmer – Carol Davila University of Medicine and Pharmacy, Bucharest

Gabriel Kevorkian, Dipl. Eng.
Graduate of University POLITEHNICA of Bucharest – Faculty of Physics
Engineering Lead – Systems Integration
Major in Biomedical Technology
† Deceased

INTRAORAL WELDING OF TITANIUM IMPLANTS ISBN: 978-973-0-42335-8

Copyright © 2025.

All rights reserved. No part of this publication may be reproduced or transmitted in any form or by any means, electronic or mechanical, including photocopying, recording, or any information storage and retrieval system, without permission in writing from the authors.

Notices

Clinical knowledge and protocols in implant dentistry are constantly evolving. As research deepens and experience accumulates, clinical practices and technical approaches may require adaptation and refinement.

Readers are encouraged to apply the information presented in this book with professional judgment and critical thinking. The described techniques—particularly those involving intraoral welding, immediate loading, and monobloc or needle implants—must be interpreted and adapted according to the clinical context, the available equipment, and the specific needs of each patient.

While this book illustrates procedures, materials, and strategies used successfully by the authors and contributors, it remains the responsibility of each practitioner to verify indications, follow safety protocols, and act in accordance with current clinical standards and manufacturer guidelines.

To the fullest extent permitted by law, the authors, contributors, and technical editors of this work assume no liability for injury or damages resulting from the use or misuse of the techniques, instruments, or clinical decisions described herein.

This book is not a substitute for hands-on clinical training, continuing education, or sound medical judgment. It is an invitation to explore, to question, and to evolve, always with respect for biology, biomechanics, and the patient in front of you.

Lead Author & Scientific Reviewer
Dr. Grigore Lăzărescu, *MD, DDS, PhD*
Co-authors
Dr. Marco Bellina, MD, DDS
Dr. Adam Aleksander Nowicki, *MD, DDS, PhD*
Photography & Clinical Documentation
Dr. Grigore Lăzărescu, *MD, DDS, PhD*
Dr. Marco Bellina, *MD, DDS*
Dr. Adam Aleksander Nowicki, *MD, DDS, PhD*
Technical Editor & Scientific Proofreader
Gabriel Kevorkian, *Dipl. Eng.*
Dr. Elizabet-Zahra Sareh, *DDS, BEng*
Narrative Development & Medical Technical Editing
Design, Layout & Multimedia Integration
Dr. Elizabet-Zahra Sareh, *DDS, BEng*

If you would like to share your feedback, clinical experience, or simply reach out, feel free to contact us at: grigore.lazarescu@thedentist.ro
We welcome your thoughts!

Printed in Romania, Bucharest

Index

1 A Friendly Welcome 11

1.1 Tribute to The Italian School 13

1.2 An Invitation to Read 19

1.3 Uncovering the Mysteries of Bone 21

2 Titanium in Dentistry 27

2.1 The Chemical Element 27

2.2 Characteristics 32

2.3 Compounds 36

2.4 Diffusion 38

2.5 Historical Background 39

2.6 Production and Fabrication 44

2.7 Applications 47

2.8 Safety Cautions 55

3 The Joule Effect and Methods for its Mitigation 57

3.1 Electrical Power in Metallic Conductors 57

3.2 Ohm's Law 61

3.3 The Electric Energy and Power 67

4 Welding, Splinting, Syncrystallization 81

4.1 Considerations Regarding Welding 81

4.2 Fundamental Notions 101

4.3 Intraoral Electrowelding 109

5 Devices and Materials 121

5.1 Introduction 121

5.2 General Characteristics 122

5.3 Functioning Principle 126

5.4 The Macroscopic Test 130

6 Indications and Clinical Cases 137

6.1 The Solo Implant 138

6.2 Multiple Implants in Short Edentulous Spans 140

6.3 Multiple Implants in Long Edentulous Spans 148

6.4 Monoblock Implants with Ball Attachments for Retention of Removable Prosthetics 155

6.5 Special Interventions 157

7 The Operating Technique 161

7.1. Preparing the Surfaces 161

7.2. Choosing the Type of Connector 162

7.3 Preparation and Calibration of the Welding Apparatus 165

7.4 Position and Direction of the Titanium Bars 166

8 Going Digital – Predictability at Its Finest ***by Dr. Adam Aleksander Nowicki*** **.. 171**

8.1 Case 1 171

8.2 Case 2 174

8.3 Case 3 178

9 Retro-Innovation and Clinical Elegance: Functional Rehabilitation with Intraoral Welding and Needle Implants ***by Dr. Marco Bellina and Dr. Grigore Lăzărescu*** **..... 183**

9.1 Clinical Cases by Dr. Marco Bellina 183

9.2 Clinical Cases by Dr. Grigore Lăzărescu 214

About The Authors 223

Bibliography 227

Acknowledgements

The illustrations used in this book were previously featured in the 2011 edition and provided courtesy of, and with agreement from, Implamed SRL, AthenaDent SRL, Implafavourite, Dr. Lorenzo Noveri, Dr. Silvano Tramonte, or sourced from personal casuistic. Further on, for this English edition, we have added additional cases and invited colleagues, to share their clinical results e.g. Dr. Marco Bellina and Dr. Adam Aleksander Nowicki.

The pre-operative preparation, as well as the provisional and final prosthetic restorations for most of my cases, were performed by DT. Răzvan Dumitrescu-Bucharest.

1 A Friendly Welcome

I began a long time ago in Dr. Noveri's office, learning about new and spectacular techniques used in „in-office implantology". After reaching a certain experience in personal practice, I took the challenge to write about it, to present the parallel universe of the implantation techniques. The reading will be more instructive for the colleagues working on a daily basis with cases that don't fit in the protocol rules, that have to resolve technical, medical and economical problems. I have considered a very important fact: that there are clinically reported cases of over 30 years – in the case of the intraoral welding – and of over 50 years in the case of the monocorp Ti2 implants. Those at the beginning of their journey in complex oral rehabilitation will find in this paper a bit more than the exactness of some technical information, namely, a clinically tested alternative and scientifically documented.

It will be, I think, a significant gain the fact that this way we will come closer to what a doctor needs to be, namely a permanent researcher, always dissatisfied with what he knows, always keen to learn.

I wish I could write more about the notable results obtained by the Romanian school, as it has proved through its representants a distinguished innovative capacity and clinical outcomes comparable to those of ones we can find today in international literature.

Unfortunately, there are only few references of whom I recall with respect: Valerian Popescu, Mihail Sturdza, Cicerone Mihail, Herman N., Pambuccian Gr., Dan Vasiliu, Burlibaşa C., Paul Orleanu, Ene L., Mărginean O., Heinrich Benedict and S. Sandhaus and many others I haven't had the chance to read about yet. A history of the Romanian creativity is useful and expected, especially when you find out that in 1951, Valerian Popescu was already practicing and then communicated in 1956 the subperiosteal implants technique, long before the titanium and Brånemark protocols era.

The first part of the work is a direct introduction into the physical basis of this application to understand <<*how*>> and <<*why*>> happens in the intraoral welding. I didn't talk about the necessity of the implant solidarization, because, on one hand, is a vast subject that deserves a separate approach when we talk about immediate loading and conducted osteo-integration, and on the other hand, it is treated at length in most of the specialty works, even though they seldom or more likely never refer to the intraoral welding.

I hope that after reading this book, you will want to find out more about the special techniques and you will have another solution in your therapeutical arsenal.

Grigore Lăzărescu

MD, DDS, PhD

1.1 Tribute to the Italian School

The Italian School has played an essential role in shaping the course of implantology. Among its contributors stand Dr. Pier Luigi Mondani and his son, Pier Maria Mondani, whose pioneering work in intraoral electric welding has left a lasting mark on the evolution of dental surgical techniques.

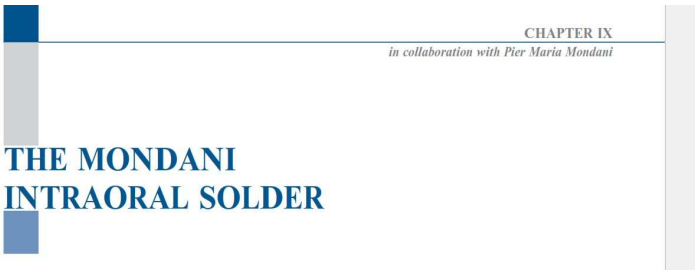

Figure 1.1.1 Title page of Chapter IX – "The Mondani Intraoral Solder", co-authored with Pier Maria Mondani, outlining the clinical protocol and impact of intraoral electric welding.

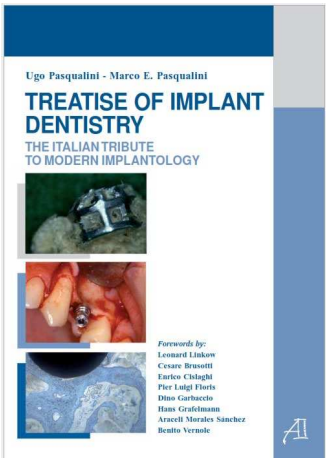

Figure 1.1.2 Cover of the book Treatise of Implant Dentistry: The Italian Tribute to Modern Implantology by Ugo Pasqualini and Marco E. Pasqualini, highlighting clinical imagery and international contributions in the field of implantology.

Dr. Pier Luigi Mondani was among the first to introduce the concept of **intraoral electric welding** – a technique that allowed for the stabilization of titanium frameworks directly within the oral cavity. His clinical and theoretical contributions, later expanded in collaboration with his son, Dr. Pier Maria Mondani, played a pivotal role in the

development of **syncrystallization** protocols, which facilitated immediate and precise prosthetic fixation.

Their publications, including *La saldatrice elettrica intraorale* and *Sincristallizzazione a flusso diretto*, provide a comprehensive overview of both the principles and practical applications of their method. These documents – many of which are still referenced today – highlight the clinical reliability and biomechanical stability made possible by intraoral welding.

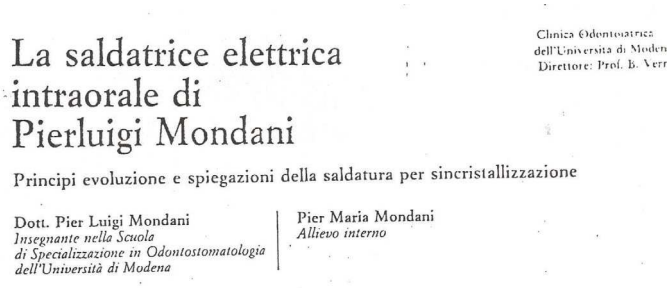

La saldatrice elettrica intraorale di Pierluigi Mondani

Clinica Odontoiatrica dell'Università di Modena
Direttore: Prof. B. Verr

Principi evoluzione e spiegazioni della saldatura per sincristallizzazione

Dott. Pier Luigi Mondani
Insegnante nella Scuola di Specializzazione in Odontostomatologia dell'Università di Modena

Pier Maria Mondani
Allievo interno

Figure 1.1.3 Title page of „La saldatrice elettrica intraorale di Pier Luigi Mondani", co-authored with Pier Maria Mondani. The document presents the principles and clinical explanations of intraoral electric welding and syncrystallization.

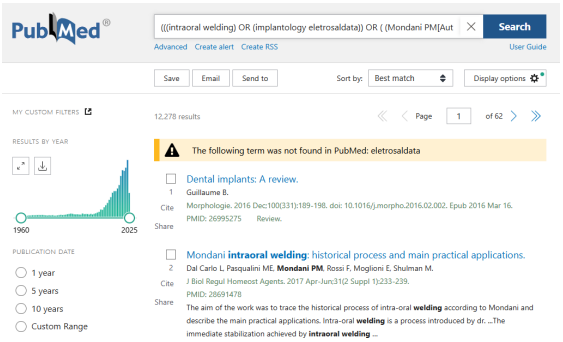
PubMed
(((intraoral welding) OR (implantology eletrosaldata)) OR ((Mondani PM[Aut
Search
Advanced
Create alert
Create RSS
User Guide
Save
Email
Send to
Sort by: Best match
Display options
MY CUSTOM FILTERS
12,278 results
Page 1 of 62
RESULTS BY YEAR
1960
2025
The following term was not found in PubMed: eletrosaldata
Dental implants: A review.
Guillaume B.
Morphologie. 2016 Dec;100(331):189-198. doi: 10.1016/j.morpho.2016.02.002. Epub 2016 Mar 16.
PMID: 26995275 Review.
Cite
Share
PUBLICATION DATE
1 year
5 years
10 years
Custom Range
Mondani intraoral welding: historical process and main practical applications.
Dal Carlo L, Pasqualini ME, Mondani PM, Rossi F, Moglioni E, Shulman M.
J Biol Regul Homeost Agents. 2017 Apr-Jun;31(2 Suppl 1):233-239.
PMID: 28691478
The aim of the work was to trace the historical process of intra-oral welding according to Mondani and describe the main practical applications. Intra-oral welding is a process introduced by dr. ...The immediate stabilization achieved by intraoral welding ...

Figure 1.1.4 Archival digital documents related to the work of Pier Luigi and Pier Maria Mondani, including publications on intraoral welding and syncrystallization protocols.

The influence of the Mondani approach extended beyond Italy. Their technique became a benchmark for what is now referred to as *immediate loading* in modern implantology – a concept widely adopted in contemporary dental practices. The devices developed under their guidance were not only innovative at the time but served as prototypes

for the intraoral soldering units currently used in advanced prosthodontics and maxillofacial surgery.

1800 e prima metà 1900	pag. 77
Maggiolo	pag. 79
Grienfield	pag 80
Adams	pag. 81
Fratelli Strock	pag 81
Dal 1950 agli anni '80	pag. 83
Formiggini M.S.	pag. 85
Pasqualini U.	pag. 87
Zepponi.	pag. 96
Tramonte St.	pag. 97
Storia del *Carico Immediato*	pag. 107
Perron A.	pag. 109
Cherceve R.	pag. 110
Muratori G.	pag. 116
Scialom J.	pag. 117
Linkow L.	pag. 118
Marini N.	pag. 119
Pierazzini A.	pag. 120
Mondani P. L.	pag 121
Garbaccio D.	pag. 127
Lobello S.	pag. 139
Zaninari A.	pag. 143

Figure 1.1.5 Excerpt from a historical index of implantology pioneers, listing Dr. Pier Luigi Mondani (pag. 121) among key figures of the 1950s-1980s.

Their contribution is acknowledged in various international works, including recent historical reviews of implantology pioneers, such as the one featured in *Stomatologia şi Chirurgia Maxilo-Facială în România (1935-1985)*, where Dr. Mondani is referenced alongside other figures who shaped the 20th-century evolution of the field.

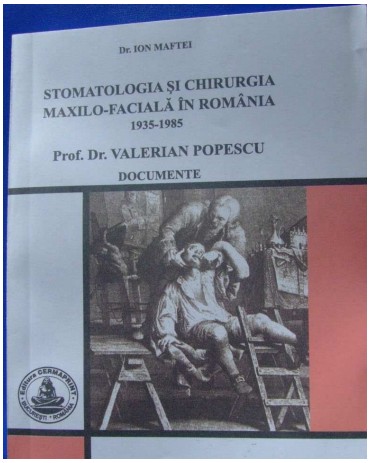

Figure 1.1.6 Cover of „Stomatologia şi Chirurgia Maxilo-Facială în România (1935-1985)" by Dr. Ion Maftei and Prof. Dr. Valerian Popescu, a historical documentary work referencing international figures such as Dr. Pier Luigi Mondani.

Italian School of implantology continues to thrive through the visionary work of contemporary experts such as **Professor Stefano Fanali**, whose advancements in *Corso di aggiornamento teoretico pratico in IMPLANTOLOGIA ELETTROSALDATA* have refined clinical precision and expanded the scope of immediate loading protocols. His work, as presented in dedicated training programs and academic materials, upholds the spirit of innovation rooted in Mondani's legacy, while addressing the demands of modern clinical practice.

Figure 1.1.7 Cover of the official course in „Implantologia Elettrosaldata" directed by Prof. Stefano Fanali. A milestone in continuing education on electrowelded implant protocols in Italy.

Figure 1.1.8 The cover of Trattato di Implantologia Integrale Elettrosaldata, a comprehensive work by Stefano Fanali (published at Youcanprint, 2014).

Furthermore, the interdisciplinary bridge between engineering and dentistry has been eloquently explored by **Professor Arturo N. Natali** in his work *Dental Biomechanics*. His integration of mechanical modeling, material science, and biological function has provided clinicians and researchers with a deeper understanding of how prosthetic structures interact with the surrounding oral environment. Natali's contributions remain essential for those seeking to design restorations and implants that are not only functional, but biomechanically harmonious and long-lasting.

Figure 1.1.9 Cover of „Dental Biomechanics", edited by Arturo N. Natali – a fundamental interdisciplinary reference bridging dentistry and mechanical engineering.

Through a blend of technical ingenuity, academic rigor and clinical foresight, the Italian School – is bridging theory and practice in ways that continue to resonate in modern dental education and surgery.

Other publications mark the principles of Italian school of Implantology and especially the advantages of Intra Oral Welding (IOW), like Dr. Giorgio Lorenzon's *Implantologia Funzionale dalla Osteointegrazione alla Fisiointegrazione*.

Figure 1.1.10 The cover of Implantologia Funzionale: dalla Osteointegrazione alla Fisiointegrazione, authored by Giorgio Lorenzon and published by Edizioni Martina in 2010.

The number of contributors to the values of Italian school is far bigger and should be honored as such, as Dr. Massimo Corradini did in his. In *Storia dell'Implantologia* (RC Libri, 2009), co-authored with Diana Naiche and Andrea Rossi, Dr. Corradini offers not only a historical account but also a tribute to the many professionals whose innovations and dedication have defined and enriched Italian dental implantology.

Figure 1.1.11 The cover of Storia dell'Implantologia, authored by Massimo Corradini, Diana Naiche, and Andrea Rossi, published by RC Libri in 2009.

1.2 An Invitation to Read

This is not a book about showing off. It's not about brands, trends, or shiny digital books. It's about hands that think and minds that respect biology. About clinical elegance, not decorative, but deeply functional.

What you will find in these pages is not perfection. It's clarity. It's biomechanics applied with common sense, adapted to the patient in front of you, not to a protocol on paper. You will see cases solved under pressure, with limited time, limited resources, and sometimes limited options, but never with limited responsibility.

Intraoral welding is not new. Neither are Tramonte or Garbaccio implants. Yet what's old is not obsolete, it's simply waiting to be rediscovered with a better understanding, with curiosity, with humility. And with the quiet confidence of someone who knows that, sometimes, the future doesn't mean reinventing everything, but doing what already works better.

We wrote this for the ones who believe that innovation is not always digital. That science can be simple. That elegance in dentistry can mean stabilizing a full arch in one session, not one year. This is for clinicians who still believe that medicine is an act of intelligence, not only a sequence of clicks.

This isn't a closed chapter. It's an open door. It's a step into a parallel clinical world that has been here all along – quiet, efficient, and powerful.

This is just the beginning. If these pages sparked your curiosity, imagine what you'll discover in dialogue with others walking the same path. Join our community of clinicians who believe in simplicity backed by science, and in techniques that stand the test of time. Share your cases. Ask questions. Learn from real experiences.

Facebook Group: Welding Implants – Immediate Loading

The next edition is already in the making, featuring even more clinical cases, new voices, and refined techniques.

We're building it together, and your contribution might just shape the next chapter.

We invite you to explore it.

The Authors

For any further references and contact, please reach us at:

grigore.lazarescu@thedentist.ro

1.3 Uncovering the Mysteries of Bone

1.3.1 Introduction

No further explanation of various dental implant techniques could be proposed without first establishing a common understanding and acceptance of basic knowledge. Among the characters, the primary one involved is the bone, the recipient and support of our implants, a character that impresses us through its absence, form or unexpected reactions during function.

While studying the literature, a medically trained researcher will naturally be inclined to focus on medical papers conducted by, supervised by, or inspired by challenges within the medical field.

It is also common for medically educated specialists to employ particular tools and methods of research, which are often biased, influenced, oriented or constrained by their educational background.

A true gem of medical and scientific research is the book authored by Prof. Arturo N. Natali and his colleagues at the Center for Mechanics of Biological Materials at the University of Padua, Italy.

On behalf of our profession, I would like to express my gratitude for this book, simply titled *Dental Biomechanics*, published in 2003.

The work of Prof Arturo N. Natali provides a comprehensive mechanical analysis of dental problems related to implant procedures, dental materials, titanium cast devices, and implant surface treatments. It also covers mechanical testing procedures for evaluating the reliability of dental devices, addresses relevant aspects of clinical practice concerning biomechanical issues, and explores numerical modeling in dental biomechanics, highlighting the importance of this approach in investigating dental problems. Overall, it presents a multidisciplinary perspective on dental

biomechanics, integrating mechanical, clinical, and chemical-physical knowledge.

As a practitioner, I am confident you will find great value in this reading experience. I will highlight here some of the most interesting factors described and studied in the book, but I encourage you to take the time and explore the rest of it yourself, believe me, it truly is a treasure.

1. **Mechanical Responses of Bone Tissue**

The properties of bone are highly dependent on the surrounding conditions, including:

- hydration levels,
- patient's age,
- type of mechanical stress, such as velocity and the duration of the applied load,
- environmental factors like temperature and humidity during the attempts.

2. **Numerical Methods of Data Analysis**

Numerical methods, particularly the finite element method, provide powerful tools for simulating and predicting the mechanical behavior of biological tissues. An interesting debate arises here due to the anisotropic characteristics of bone tissue and the clear advantages of using finite element analysis in research applications.

3. **Bone Maintenance Mechanism**

Bone is classified as a hard tissue; however, its macroscopic behavior reflects the complexity of its microstructure, which is intricately connected to the functional demands that drive bone evolution throughout life.

Bone can be described as the result of the activities of three principal types of cells: osteoblasts, osteoclasts, and osteocytes. Osteoblasts are the cells responsible for the production of new tissue. Osteoclasts are involved in bone resorption. Osteocytes are the cells embedded within fully formed, mature bone.

The local resorption of bone, followed by new bone formation during the remodeling process, is not yet fully understood.

Bone can be stimulated to change its form and dimensions through a process known as modeling or remodeling of the bone network. Most modeling occurs during growth, involving modifications of bone shape and size. However, even after reaching maturity, bone can still be stimulated to adapt by altering mechanical stress or through various agents that influence its form and/or its properties modification.

4. Anisotropy: The Biological Researcher's Nightmare

The anisotropic properties of cortical bone are discussed by Prof. Natali through the measurement of various physical characteristics of bone samples.

In the case of human bone, we may dare to propose two main types of anisotropic classification, those being:

- having different physical properties in different directions and,
- having different physical properties along a certain axis and direction, as the structure of the bone differs along.

Of course, this second approach is very much related to the very focused universe of our profession. It is a well-known fact that even creating a neo-alveolus for an implant often requires different types of drills, according to the varying qualities of the bone at different depths and widths.

1.3.2 Time-Dependent Response

Bone exhibits time-dependent behavior, being described as a viscoelastic material in certain conditions. The viscoelastic typical behavior, where deformation continues to increase over time in response to a constantly applied load, is known as creep. This phenomenon is relevant when discussing bone

compression, orthodontics, clenching, bruxism, and similar conditions.

1.3.3 Bone Hydration

The mechanical response of bone depends on its liquid content. Naturally, arguments for this specific aspect are mainly derived from in vitro studies. However, in our daily practice, we can recognize a well-hydrated bone (with abundant vascular supply), which reacts more resiliently to applied stress, and a less hydrated bone, with a more mineralized structure, that responds in a more brittle manner.

Another way to approach bone hydration is through the methods used to collect and examine bone samples. Although various precautions are taken to prevent bacterial or chemical contamination, the process itself can interfere with the water content of the sample, thus altering its physical characteristics.

The authors' work continues with important concepts in scientific research, such as constituent bone models, structural properties, the limit state of bone, phenomenological models, and others.

One important note (and last) is that reading this book today feels like time traveling, because you will have the objective arguments – ideas, concepts, and facts presented in the book – and you can observe their materialization and development over time up to the present day. These foundations enabled numerous researchers to further develop our scientific approach.

In our field, simple examples include the concept of implant cleanliness, which became a crucial milestone to monitor; the evolving definition of intraoperative implant stability; and shift in focus from achieving high tension stress at the bone-implant interface to ensuring immobility. In my opinion, one of the most direct

consequences of this foundational work is the article (and concept) by S. Raghavendra, M. C. Wood, T. D. Taylor, titled *Early Wound Healing Adjacent to Endosseous Dental Implants: A Review of the Literature*, published in the *International Journal of Oral Maxillofacial Implants* (2005, May-June; 20(3):425-31), which actually set the rules for timing in implant dentistry.

And the list of examples continues.

In addition to the pioneering work of Prof. Arturo Natali, modern implant biomechanics has been further explored in several recent contributions. Notably, the works of Ishak and Abdul Kadir (Figure 1.3.3.12), as well as the research compiled by Çehreli (Figure 1.3.3.13), offer a deeper understanding of the mechanical response of bone and implant interfaces, especially in complex clinical cases such as atrophic maxilla.

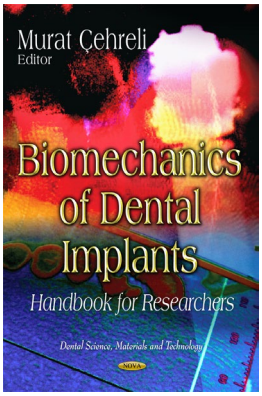

Figure 1.3.3.14 Cover of the book Biomechanics of Dental Implants: Handbook for Researchers, edited by Murat Çehreli, published by Nova Science Publishers, part of the "Dental Science, Materials and Technology" collection.

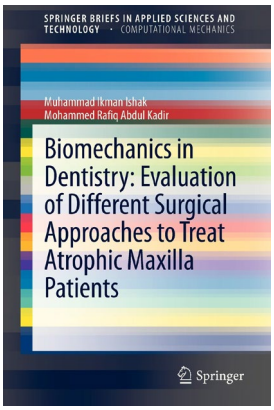
SPRINGER BRIEFS IN APPLIED SCIENCES AND TECHNOLOGY · COMPUTATIONAL MECHANICS
Muhammad Ikman Ishak
Mohammed Rafiq Abdul Kadir
Biomechanics in Dentistry: Evaluation of Different Surgical Approaches to Treat Atrophic Maxilla Patients
Springer

Figure 1.3.3.15 Cover of the book Biomechanics in Dentistry: Evaluation of Different Surgical Approaches to Treat Atrophic Maxilla Patients, by Muhammad Ikman Ishak and Mohammed Rafiq Abdul Kadir, published by Springer in the Computational Mechanics series in 2013.

2 Titanium in Dentistry

2.1 Introduction

Imagine this: a metal so light it floats in engineering dreams, so strong it withstands the crushing pressures of the ocean floor, so stable it resists corrosion from seawater, acid, and even chlorine, and yet, so biologically friendly that your body accepts it as one of its own.

That metal… is titanium.

You may know it from aerospace or military technology, or maybe from luxury watches, racing bikes, or surgical implants, but here's the twist: some of its most life-changing applications happen at the micrometric level, within the confined, complex space of the human mouth.

This chapter isn't just about titanium, it's about the silent revolution behind your smile.

Titanium is no ordinary metal. Born from cosmic processes, first identified in 1791 by a British pastor who stumbled upon a strange black sand in Cornwall, and named after the mighty Titans of Greek mythology, it has always been destined for greatness. But its real journey didn't begin until centuries later, when technology finally caught up with its promise.

As you'll soon learn, titanium exists in two allotropic forms, boasts five naturally occurring isotopes, and has a Young's modulus that's surprisingly close to that of bone, making it uniquely suited for load-bearing implants. Its passive oxide layer acts like a self-healing armor, allowing it to resist corrosion and integrate into living tissue with elegance and efficiency.

This chapter isn't just about the science, it's about the story.

We'll trace titanium's rise from a lab curiosity to a strategic military asset, from Soviet submarines to high-performance jets, and finally… to dental clinics across the world. We'll explore the chemistry, the crystallography, the fabrication

methods, from the intricate Kroll process to cutting-edge innovations like FFC Cambridge and we'll show you why titanium is still, after decades, the undisputed king of dental biomaterials.

You'll see how titanium alloys are tailored for very specific functions. Why pure grades are selected for ductility, and why certain alloys, like Ti-6Al-4V, are chosen for their tensile strength. You'll understand how microscopic surface topography influences osseointegration. How crystal structure, elasticity, and corrosion resistance dictate the long-term success of an implant.

And then… we'll zoom out, because titanium isn't just used for implants. It's used for endodontic files, orthodontic wires, prosthetic frameworks, surgical instruments, and even the invisible coatings that make tools last longer and perform better. It has infiltrated every corner of modern dentistry, and yet, it's still evolving. Lighter, stronger, more biocompatible versions are being researched as we speak.

In many ways, titanium has become the skeleton of our second skeleton, the artificial structures we rely on when nature fails us. It stands at the intersection of biology and engineering, where atoms and empathy meet. It's the reason a grandmother can chew again, a teenager can smile without fear, a surgeon can place a full-arch restoration with confidence.

So whether you're here for the material science, the medical breakthroughs, or the sheer elegance of a metal that bridges the gap between machine and man, welcome to Chapter 2.

2.2 The Chemical Element

Titanium is a chemical element with the symbol Ti and the atomic number 22, often referred to as „the metal of the space age". It is a low-density transition metal with a silver color, lustrous appearance. It exhibits high resistance to mechanical stress and chemical corrosion (including the one exerted by seawater, aqua regia and chlorine).

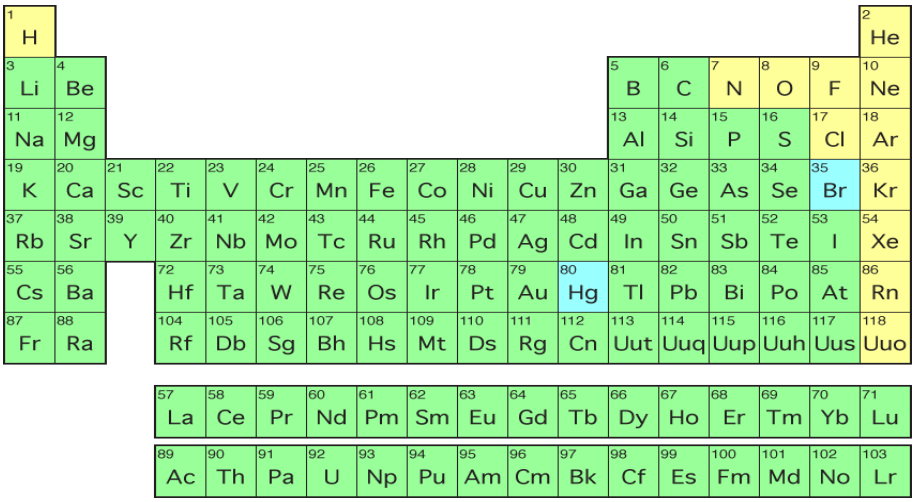

Figure 2.2.1 The periodic table of elements: Titanium's position (transition metal) in the periodic table of elements (Mendeleev) – group 4, period 4, d-block, atomic number 22.

Grupa	**3**	**4**	**5**	**6**	**7**	**8**	**9**	**10**	**11**	**12**
Perioada 4	Sc 21	Ti 22	V 23	Cr 24	Mn 25	Fe 26	Co 27	Ni 28	Cu 29	Zn 30
Perioada 5	Y 39	Zr 40	Nb 41	Mo 42	Tc 43	Ru 44	Rh 45	Pd 46	Ag 47	Cd 48
Perioada 6	La 57	Hf 72	Ta 73	W 74	Re 75	Os 76	Ir 77	Pt 78	Au 79	Hg 80
Perioada 7	Ac 89	Rf 104	Db 105	Sg 106	Bh 107	Hs 108	Mt 109	Ds 110	Rg 111	Cn 112

Figure 2.2.2 The d-block of the periodic table of elements.

The term „transition metal" (sometimes named also transition element) has two possible meanings:

1) It refers to any element from the d-block of the periodic table, which includes groups from 3 to 12 from the table. All the elements from the d-block are metals. (In reality, the f-

block is sometimes also considered, comprising the lanthanide and actinide series).

2) According to the IUPAC definition, a 'transition element' is „an element whose atom has an incomplete d sub-shell, or which can give rise to cations with an incomplete d sub-shell". In terms of this definition, the 12th group elements are not transition metals.

Figure 2.2.3 As can be noted, the bar with titanium crystals, obtained through the van Arkel-de Boer process, has a silver-gray aspect of a metallic white.

In 1791, pastor William Gregor, an amateur geologist, discovered titanium in Cornwall (United Kingdom) and in 1795 the German chemist Martin Heinrich Klaproth named the element „titanium" after the titans from Greek mythology.

The element can be found in certain mineral deposits, particularly in rutile and ilmenite, which are widely distributed inside the crust and lithosphere, but it can also be found in almost any living being, rocks, in the subterranean natural aquifer layers and in the soil. The metal was initially extracted from its principal metallic ore using the Hunter process and is now commonly produced through the Kroll process. The most widespread compound of titanium, the titanium dioxide (TiO_2), is a well-known photocatalyst and is widely used in the production of white pigments.

Figure 2.2.4 Titanium dioxide (TiO_2) powder on a glass petri dish.

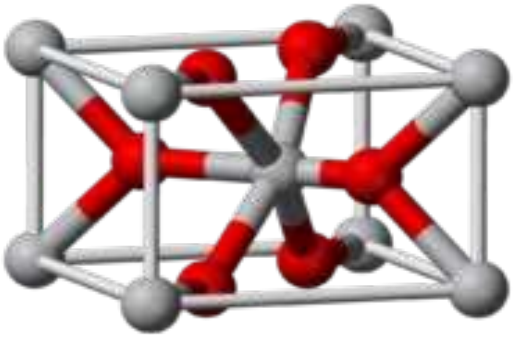

Figure 2.2.5 Crystal structure of titanium dioxide (TiO_2).

Other compounds include the titanium tetrachloride ($TiCl_4$), in the production of smoke screens and catalysts and the titanium trichloride ($TiCl_3$), which serves as a catalyst in the manufacturing of polypropylene.

Titanium can be alloyed with iron, aluminum, vanadium, molybdenum, among other elements to produce strong and lightweight alloys used in the aerospace industry (the jet aircraft engines, missiles and spacecrafts), military applications, industrial processes (including chemical and petrochemical production, seawater desalination, plants, paper and cellulose), as well as in the automobile and agri-food sectors. Titanium alloys are also widely used to manufacture medical prosthetics, orthopedic implants, dental and endodontic instruments and files, dental implants, sports equipment, jewels, mobile phones and various consumer products.

Figure 2.2.6 Common applications of titanium: hip implants, bicycle frames, earrings, and eyeglass frames.

Two of the most important characteristics of a metal are the corrosion resistance and its strength-to-density ratio, which is intended to be as high as possible. Unalloyed titanium is as strong as certain types of steel, but yet approximately 45% lighter. Titanium exists in two allotropic forms and has five naturally occurring isotopes of titanium, ranging from ^{46}Ti to ^{50}Ti, with ^{48}Ti being the most abundant (73.8%).

Table 2.2.1 Natural Isotopes of Titanium

MASS NUMBER	NATURAL ABUNDANCE	STABILITY AND NEUTRONS
46	8,25%	**^{46}Ti** stable with **24 neutrons**
47	7,44%	**^{47}Ti** stable with **25 neutrons**
48	**73,72%**	**^{48}Ti** stable with **26 neutrons**
49	5,41%	**^{49}Ti** stable with **27 neutrons**
50	5,18%	**^{50}Ti** stable with **28 neutrons**

The chemical and physical properties of titanium are similar to those of zirconium, as both elements have the same number of valence electrons and belong to the same group of the periodic table of elements.

2.3 Characteristics

2.3.1 Physical properties

Titanium is a metallic element notable for its high strength-to-density ratio. It is a strong metal with a low density, slight ductility (it can undergo plastic deformation without breaking), especially in an oxygen-free environments. It has a lustrous appearance and a white metallic color. Its melting point is relatively high (above 1650°C), which classifies it as a refractory metal. It is paramagnetic and it exhibits relatively low thermal and electrical conductivity.

Commercially pure titanium grades (with 99,2% purity) have the tensile strength of approximately 434MPa, comparable to that of lower-grade steels, yet titanium is 45% lighter than steel. Titanium is about 60%

denser than the aluminum, but it is nearly twice as strong as the most commonly used aluminum alloy, 6061-T6. Certain titanium alloys, such as Beta-C), can achieve tensile strengths exceeding 1,400 MPa. However, titanium loses its mechanical strength when heated above 430℃.

Machining titanium components requires strict safety precautions, as titanium tends to „soften" and „smears" if sharp tools and appropriate cooling techniques are not used.

As with steel structures, titanium-based structures exhibit fatigue resistance that ensures long service life in certain applications. However, the specific stiffness of the titanium alloys is lower than that of other materials, such as aluminum alloys of carbon fibers, which limit their use in structures where high rigidity is required.

Titanium is an allotropic, dimorphic metal, whose hexagonal close-packed alpha (α) crystal structure transforms into the beta (β) phase at 882℃, which has a body-centered cubic (BCC) crystal structure.

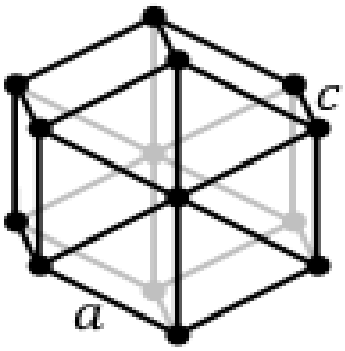

Figure 2.3.1.1 Body-centered cubic (BCC) crystal structure of β-titanium.

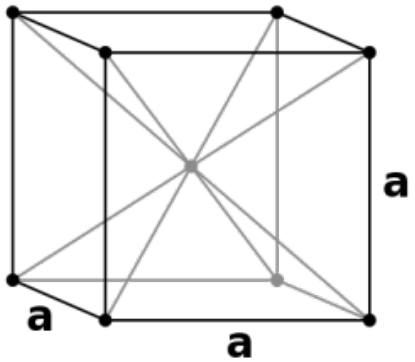

Figure 2.3.1.2 Hexagonal close-packed (HCP) crystal structure of α-titanium.

The specific heat of the α phase increases significantly as it approaches the transformation temperature, but then drops abruptly and remains nearly constant for the β phase,

regardless of further temperature increases.

Table 2.3.1.1 Titanium – Physical Properties

PROPERTY	VALUE
Phase at room temperature	**Solid**
Density (at **293*K* / 20**℃*)*	**4.500 kg/m^{-3}**
Density of liquid titanium at melting point (at 1941 K / 1668^{o}C)	**4.110 kg/m^{-3}**
Melting point	**1941 K (1668 °C)**
Boiling point	**3560 K (3287 °C)**
Heat of fusion (latent heat of melting)	**14.15 kJ/mol**
Heat of vaporization (latent heat)	**425 kJ/mol**
Specific heat capacity (at **298*K* / 25**℃*)*	**0.52 × 10^{3}J/kg·K**
Thermal conductivity	**22 W/m·K**
Coefficient of linear thermal expansion	**8.6 × 10^{-6}K^{-1}**
Young's modulus	**116 GPa**
Poisson's ratio	**0.32**
Brinell hardness	**716 MPa**
Vickers hardness	**970 MPa**
Electrical resistivity	**40 × 10^{-8}Ω·m**

2.3.2 Chemical properties

Titanium's excellent corrosion resistance is the most notable chemical property. It is nearly as resistant as platinum and can withstand attacks from diluted sulfuric acid mixture and hydrochloric acids, chloride solutions, and most organic acids. However, titanium is soluble in concentrated acids.

On the other hand, titanium reacts slowly with water and air, forming a passive, protective oxide film that shields it from the further reactions. When first formed, this protective layer has a thickness of only 1-2 nm (1 nm = 10^{-9} m), but it continues to grow gradually, reaching up to 25 nm over a period of four years.

When exposed to high temperatures, titanium reacts readily with oxygen – at 1,200℃ in the air and at 610℃ in pure oxygen – forming titanium dioxide. As a result, titanium cannot be melted in contact with air, as it burns before reaching its melting point. Melting is only

possible in an inert atmosphere or in a vacuum. At 550°C it reacts with chlorine, and it also reacts with other halogens and absorbs hydrogen.

Titanium is one of the few elements that burn in pure nitrogen, reacting at 800°C to form titanium nitride (TiN), which causes embrittlement in metallic alloys.

Experiments have shown that natural titanium becomes radioactive when bombarded with deuterons, emitting primarily positrons and high-energy gamma rays.

Table 2.3.2.1 Titanium – Chemical and Physical Properties Table

PROPERTY	VALUE
Atomic number	**22**
Symbol	**Ti**
Atomic mass	**47.88 u**
Oxidation states	**+4, +3, +2**
Crystal structure	
• *Below* **882**°C	*Hexagonal close-packed (a-phase)*
• *Above* **882**°C *to* **1688**°C	*Body-centered cubic (β-phase)* 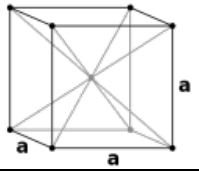
Electronic configuration	**$1s^2\ 2s^2p^6\ 3s^2p^6d^2\ 4s^2$**
Electron energy levels	**2,8,10,2** 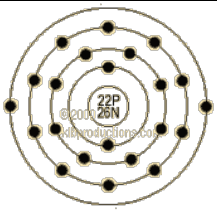
Hardness (Mohs' scale)	**6**

2.4 Compounds

The +4 oxidation state dominates titanium chemistry, although compounds with the +3 oxidation state also exist. Due to this high oxidation state, many titanium compounds exhibit a high degree of covalent bonding. Sapphires and rubies owe their asterism to the titanium dioxide (TiO_2) impurities present within their crystalline structure.

ASTERISM (gemstones)

Asterism is an optical phenomenon observed in certain rubies, sapphires and other gemstones, characterized by a star-shaped pattern of light that appears on the surface of a cabochon-cut stone due to highly reflective inclusions or structural features.

Figure 2.4.1 Asterism visible on the surface of the 182-carat Star of Bombay sapphire (36.4 g), housed at the National Museum of Natural History, Washington D.C.

Titanates are compounds based on titanium dioxide. Barium titanate exhibits piezoelectric properties, enabling its use as a transducer for converting sound into electrical signal and vice versa. Titanium esters are formed by the reaction of alcohols with titanium tetrachloride and are used in the production of water-repellent fabrics.

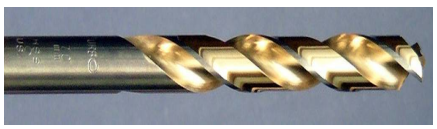

Figure 2.4.2 Spiral steel drill coated in titanium nitrogen (TiN), featuring golden fluted channels.

Table 2.4.3.1 Mohs Hardness Scale (Friedrich Mohs)

SUBSTANCE	MOHS HARDNESS
Talc	**1**
Gypsum (Plaster)	**2**
Calcite	**3**
Fluorite	**4**
Apatite	**5**
Orthoclase (Feldspar)	**6**
Quartz	**7**
Topaz	**8**
Corundum	**9**
Sapphire	
Tungsten carbide	
Titanium nitride (TiN)	
Silicon carbide (SiC)	
Diamond	**10**

Titanium nitride (TiN), which has a hardness equivalent to sapphire or corundum (9 on the Mohs scale), is commonly used to coat cutting tools such as drill bits. It is also used for the decorative gold-colored finishes and as a barrier metal film in semiconductor manufacturing.

Titanium tetrachloride ($TiCl_4$) is a colorless liquid used as an intermediate in the production of titanium dioxide (TiO_2) for use in paints and pigments. It is also widely employed in organic chemistry as a Lewis acid, particularly in the Mukaiyama aldol reaction – an aldol-type organic reaction between a silyl enol ether and an aldehyde, catalyzed by a Lewis acid. Titanium also forms lower chlorides, such as titanium trichloride ($TiCl_3$), which is used as a reducing agent.

Dichlorobis(cyclopentadienyl)titanium ($(\eta^5-C_5H_5)_2TiCl_2$) is an important catalyst in carbon–carbon bond formation. Titanium isopropoxide ($Ti[OCH(CH_3)_2]_4$) is used in the Sharpless epoxidation, a key asymmetric reaction in organic synthesis. Other compounds include titanium tetrabromide ($TiBr_4$), used in metallurgy, superalloys, high-temperature electrical coatings, as well as titanium carbide (TiC),

which is applied in the manufacturing of cutting tools and thermal protection coatings.

2.5 Diffusion

In nature, titanium is always found in combination with other elements. In the Earth's crust, it is the ninth most abundant element by mass (0,63%) and ranks seventh among metals. It is present in igneous rocks, in the sediments derived from them, as well as in living organisms and natural water sources. Out of 801 types of igneous rocks analyzed by the United States Geological Survey, 784 were found to contain titanium. In soil, its concentration typically ranges from 0,5% to 1,5%. Titanium is widely distributed and is primarily found in the minerals anatase, brookite, ilmenite, perovskite, rutile, and titanite, as well as in various iron ores.

Figure 2.5.1 Brookite.

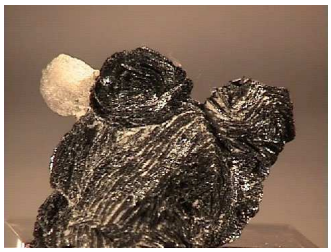

Figure 2.5.2 Ilmenite.

Figure 2.5.3 Perovskite.

Fig. 2.5.4 Rutile.

Figure 2.5.5 Titanite.

Among these minerals, rutile and ilmenite are of particular economic importance, despite being relatively scarce in high concentrations. Significant ilmenite deposits containing

titanium are found in Western Australia, Canada, China, India, Mozambique, New Zealand, Norway, and Ukraine. Sizable quantities of rutile are also extracted in North America and South Africa, contributing to the annual global production of approximately 90,000 tons of metallic titanium and 4.3 million tons of titanium dioxide. Global titanium reserves are estimated to exceed 600 million tons.

Table 2.5.1 Worldwide production of titanium dioxide in 2003

PRODUCER	PRODUCTION (thousand tons)	% OF TOTAL PRODUCTION
Australia	**1,291.0**	**30.58**
South Africa	**850.0**	**20.14**
Canada	**767.0**	**18.17**
Norway	**382.9**	**9.07**
Ukraine	**357.0**	**8.46**
Other countries	**573.1**	**13.58**
TOTAL	**4,221.0**	**100**

Titanium has been detected in meteorites, and spectral analysis confirms its presence in the Sun and in type M stars – the „coolest" among the stellar types – some of which have surface temperature 3,200°C. Samples of lunar rock collected during the Apollo 17 mission were found to contain up to 12.1%. Titanium can also be found in the coal ash, in various plants, and even in the human body.

2.6 Historical Background

In 1791, an amateur geologist and pastor, William Gregor, discovered titanium in a mineral found in Cornwall, United Kingdom. The pastor noticed the presence of a new element when he found black sand in the running water near the Manaccan parish and concluded that the sand was attracted by a magnet. The sand analysis (of the mineral named menaccanite) showed the presence of two metal oxides and those are the iron

oxide (which explained the attraction made by the magnet) and an unidentified white metallic oxide in a proportion of 45,2%.

Understanding that the unidentified oxide contains a metal whose properties don't match the properties of any known element, Gregor presented the results of his investigations in front of the Royal Geological Society of Cornwall and in the German scientific journal, Annals of Crell.

Almost at the same time, Franz-Joseph Müller von Reichenstein obtained a similar substance but didn't manage to identify it. Independently, the German chemist Martin Heinrich Klaproth rediscovered the titanium oxide in 1795, in rutile.

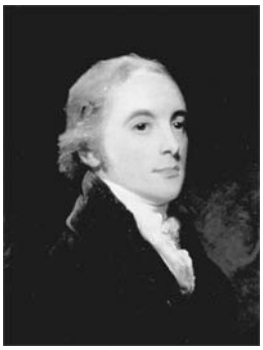

Figure 2.6.1 William Gregor (1761-1817).

Figure 2.6.2 Martin Heinrich Klaproth (1732-1817).

Klaproth established that the oxide contained a new chemical element and gave it the name of titanium after the names of the Titans from Greek mythology, the first born of the Earth. After he found out about the anterior discovery of Gregor, Klaproth obtained a menaccanite sample and confirmed that it contained titanium.

Figure 2.6.3 Jöns Jakob Berzelius

(1779-1848).

Only in 1825, Jöns Jakob Berzelius, the well-known Swedish chemist, managed to obtain the impure metallic titanium. The road towards the industrial production of titanium was long and required the use of all resources and abilities.

In 1875, in Russia, Kirillov managed to obtain almost pure titanium. In 1887, Lars Nilson and Otto Pettersson also managed to obtain titanium with a purity of 95%. Using his electric oven, Henri Moissan managed to obtain titanium with a purity of 98%.

The necessary processes for the obtainment of titanium from its different ore are laborious and expensive. The common reduction through heating in the presence of carbon is not possible because this way it is being produced titanium carbide.

In 1910, Matthew A. Hunter from Rensselaer Polytechnic Institute obtained pure metallic titanium (99,9% purity) for the first time by heating up $TiCl_4$ with sodium at $700 \div 800°C$ and established the procedure that carries his name (the Hunter procedure).

Figure 2.6.4 Matthew A. Hunter (1878-1961).

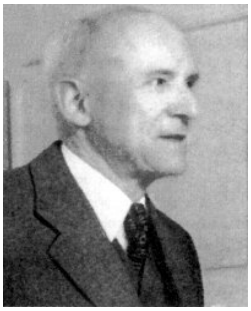

Figure 2.6.5 Guillaume (William) Justin Kroll (1889-1973).

Titanium metal was never used outside of the lab until 1932 when Guillaume (William) Justin Kroll proved that it can be produced through the reduction of titanium tetrachloride ($TiCl_4$) with calcium. Eight years later, he was perfecting the procedure by using magnesium and even sodium, becoming known as the Kroll procedure. Even though the research for the establishment of more effective and cheaper procedures continues (for example, the FFC Cambridge procedure), the Kroll procedure is still used for commercial production.

The high purity titanium was obtained in small quantities in 1925, when Anton Eduard von Arkel and Jan Hendrik de Boer discovered the iodide procedure (the crystal bar procedure), through the reaction with iodine and the decomposition of the vapors formed on a hot filament for obtaining pure metal.

Between 1950 and 1970 the former Soviet Union developed a pioneering activity for the use of titanium in military applications such as the construction of submarines (classes Alpha and Mike according to the NATO encoding) as part of the programs regarding the Cold War.

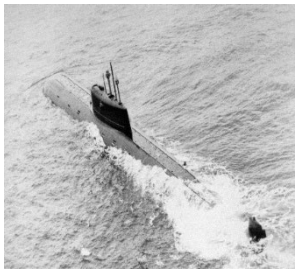

Figure 2.6.6 Ex-soviet submarine (Mike class).

Figure 2.6.7 Ex-soviet submarine (Alpha class).

Starting from the first year of the 1950-1960's, titanium began to be used on a wide scale of the military aviation domain, especially on the high performance reaction jets, starting with the combat aircrafts like F100 Super Sabre and Lockheed A-12 from the U.S.A.

Figure 2.6.8 F100 Super Sabre Airplane.

Figure 2.6.9 Lockheed A-12 Airplane.

In the U.S.A. the Department of Defense understood the strategic importance of metal and supported the first marketing efforts. For the entire duration of the Cold War, the U.S government considered titanium a strategic material and stocked high reserves at Defense National Stockpile Center which weren't cleared until 2005.

Nowadays, the biggest producer is VSMPO-Avisma of Russia whose worldwide market share is estimated at 29%.

In 2006 the US Defense Agency granted a contract of 5,7 million$ to the consortium made of two companies for the development of a new procedure of obtaining metallic titanium powder. Under heating and

pressure, the titanium powder can be used for the manufacture of light and resistant items, ranging from armor plating to components for the aerospace, to transportation and chemical processing industries.

2.7 Production and fabrication

The process of titanium obtainment is made in 4 big steps:

- the reduction of the titanium ore to a sponge, a porous body.
- melting the sponge or the sponge with an intermediary alloy (pre-alloy) shaped as an ingot.
- the primary fabrication in which the ingot is transformed into general products of lamination such as: billet, bar, plaque, sheet, band and pipe.
- the secondary fabrication of finite profiles from laminated products.

Because of the fact that titanium reacts with oxygen at high temperatures, it cannot be produced through the reduction of this dioxide. Therefore, titanium metal is produced for commercial purposes through the Kroll procedure, a desultory, complex and expensive procedure. The relatively high market value of titanium is mainly the result of the elaboration processes which involve the use of magnesium, another expensive metal.

In the Kroll procedure, the dioxide is turned into chloride through carbochlorination. The chlorine gas is being passed, in the presence of carbon, over rutile or ilmenite heated to red for the obtainment of $TiCl_4$. This is condensed and purified through fractional distillation and then reduced with magnesium melted at 80℃ in an argon atmosphere.

Figure 2.7.1 Titanium sponge obtained through the Kroll procedure.

The Kroll procedure is an industrial metallurgic used for the production of metallic titanium. This was invented by Guillaume (William) Justin Kroll in Luxembourg. After he moved to the United States, Kroll continued to develop the procedure for the production of zirconium. The Kroll procedure replaced the Hunter procedure for almost all the commercial production of titanium.

The refined rutile (or ilmenite) from ore is reduced with petroleum obtained coke in a fluidized bed reactor at 1000℃. Then the mixture is treated with gassy chlorine, obtaining the titanium tetrachloride ($TiCl_4$) and other volatile chlorides which are subsequently separated through a continuous fractional distillation. In a separate reactor, in a stainless steel flask, $TiCl_4$ is reduced to $800 \div 850$℃ *with excessive liquid magnesium with* $15 - 20\%$ *to ensure complete reduction.*

The reaction is:

$$2 \cdot Mg\ (liquid) + TiCl_4\ (gas) \rightarrow 2 \cdot MgCl_2\ (l) + Ti\ (solid)\ (temperature = 800 \div 850℃)$$

The complications result from the partial reduction of the titanium to inferior chlorides $TiCl_2$ *and* $TiCl_3$. *c* $MgCl_2$ *can still be refined in opposite direction, obtaining this way magnesium. The resulted porous metallic titanium sponge is purified through solution (extraction through solution) or void distillation through heat. The sponge is broken with a drop hammer, crushed and pressed before melting it in void as an electrode in an electrical arch oven.*

A more recent procedure, named FFC Cambridge, may eventually replace the Kroll technological process. This procedure uses titanium dioxide powder (which is a refined form of rutile) as an intermediary product for the obtainment of the final product which is either a powder or a sponge. If oxide powders are mixed, the resulting product is an alloy manufactured at a lower cost than that of the multi-step melting fabrication process.

The FFC Cambridge process can make titanium, a rare and expensive material, designed for the aerospace industry and luxury products market, to be used for the manufacture of many products made nowadays from aluminum alloys and special steel grades. Common titanium alloys are obtained through reduction. Thus, alloys such as cupro-titanium (the rutile is reduced with added copper), steel-carbon titanium (ilmenite reduced with coke in the electric oven), and manganese-titanium alloy (rutile

reduced with manganese or manganese oxides) are produced.

$$2 \cdot FeTiO_3 + 7 \cdot Cl_2 + 6 \cdot C \rightarrow 2 \cdot TiCl_4 + 2 \cdot FeCl_3 + 6 \cdot CO$$

($temperature$ 900℃)

$$TiCl_4 + 2 \cdot Mg \rightarrow 2 \cdot MgCl_2 + Ti$$

($temperature$ 1100℃)

About 50 grades of titanium and titanium alloys are indicated and currently used even though only two dozen are truly available commercially. ASTM International acknowledges 31 titanium and titanium alloy grades from which from grade 1 to grade 4 are those of pure commercial titanium (unalloyed). Grades from 1 to 4 distinguish themselves through the different size of the tensile strength depending on the oxygen content, grade 1 being the most ductile (the lowest tensile strength suitable for a 0,18% oxygen content) and grade 4 the least ductile (the highest tensile strength for an oxygen content of 0,40%). The rest of the grades, from 5 to 31 are alloys, each of them conceived for certain uses and, depending on the use, have a specific deformation behavior, tensile strength, toughness, electric resistivity, creep resistance, corrosion resistance in certain environments, or a combination of all these characteristics.

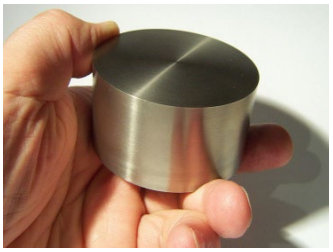

Figure 2.7.2 A titanium cylinder GRADE 2.

Both the grades acknowledged by ASTM and other alloys are produced in a way that they satisfy both aerospace requirements (SAE-AMS standards) and/or military

requirements (MIL-T standards) and ISO and one country's standards but also the standards of the final user from the aerospace, military, medical and industrial domains.

Regarding the fabrication, all the welding joints of titanium must be executed in an inert argon or helium atmosphere to protect the titanium from contact with atmospheric gases such as oxygen, nitrogen, or hydrogen. The contact has a diversity of consequences, such as brittleness, which entirely jeopardizes the weld joints of the ensemble and leads to welding defects. Even if, commercially, the completely flat products (sheets and plaques) can be made rapidly, the processes must take into consideration the fact that the metal has a „memory" and has the tendency of reverting to its initial form. This fact is obvious, especially in the case of certain high-strength alloys. Titanium can be processed by cutting using the same equipment and the same procedures as for stainless steel.

2.8 Applications

Titanium is used as an alloying element (ferrotitanium) in steel for reducing grain size and as a deoxidizer, and in the alloyed steel for the reduction of the carbon content. Titanium is often alloyed with aluminum (for the improvement of the grain dimension), with vanadium, copper (for hardening), with iron, molybdenum and other materials.

Titanium as laminated products (sheets, plaques, bars, wires), forged pieces and turned pieces can be found in the industrial, aerospace, recreational and emerging product markets.

Titanium as a powder is used in the pyrotechnics domain as a source of particles that when burning become luminous.

2.8.1 Pigments, additives and coverings

Almost 95% of titanium ore extracted from the ground is intended for the refinement into titanium dioxide (TiO_2), a

permanent pigment of an intense white, used in the painting, paper, toothpaste and plastic materials industry. It is also used in the cement and gems industry, as a substance of optical opaqueness in the paper industry and as a hardening agent of the graphite-based compounds for angle tools and golf clubs.

TiO_2 powder is chemically inert, resistant to discoloration from sunlight, and highly opaque. This allows it to imprint a shiny and pure white color to the brown and grey chemical substance contained in most household plastics. In nature this titanium compound is found in the anatase, brookite and rutile minerals. The paint made with titanium dioxide behaves well at extreme temperatures, it presents a somewhat self-cleaning and resists in the marine environment. The pure titanium dioxide has a very high refractive index and a higher optical dispersion than the diamond. Besides the fact that it is a very important pigment, titanium dioxide is also used for sunscreen products thanks to its intrinsic capacity of protecting the skin.

Recently, it has been used in the air purifiers (as a filtering layer) or as a coating film on the building windows, because when it is exposed to UV light (be it solar or human produced) and the air humidity, it produces hydroxyl radicals that purify the air and keeps the windows surface clean.

2.8.2 Aerospace and marine domains

Titanium alloys are used in the construction of aircraft, spacecraft, ships, and missiles, as well as in the manufacturing of armored protection, due to their high tensile strength-to-density ratio, excellent corrosion resistance, fatigue resistance and their ability of resisting pretty high temperatures without creep deformation.

In these applications, titanium alloys with aluminum, vanadium and other elements are used for a multitude of components including critical structural benchmarks such as firewalls, landing gear, exhaust

pipes (of helicopters), and hydraulic systems. In fact, almost two thirds of all the produced titanium metal is used for the construction of engines and aircrafts structures.

The SR-71 „Blackbird" was one of the first aircrafts that used, on a large scale, titanium in its structure, opening the road of titanium usage in the construction of military and commercial modern aircrafts.

Figure.2.8.2.1 SR-71 „Blackbird" aircraft.

59t of titanium are estimated to be used on a Boeing 777, 45t on a Boeing 747, 18t on a Boeing 737, 32t on Airbus 340, 18t on Airbus 330 and 12t on an Airbus 320. Airbus A380 uses 146t from which 26t on the engines. In jet engines, titanium is used for rotors, compressor blades, hydraulic system components and nacelles. It is considered that the 6Al-4V titanium alloy represents almost 50% of the total alloys used in the aircraft's domain.

Thanks to its high resistance to seawater corrosion, titanium is used for the construction of propeller shafts, heat exchangers in seawater desalination plants, heating systems in crystallized saltwater aquariums, and diving knives. Titanium is also used for the manufacture of hulls and other components of the inspection and surveillance devices installed in the ocean for military and scientific purposes. The former Soviet Union developed technologies for the manufacture of submarines mostly made of titanium.

2.8.3 Industrial domain

Titanium welded pipes and the processing equipment (heat exchangers, reservoirs, processing dishes, valves) are used in the chemical and petrochemical industries thanks to mainly the

corrosion resistance. Certain alloys are used in the drilling and nickel hydrometallurgical domains thanks to the high resistance of the Beta-C titanium, the corrosion resistance or both properties.

The cellulose and paper industry uses titanium in the processing equipment submitted to the corrosive environments such as sodium hypochlorite or moist chlorine gas (e.g., in whiteners/whitening sections). Among other uses there is ultrasonic welding, bonding electronic components and sediment of film-layers through spreading of atoms from a bombed target with high energy particles.

Titanium tetrachloride ($TiCl_4$), a colorless liquid is important as an intermediary substance in the process of obtaining TiO_2 and the obtainment of the Ziegler-Natta catalyst. It is also used for the treatment with iridium of glass but also for the making of smoke curtains thanks to the strong smoking in moist air.

2.8.4 Consumer goods domain

Titanium metal is used in the automobile industry, especially for the racing automobiles and motorcycles, where the weight reduction is extremely important along with maintaining of high resistance and toughness. The metal is, virtually, too expensive to be marketed on the common consumer market, other than the one of the hi-tech products such as the racing cars products market. We remember the existence of one of the last Corvette models equipped with titanium exhaust pipes.

Figure 2.8.4.1 Chevrolet Corvette Z06 Hardtop Coupe is equipped with titanium exhaust pipes

Titanium is used for many sports designed products: rackets, golf clubs, cricket clubs and hockey but also for the American football helmet grids and for the bicycle frame. Even though it is not a material used on a high scale in the construction of bicycles, titanium bicycles are used by racing teams and in cycling. Titanium alloys are also used for spectacle frames, they are more expensive but with a higher durability, a reduced weight and are allergy free.

Figure 2.8.4.2 Three golf clubs of different classes. From left to right: a driver, a putter and an iron.

Many tourists that spend their vacations camping use titanium items, including dishes, cutlery, pots, and tent stakes. These items are a bit more expensive than those made of steel or aluminum, but they are much lighter without having their resistance compromised. For racing horses there can be titanium horseshoes, lighter and more durable.

Thanks to its durability, titanium has begun to be used for jewelry making (especially for titanium rings manufacture). As a result of its chemical inactivity, the titanium made jewelry able to be worn by those with allergies or by those who wish to wear them in a pool.

Figure. 2.8.4.3 Titanium Ring.

The durability of titanium, its reduced mass, its resistance to chipping and corrosion makes it adequate for the production of watch cases.

2.8.5 Art and architecture domain

There are artists that make works of art from titanium, such as sculptures, decorative objects and furniture. Titanium has also been used in architectural applications such as the monument built in Moscow (with a height of 40m), in the memory of Iuri Gagarin, the first man who travelled in space. The Guggenheim Museum of Bilbao and the Cerritos Millennium Library are the first buildings in Europe and respectively North America, covered with titanium panels. Titanium layers were also used at the Frederic C. Hamilton Building in Denver, Colorado and at the Space Conquerors Monument in Moscow, with a height of 107m.

Figure 2.8.5.1 The Guggenheim Museum (Bilbao) is wrapped in glass, titanium and limestone.

Figure 2.8.5.2 The Guggenheim Museum (Bilbao), the titanium panels.

2.8.6 Weaponry, IT and luxury tools domains

Thanks to its superior resistance and its reduced mass compared to other metals used traditionally for firearms (steel, stainless steel and aluminum) and thanks to the development of the metal processing techniques, the use of titanium in firearms manufacturing has spread. Among the first uses of titanium in this domain there are pistol frames and revolver kegs (cylinders).

Figure 2.8.6.1 9mm caliber pistol TAURUS MILLENIUM PROTM TITANIUM 111 (Titanium made frame).

Figure 2.8.6.2 357 caliber revolver Smith & Wesson 360 PD (Titanium made keg).

The same reasons determine the use of titanium for laptop bodies (for example, the Apple Titanium PowerBook G4).

Some luxury articles categories are made of titanium to be light and corrosion resistant such as shovels and lantern.

Figure 2.8.6.3 Titanium-bodied laptop – Apple PowerBook G4, featuring a titanium casing for improved strength, reduced weight, and heat resistance.

2.8.7 Medical domain

2.8.7.1 Orthopedic implants

Because of its biocompatibility (it is not toxic and not rejected by the organism), titanium is used on a large range of medical applications, including the surgical and implant ones, such as the hip articulation (the articulation replacement), with a functional span of about 20 years. Titanium is often alloyed with approximately 4% aluminum or with 6% aluminum and 4% vanadium.

Titanium has the intrinsic property of integrating in the bone mass, which allows the use of dental implants with a functional span of over 30 years. This property is also useful for orthopedic implants. These implants benefit from titanium's relatively low elastic modulus (Young's modulus), much closer to the bones', compared to other devices with which they try to remake the articulation. As a result, the loads transferred through the skeleton are more homogeneously distributed between the bone and implant, leading to a lower incidence of the bone degradation caused by the mechanical stress exerted by the metallic reinforcement and the periosteal fractures, at the interface of the orthopedic implants. Nevertheless, the rigidity of titanium alloys is still twice as high compared to the bone's so that the bone near the implant can deteriorate in time, because it takes on a reduced mechanical loading.

Because titanium is not a ferromagnetic material, patients with titanium implants can safely undergo magnetic resonance imaging (MRI), which is convenient for long-term implanted devices. The preparation of titanium for inside the body implants implies cleaning its surface atoms with a high temperature plasma jet so that the cleaned titanium is instantly oxidized.

2.8.7.2 Piercings

Its chemical inertness and its capacity of attractive coloring determine the use of titanium, as a metal, for piercings. Titanium can be anodized to produce different colors, which vary depending on the thickness of the surface oxide layer and create interference fringes.

2.8.7.3 Other usages

Titanium is used for surgical instruments in image guided surgery, as well as in wheelchairs, crutches and any other products which imply a high strength and a low weight.

2.9 Safety cautions

Titanium is non-toxic, even in high doses, and has no influence on the human body. It is estimated that 0,8 milligrams of titanium are ingested by a human each day, but it passes through the organism without being absorbed. There is though the tendency of being accumulated in the tissues that contain silicon. Plants have an unclear mechanism that uses titanium in the simulation of the carbohydrate synthesis, thereby promoting growth. This way is explained by the fact that most of the plants contain about 1 part per million (ppm) of titanium, the edible plants contain about 2 ppm and the Equisetum arvense (common horsetail) and Urtica dioica (stinging nettle), have been found to contain up to 80 ppm.

Titanium, as a powder or metal chips, presents a high fire risk, and if it is heated in air, it presents an explosion risk. Firefighting methods based on water and carbon dioxide are ineffective against burning titanium. These fires are put out by using dry powder-type Class D firefighting agents.

When it is used in the production or manipulation of chlorine, the titanium must be used only in the places where it won't be exposed to dry gaseous chlorine, because this kind of

exposure can lead to a titanium/chlorine fire. There is also a fire risk even when the titanium is used in contact with moist chlorine, because of possible and unpredicted drying of chlorine caused by extreme meteorological conditions.

Titanium can ignite when a newly exposed and unoxidized surface comes in contact with liquid oxygen. These types of surfaces can appear when the oxidized surface is hit with a hard object and then, under mechanical stress, a fracture appears. This fact limits the possible use of titanium in liquid oxygen systems such as those from the aerospace field.

3 The Joule Effect and Methods for its Mitigation

3.1 Electrical power in Metallic Conductors

3.1.1 Metallic Structure

The simplest model for a metallic structure is that of a network of positive ions within which negatively charged electrons move freely (Figure 3.1.1.1). Thermal agitation is reflected by small-amplitude oscillations of the ions around their equilibrium position, while the electrons exhibit random motion through the lattice, similar to the movement of gas molecules confined within a container. In their random motion among the positive ions, the electrons form what is known as an electron gas. The number of the electrons forming this electron gas is relatively high.

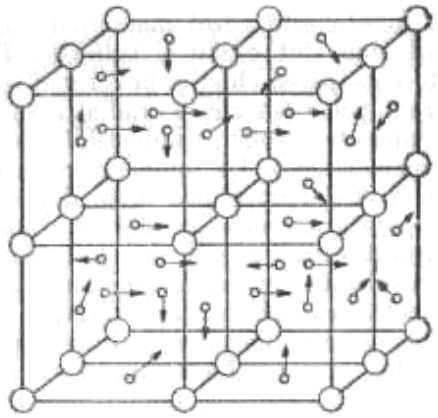

Figure 3.1.1.1 The crystalline lattice of a metal and the free electrons (electron gas).

The total electric charge of the free electrons is negative and equal in magnitude to the positive charge of all the ions forming the crystalline lattice of the metal. As a result, the metal is usually electrically neutral.

3.1.2 The Electric Potential

Let there be two conductive bodies: one labeled $\boldsymbol{A}$, with electric potential $\boldsymbol{V_A}$, and another one labeled $\boldsymbol{B}$, with electric potential $\boldsymbol{V_B}$, where $\boldsymbol{V_A} < \boldsymbol{V_B}$ (Figure 3.1.2.1). If the two bodies are connected through a metallic conductor, the electrostatic forces generated by the electric field between bodies $\boldsymbol{A}$ and $\boldsymbol{B}$ will induce a directed motion of the free electrons within the crystalline lattice of the metallic conductor.

As a result, some of the free electrons from body ***A*** will flow toward body ***B*** until the electric potentials of ***A*** and ***B*** equalize. This transport of free electrons (the charge carriers) through the metallic conductor is called **electric current.**

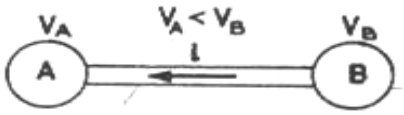

Figure 3.1.2.1 The electric current between two conductive bodies with different potentials.

Obtained this way, the electric current lasts in time if the difference of potential between the conductive bodies ***A*** and ***B*** is maintained constant. In other words, the condition that the free electrons to return from body ***B*** to body ***A*** must be fulfilled. This condition is fulfilled if an electric source ***S*** (an electric generator) is introduced between the two conductive bodies**.** The electric source ***S*** (the electric generator) is connected through two conductive wires to bodies ***A*** and ***B*** so that a closed circuit is formed (Figure 3.1.2.2).

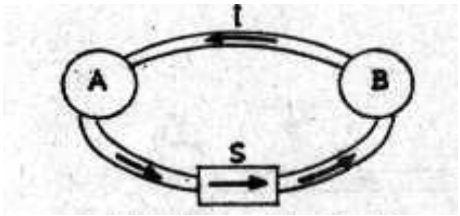

*Figure 3.1.2.2 The electric current established by means of the electric source **S** (generator).*

The electric source ***S*** (the electric generator) ensures a constant potential difference between bodies ***A*** and ***B***, i.e., an electric field capable of driving the free electrons into a collective movement, characterized by an average constant drift velocity, which leads to the presence of electric current within the closed circuit from Figure 3.1.2.3.

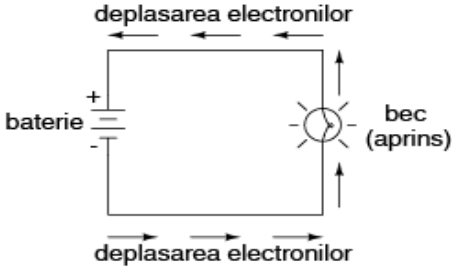

Figure 3.1.2.3 Electric current in a simple circuit composed of a source (battery), a consumer (light bulb), and connecting conductors.

Over distances of hundreds of kilometers, electric power is transmitted almost instantaneously, even though the

drift velocity of the charge carriers has a magnitude on the order of 10^{-5} m·s^{-1}. The near-instantaneous transmission is due to the extremely high speed $3 \cdot 10^{8}$ m·s^{-1}, at which the electric field propagates through the conductors (field guides). When the electric field is established at a point within the conductor, the surrounding electrons at that point are induced into a secondary ordered motion, which produces the stationary electric current. This produces a stationary electric current, characterized by a collective drift velocity of the electrons that is constant and time-independent across any section of the conductor. The electric source (generator) converts another form of energy into electric current.

Depending on the type of energy converted into electric current, the electric sources (electric generators) can be classified as follows:

- Electric accumulators and cells, which convert the chemical energy into electric current;
- Dynamos and alternators, which convert the mechanical energy into electric current;
- Thermo-elements, which convert the thermal energy into electric current;
- Photo-elements, which convert the luminous energy into electric current.

The existence of electric current manifests through three main effects:

- The thermal effect, observed as the heating of conductors through which the electric current passes;
- The chemical effect, evident in the deposition of a certain quantity of substance at the negative electrode when electrical current passes through an electrolyte solution;
- The magnetic effect, highlighted by the appearance of a magnetic field around a conductor carrying an electric current.

3.1.3 The Electric Circuit

The electric source (or generator), the field guides (conductive wires), and one or more consumers together form an electric circuit (Figure 3.1.3.1).

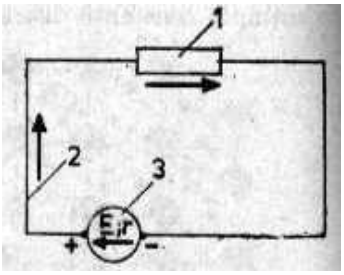

Figure 3.1.3.1 Electric circuit: 1 – Consumer; 2 – Conductive wire; 3 – Electric source (generator).

3.1.4 The Intensity of the Electric Current

The effects of electric current can be stronger or weaker, depending on how intense the electric current is. A current is considered more or less intense depending on the amount of electric charge transported by the charge carriers (electrons) through a cross-sectional area of the conductor in a given time interval.

The physical quantity that defines this characteristic of the electric current is called **the intensity of the electric current.**

The intensity of the electric current is the physical quantity that expresses the amount of electric charge passing through the cross-sectional area of a conductor per unit of time.

$$I = \frac{Q}{t} \qquad (3.1.4.1)$$

Where:

Q is the electric charge (in coulombs);

t is the time interval during which the charge Q passes through the surface of the cross-section of the circuit;

I is the electric current intensity (in amperes).

The electric current intensity is a fundamental scalar quantity in the International System of Units (SI). **The unit of measurement for intensity** is

called the ***ampere***, abbreviated as ***A***.

The intensity of the electric current is measured using a device called ammeter, which, when placed at any point in the circuit, indicates the same intensity. The ammeter is schematically represented in Figure 3.1.4.1.

Figure 3.1.4.1 Schematic representation of an ammeter.

Since some of the effects of the electric current depend on the direction in which the charge carriers flow through the circuit, a conventional direction is chosen for the electric current: the direction of movement of positive charge carriers.

3.2 Ohm's Law

3.2.1 Ohm's Law for a Homogeneous and Isotropic Conductor

Ohm's law, also known as the law of electric conduction, establishes the relationship between the **intensity *I* of the electric current** flowing through a homogenous and isotropic conductor, **the voltage *U*** applied at its ends, and **the electrical resistance *R*** of the conductor.

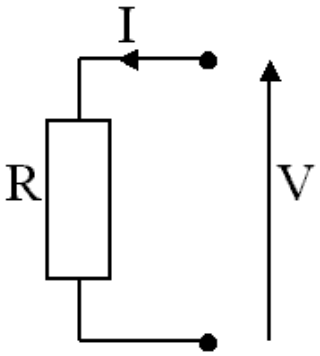

*Figure 3.2.1.1 A conductor with electrical resistance **R**, with voltage **U** applied at its ends, and electric current of intensity **I** flowing through it.*

Inside a conductor, **the electric current intensity I** is directly proportional **to the voltage U** applied at the ends of the conductor and inversely **proportional to its resistance R**.

These dependances between the measurements can be grouped inside the formula:

$$I = \frac{U}{R} \qquad (3.2.1.1)$$

Formula (3.2.1.1), known by the name of **Ohm's law for a homogenous and isotropic conductor (or a portion of an electric circuit)**, was discovered experimentally by **Georg Simon Ohm** in 1826 and represents **the macroscopic form** of the law.

3.2.2 The Ohm's Law for a Simple Circuit

Ohm's law can be extended to a simple circuit that contains a generator of electromotive force E, with an internal resistance r, in series with a resistive consumer R (Figure 3.2.2.1).

To extend Ohm's law to such a circuit, the following aspects must be taken into consideration:

The electric field generated by the source performs mechanical work L on the charge carriers, displacing them along the entire circuit.

The energy consumed by the source to perform this mechanical work L upon the charge carriers is regained by the source through the internal transformation process taking place inside the source. For example, in the case of an electrical battery, this energy results from the continuous transformation of chemical energy into electrical energy.

The electromotive force is numerically equal to the mechanical work performed to transport a unit of positive charge along the entire circuit.

Let W be the total energy provided by the source. This splits into the energy W_1,

necessary for the transport of the charge carriers through the external circuit, and the energy $\boldsymbol{W_2}$, necessary for the transport of the charge carriers through the source. Thus, we can write:

$$\boldsymbol{W = W_1 + W_2} \qquad (3.2.2.1)$$

If $\boldsymbol{Q}$ is the total electric charge of all the charge carriers, then expression (3.2.2.1) becomes:

$$\frac{\boldsymbol{W}}{\boldsymbol{Q}} = \frac{\boldsymbol{W_1}}{\boldsymbol{Q}} + \frac{\boldsymbol{W_2}}{\boldsymbol{Q}} \qquad (3.2.2.2)$$

Each one of the terms in expression (3.2.2.2) has the significance of a voltage, because, by definition, the electric potential difference $\boldsymbol{V_A - V_B}$ between two points $\boldsymbol{A}$ and $\boldsymbol{B}$ – or the voltage $\boldsymbol{U}$ between these two points – is a physical quantity equal to the ratio between the mechanical work $\boldsymbol{L}$ performed by the field to move a charged body and the electric charge $\boldsymbol{Q}$ of that body:

$$\boldsymbol{U = V_A - V_B = \frac{L}{Q}} \qquad (3.2.2.3)$$

According to the definition of the electromotive voltage, the term $\frac{\boldsymbol{W}}{\boldsymbol{Q}} = \frac{\boldsymbol{L}}{\boldsymbol{Q}}$ from equation (3.2.2.2) represents the electromotive voltage of the source, denoted by $\boldsymbol{E}$.

The term $\frac{\boldsymbol{W_1}}{\boldsymbol{Q}}$ represents the energy required to transport one unit of electric charge through the external circuit. Taking into account that $\boldsymbol{W_1 = L_1 = QU}$, where $\boldsymbol{U}$ is the voltage across the terminals, then $\frac{\boldsymbol{W_1}}{\boldsymbol{Q}}$, which is the voltage drop across the external part of the circuit.

Analogue, $\frac{\boldsymbol{W_2}}{\boldsymbol{Q}} = \frac{\boldsymbol{L_2}}{\boldsymbol{Q}} = \frac{\boldsymbol{Q \cdot u}}{\boldsymbol{Q}} = \boldsymbol{u}$, which is the voltage drop across the internal resistance of the source.

Taking the above into account, the equation (3.2.2.2) becomes:

$$\boldsymbol{E = U + u} \qquad (3.2.2.4)$$

The electromotive tension and the voltage drop are scalar physical quantities, and the unit of measurement for both is the **volt** (***V***)**.**

Considering the above, we move on to establishing the Ohm's law for a simple circuit. The electromotive tension (EMF) $\boldsymbol{E}$ of the source (generator) is the immediate cause of the movement of charge carriers, both through the external circuit of resistance $\boldsymbol{R}$, and through the internal circuit of the generator with resistance $\boldsymbol{r}$, determining the voltage drop $\boldsymbol{U}$ across the external circuit and, respectively, the voltage drop $\boldsymbol{u}$ across the source (generator). The physical meaning of the voltage drop is the energy per unit charge, dissipated by the system as a result of collisions within the crystalline lattice.

According to the equation (3.2.1.1), these voltage drops can be written as:

$$\boldsymbol{U = I \cdot R} \qquad (3.2.2.5)$$

$$\boldsymbol{u = I \cdot r} \qquad (3.2.2.6)$$

Replacing these expressions into relation (3.2.2.4), we obtain:

$$\boldsymbol{E = I \cdot R + I \cdot r} \qquad (3.2.2.7)$$

From which we immediately deduce:

$$\boldsymbol{I = \frac{E}{R+r}} \qquad (3.2.2.8)$$

The equation (3.2.2.8) represents **Ohm's law for a simple circuit**, and it is stated as follows:

The intensity of the electric current through a circuit is directly proportional to the electromotive tension of the circuit and inversely proportional to the total resistance of the circuit.

3.2.3 Biographical Note – Georg Simon Ohm

Fig.3.2.3.1 Georg Simon Ohm

(1789-1854).

Georg Simon Ohm (16th of March 1789, Erlangen - 6th of July 1854, Munich) was a German physicist and professor. From the very beginning of his didactic career as a high-school teacher, Ohm studied the ***galvanic pile*** invented by the Italian count ***Alessandro Volta***. Using equipment, he built himself, the German physicist ***experimentally discovered the relationship between the potential difference, the intensity of the electric current, and the electrical resistance*** – a relationship that became known in the scientific world, starting in **1826, as the law of electrical conduction**, more commonly referred to as **Ohm's law**.

Later, after becoming a professor at the **University of Nurnberg**, Ohm made additional contributions to the **development of physics**, the most significant of which include: **Ohm's acoustic law**, proposed in **1843** and known as **the siren theory**, **and his work on the interference of polarized light in crystals (1854)**.

Among his many remarkable contributions, we must mention **the truly scientific definition of the electrokinetic phenomena – namely, the comparison of the electric power with flow, the difference of potential as a difference of level, and the precise definition of the electric charge, intensity of the electric power, and the electromotive tension**.

The unit of measurement for electrical resistance bears his name is called the **ohm** (***Ω***).

3.2.4 The Microscopic (Local) Form of Ohm's Law for a Homogeneous and Isotropic Conductor

Applying a constant potential difference, $\Delta U = U_2 - U_1$, across the ends of a cylindrical conductor with cross-sectional area ΔS and length Δl , a time-independent current of intensity I is established within the conductor (Figure 3.2.4.1). This current has the same value at any cross-section of the conductor and is referred to as **direct current.**

The macroscopic form of the Ohm's law in this case is:

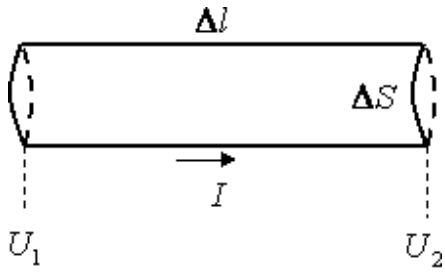

Figure 3.2.4.1 Homogenous and isotropic conductor.

$$I = \frac{U_1 - U_2}{R} = \frac{\Delta U}{R} \qquad (3.2.3.1)$$

The minus sign is a consequence of the fact that the direction of I corresponds to the movement of the positive charges, which is in the direction of decreasing potential. R **is the electrical resistance** of the conductor, measured in **ohms (Ω)** in the International System of Units (SI), and depends on the dimensions of the conductor, according to the formula:

$$R = \rho \cdot \frac{\Delta l}{\Delta S} \qquad (3.2.3.2)$$

where ρ is the **resistivity** of the conductor, measured in $\Omega \cdot m$ in the SI, and depends on the nature of the material from which it is made, as well as the environmental conditions. The inverse of resistivity is called **electrical conductivity** (σ), and is measured *in* $\Omega^{-1}\, m^{-1}$ in the SI. Therefore,

$$\sigma = \frac{1}{\rho} = \frac{\Delta l}{R \cdot \Delta S} \qquad (3.2.3.3)$$

From the macroscopic form of the Ohm's law, we can deduce **its microscopic (local) form.** Let us consider an infinitesimal length of conductor $\boldsymbol{dl}$ with a corresponding resistance $\boldsymbol{dR}$, across which a differential potential $\boldsymbol{dU}$ appears. The relation (3.2.3.1) can be written as:

$$\boldsymbol{I = -\frac{dU}{dR} = -\frac{dU}{\frac{\rho \cdot dl}{S}} = -\sigma \cdot S \cdot \frac{dU}{dl} = \sigma SE} \qquad (3.2.3.4)$$

Marking the current density with $\boldsymbol{j = \frac{I}{S}}$, it immediately results that:

$$\boldsymbol{j = \sigma \cdot E} \qquad (3.2.3.5)$$

Taking into account that, within a homogenous and isotropic conductor, the current density at a given point is a vector having the same direction and orientation as the electric field intensity vector at that point, **the local (vectorial) form of Ohm's law can be written as**:

$$\boldsymbol{\vec{j} = \sigma \vec{E}} \qquad (3.2.3.6)$$

3.3 The Electric Energy and Power

3.3.1 The Effects of Electric Power

Thanks to its multiple applications, the effects of electric power are familiar to us from everyday life. **The thermal, electrochemical and magnetic effects of electric power** originate from the same cause: the electric field. The electric field transmits the energy generated by the source to the consumers, through the conductive pathways. Upon reaching the consumers, the energy is transformed, depending the case, into:

- mechanical work;
- thermal energy;
- chemical energy.

3.3.2 The Energy Dissipated to the Consumer

Let there be a circuit formed by a source with an electromotive tension $\boldsymbol{E}$, an internal resistance $\boldsymbol{r}$, and a consumer $\boldsymbol{X}$ with resistance $\boldsymbol{R}$ (Figure 3.3.2.1).

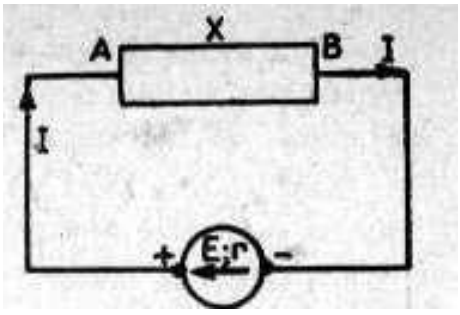

Figure 3.3.2.1 The energy dissipated to the consumer.

The terminal $\boldsymbol{A}$ of the consumer, connected to the positive terminal of the source, is at a higher electric potential than terminal $\boldsymbol{B}$. Therefore, the electric field generated by the source determines the charge carriers to move in an ordered manner through the consumer $\boldsymbol{X}$, which has the resistance $\boldsymbol{R}$.

Let $\boldsymbol{q}$ be the electric charge of the carriers passing through the consumer.

$$\boldsymbol{W = U \cdot q} \qquad (3.3.2.1)$$

or

The mechanical work carried out to maintain the constant-velocity motion of these carriers is given by $\boldsymbol{L = U \cdot q}$, where $\boldsymbol{U}$ is the voltage drop across the consumer. The energy required to perform this mechanical work is provided by the electric field.

The law of energy conservation shows that this electric power is transformed within the consumer into another form of energy, depending on the nature of the consumer. If the consumer is an electric motor, the received energy is converted into mechanical work, and if it is a heating device, the received energy is converted into thermal energy.

The energy $\boldsymbol{W}$ transformed by the consumer during the time interval of time $\boldsymbol{t}$ is:

$$W = U \cdot I \cdot t \qquad (3.3.2.2)$$

taking into account that $q = I \cdot t$.

Observation. Formulas (3.3.2.1) and (3.3.2.2) apply to the transformation of electric power into any other form of energy.

The unit of measurement in the SI for the energy resulting from these transformations is the **joule**, symbol J.

In practice, **kilowatt-hour (kWh)** is also used $1\ kWh = 3.6 \cdot 10^6\ J$.

3.3.3 The Power Dissipated to the Consumer

It is known that the energy developed per unit of time is called **power**. Therefore:

$$P = \frac{W}{t} \qquad (3.3.3.1)$$

In the case of electric circuits, the energy developed per unit of time at the terminals of a consumer is also called **electric power**. From (3.3.3.1) and (3.3.3.1), we deduce that:

$$P = U \cdot I \qquad (3.3.3.2)$$

For an entire circuit, the power developed by the source (generator) is:

$$P = E \cdot I \qquad (3.3.3.3)$$

Observation. Formulas (3.3.3.2) and (3.3.3.3) apply to the transformation of the electric power into any other form of power.

The unit of measurement in the SI for the power resulting from these transformations is a **watt** ($1\ watt = \frac{1\ \text{joule}}{1\ \text{s}}$), and its symbol is W.

In practice, the **kilowatt (kW)** is also used: $1kW = 10^3 W$.

3.3.4 Joule's Law

If the consumer is a resistor with resistance R, from formula (3.3.2.2) and Ohm's law (3.2.1.1), we deduce the following expression:

$$W = R \cdot I^2 \cdot t \qquad (3.3.4.1)$$

or:

$$\boldsymbol{W = \frac{U^2}{R} \cdot t} \qquad (3.3.4.2)$$

Taking into account that the electric energy is dissipated as heat by the consumer with resistance **R**, meaning $\boldsymbol{W = Q}$, formulas (3.3.3.1) and (3.3.3.2) become:

$$\boldsymbol{Q = R \cdot I^2 \cdot t} \qquad (3.3.4.3)$$

and respectively:

$$\boldsymbol{Q = \frac{U^2}{R} \cdot t} \qquad (3.3.4.4)$$

Formulas (3.3.3.1) and (3.3.3.2) are known as Joule's law and represent the phenomenon in its macroscopic form.

Taking into account that $\boldsymbol{P = \frac{W}{t}}$, the electric power dissipated as heat by a consumer with resistance $\boldsymbol{R}$ can be immediately derived from (3.3.3.1) as:

$$\boldsymbol{P = R \cdot I^2} \qquad (3.3.4.5)$$

or from (3.3.3.2) as:

$$\boldsymbol{P = \frac{U^2}{R}} \qquad (3.3.4.6)$$

For an entire circuit with total resistance $\boldsymbol{R + r}$, the total power dissipated as heat is:

$$\boldsymbol{P = (R + r) \cdot I^2} \qquad (3.3.4.7)$$

Observation. Formulas (3.3.3.1), (3.3.3.2), (3.3.3.3), (3.3.3.4), (3.3.3.5), (3.3.3.6) and (3.3.3.7) apply only at the transformation of the electric power into thermal energy. This transformation occurs only when there is a consumer with resistance $\boldsymbol{R \neq 0}$ present in the circuit (i.e., a **resistive consumer**).

The explanation of the dissipation phenomenon of the electric power as heat by a consumer with resistance $\boldsymbol{R}$ is as follows**:**

When passing through the input terminal of the consumer, the charge carriers possess not only potential energy but also kinetic energy, corresponding to their average drift velocity. This drift velocity remains unchanged at the output terminal of the consumer. The potential energy that the charge carriers lose inside the consumer is not transformed into kinetic transport energy of the charge carriers, but rather into vibrational kinetic energy of the crystalline lattice of the consumer. This leads to an increase in the internal energy of the lattice, and consequently, to the heating and rise in temperature of the lattice – and, implicitly, of the consumer itself. **The irreversible thermodynamic** phenomenon that occurs is known as the **Joule effect**.

The Joule's law regarding the thermal energy produced by an electric current, known as the **Joule effect**, is a physical law that describes the relationship between the heat generated and the current passing through a conductor. As a result of **James Prescott Joule**'s studies of this phenomenon in the years following 1840, the law was named in his honor. The law is expressed by formula (3.3.3.3):

$$\boldsymbol{Q = R \cdot I^2 \cdot t} \qquad (3.3.4.8)$$

or the formula (3.3.3.4):

$$\boldsymbol{Q = \frac{U^2}{R} \cdot t} \qquad (3.3.4.9)$$

where:

$\boldsymbol{Q}$ – the heat generated by the current passing through the ohmic conductor;

$\boldsymbol{I}$ – the constant current flowing through the conductor;

R – the electric resistance of the conductor;

t – the time interval during which the current flows through the conductor.

As previously mentioned, if the current intensity, the resistance of the conductor, and the time duration are expressed respectively in amperes (**A**), ohms (**Ω**) *and seconds* (**s**), *the unit of the generated heat is the joule* (**J**).

Before the introduction of the International System of Units (SI), a unit used for measuring heat was the small calorie ($1\,cal = 4.184\,J$), along with its multiple, the large Calorie ($1\,Cal = 1\,kcal = 4.184\,kJ$).

Joule's law is sometimes referred to as the **Joule-Lenz law**, because, in 1842**, Heinrich Lenz** independently discovered the same principle.

The heating effect of the conductors traversed by electric currents is commonly known as **Joule heating.**

3.3.5 Biographical Note – James Prescott Joule

Figure 3.3.5.1 James Prescott Joule (1818-1889).

James Prescott Joule (24th December 1818 – 11th October 1889) was an English brewer and self-taught physicist. He became renowned for a famous experiment designed to determine the mechanical equivalent of the calorie, which he conducted in 1842. Through this experience, Joule confirmed the principle of conservation and transformation of energy.

Figure 3.3.5.2 The apparatus used by Joule to determine the mechanical equivalent of the calorie.

In 1841, he formulated the law of energy transformation in conductors, according to which the energy dissipated as heat during the passage of the electric current through a conductor is proportional to the resistance of the conductor, the square of the current intensity, and the time interval during which the current flows, expressed as: $\boldsymbol{W = R \cdot I^2 \cdot t}$. This law is known as the **Joule's law**.

He is the discoverer of the magnetostriction effect, which he explained in 1847.

James Prescott Joule also made an important contribution in the molecular physics, being the first to establish that the internal energy of a gas depends on its temperature, and he calculated the molecular velocity of a gas.

In 1852, together with William Thomson, he observed the cooling of a gas that expands without performing mechanical work, a phenomenon known as Joule-Thomson effect. Thanks to his significant role in physics, the unit of energy in the International System of Units was named **joule** in his honor.

3.3.6 Biographical Note – Heinrich Friedrich Emil Lenz

Figure 3.3.6.1 Heinrich Friedrich Emil Lenz (1804-1865).

Heinrich Friedrich Emil Lenz (12th February 1804, Dorpat – 10th February 1865, Rome) was a Baltic German physicist from the Russian Empire. He is well known for the law of electrodynamics that bears his name (Lenz's Law), established in 1833. Lenz was born in the city of Dorpat (nowadays, Tartu), in the Livonian Governorate of the Russian Empire. After completing his secondary education in 1820, he studied chemistry and physics at the Dorpat University. He travelled with the navigator Otto von Kotzebue on his third expedition around the world (1823-1826). During this journey, Lenz studied climatic conditions and the physical properties of seawater. The results were published in "*The Memoirs of the Science Academy in Sankt Petersburg*" (1831).

After this trip, Lenz began working at the University of Sankt-Petersburg, Russia, where he later became Dean of the Faculty of Mathematics and Physics (1840-1863), and subsequently served as Rector from 1863 until his death in 1865. Lenz also taught at the Petrischule (1830-1831) and at the Mikhaylovskaya Artillery Academy.

Lenz began studying electromagnetism in 1831. In addition to the law that bears his name (Lenz's law), independently discovered Joule's law in 1842. In recognition of his contributions to this field, Joule's law is also referred to as the Joule-Lenz law. Lenz was involved since the beginning in the development of galvanic coatings, invented by his friend

and colleague, Moritz von Jacobi.

In 1839, Lenz produced several medallions using electroplating. Along with the bas-relief created by Jacobi in the same year, these were among the first sculptures made through galvanoplasty.

Heinrich Lenz died in 1865 in Rome, Italy, after suffering a stroke.

3.3.7 The Microscopic (Local) Form of Joule's Law

The mechanical work performed by the Coulomb electric field for the displacement to move an electric charge $\boldsymbol{q}$ between two points, between which there is a potential difference (voltage) $\boldsymbol{U}$, is given by the formula $\boldsymbol{L = U \cdot q}$. Given that $\boldsymbol{q = I \cdot t}$ and considering Ohm's law (3.2.1.1), it follows:

$$\boldsymbol{L = U \cdot q = U \cdot I \cdot t = I^2 \cdot R \cdot t}$$

This mechanical work $\boldsymbol{L}$ is transformed into kinetic energy of all the charge carriers. As these carriers move through the conductor, they encounter resistance, which determinates their kinetic energy to be converted into heat. Therefore, the macroscopic form of Joule's law (3.3.3.3) shows that when a continuous current of intensity $\boldsymbol{I}$ passes through a conductor with resistance $\boldsymbol{R}$, over a time interval $\boldsymbol{t}$, heat is released.

$$\boldsymbol{Q = R \cdot I^2 \cdot t}$$

We further use the notations from Figure 3.2.4.1..

To derive the microscopic form of the Joule's law, we define the thermal energy density $\boldsymbol{w}$ as the quantity of heat emitted per unit volume per unit time:

$$\boldsymbol{w = \frac{Q}{\Delta S \cdot \Delta l \cdot t}} \qquad (3.3.7.1)$$

Using the notations from Figure 3.2.4.1 and taking into account that $\boldsymbol{Q = R \cdot I^2 \cdot t}$ and $\boldsymbol{R = \rho \cdot \frac{\Delta l}{\Delta S}}$, formula (3.3.7.1) becomes**:**

$$\boldsymbol{w = \frac{\rho \cdot \frac{\Delta l}{\Delta S} \cdot I^2 \cdot t}{\Delta S \cdot \Delta l \cdot t} = \rho \cdot \frac{I^2}{\Delta S^2} = \frac{j^2}{\sigma}} \qquad (3.3.7.2)$$

Given that $\boldsymbol{j = \sigma \cdot \mathbf{E}}$, according to the formula (3.2.3.5), we obtain:

$$\boldsymbol{w = \rho \cdot E^2} \qquad (3.3.7.3)$$

We observe that, in the microscopic form of both Ohm's law (3.2.3.5) and Joule's law (3.3.7.3) the conductivity $\boldsymbol{\sigma}$ and the electric field intensity $\boldsymbol{E}$ appear in the right-hand side of the equations.

3.3.8 The Relationship Between Joule's Law and Ohm's Law

Joule's law and Ohm's law were discovered independently, through experimental methods, before the concepts of energy conservation and electric potential were well fully developed.

In the case of resistive circuits, taking into account the principles of energy conservation and electric potential, Joule's law and Ohm's law are equivalent and can be derived from one another, as demonstrated by James Clerk Maxwell, Éleuthère Élie N. Mascart, and Oliver Heaviside.

3.3.9 The Consequences of Joule's Law

In the case of electrical circuits, the consequences of the Joule's law can be either favorable or unfavorable. The former are the subject of practical applications, while the latter require specific measures to limit their effects.

3.3.9.1 Practical applications of the Joule's Law

The Joule effect – namely, the heating of conductors through which electric current flows – has numerous practical

applications. Below, we present some of the most common uses of this phenomenon.

Incandescent light bulbs

Objects that are intensely heated become incandescent, radiating both light and heat. Metallic conductors through which electric current flows can also become incandescent due to the Joule effect, thus emitting light and heat. This phenomenon forms the basis for the manufacturing of incandescent light bulbs, commonly known as electric bulbs.

The filaments of these bulbs are made from metals with very high melting points (over 2800°C), such as tungsten (wolfram), osmium, or tantalum. The glass envelope containing the filament is either vacuum-sealed or filled with an inert gas at low pressure. To improve the efficiency and durability of the bulb, the filament is executed from very thin metallic wires (hundredths of a millimeter in diameter), arranged in a spiral or double-spiral shape.

Electric Heating Apparatuses

Electric heating devices come in various forms and serve multiple purposes, including radiators, heaters, irons, soldering irons, and more. The heat source in these devices is a resistor made of a material with high resistivity, which heats up when an electric current passes through it. Since household heating appliances typically operate at temperatures below 1000^{o}C, their resistors are often made from chrome-nickel alloy wires.

In the technical and industrial applications, electrical heating equipment capable of reaching higher temperatures are required. For this purpose, resistors made from molybdenum, resistant up to 2100°C, or from tungsten (wolfram), capable of withstanding temperatures around 2800°C, are used.

Electric Ovens with Resistance

In technical and industrial applications, resistance ovens are used for heating or melting certain components. These ovens are employed in metallurgy for the quenching of iron parts, and in the glass industry for melting glass. The required heat is generated by the thermal effect produced as electric power flows through the resistors that surround the crucible made of refractory material, which contains the product intended for heating or melting.

3.3.9.2 Measures to limit the adverse consequences of the Joule's Law

The formula (3.3.3.3) shows that when a continuous current of intensity $\boldsymbol{I}$ and voltage $\boldsymbol{U}$ passes through a conductor with resistance $\boldsymbol{R}$ over a time interval $\boldsymbol{t}$, heat is emitted:

$$\boldsymbol{Q = R \cdot I^2 \cdot t}$$

The emitted heat is directly proportional with:

(i) the square ($\boldsymbol{I^2}$) of the current intensity;
(ii) the resistance ($\boldsymbol{R}$) of the conductor;
(iii) the time interval ($\boldsymbol{t}$) during which the current flows.

If it doesn't represent a wanted consequence (a practical application), the emitted heat can be reduced through:

- the shrinkage of the intensity of the current to a value that doesn't jeopardize the functioning of the electrical installations and the consumers;
- the shrinkage of the resistance through the execution of the conductors from metals with low resistivity (such as copper or aluminum), through the augmentation of the area of the cross-sectional area of the conductors, and through the limitation of the length of the conductors, considering that the resistance of a

conductor is given by the formula:

$$\boldsymbol{R = \rho \cdot \frac{l}{S}}$$

where:

$\boldsymbol{R}$ is the resistance of the conductor;

$\boldsymbol{\rho}$ is the resistivity of the conductor's material;

$\boldsymbol{l}$ is the length of the conductor;

$\boldsymbol{S}$ is the area of the cross-sectional area of the conductor

- the shrinkage of the time interval $\boldsymbol{t}$ in which the current flows, within acceptable operating limits.

4 Welding, Splinting, Syncrystallization

4.1 Considerations Regarding Welding

4.1.1 Introduction

Welding is a fabrication sculpting process in which materials – usually metals or thermoplastics – are joined together by causing their interpenetration. In terms of assembly, welding creates a non-removable connection.

Sculpting through welding (related to the visual arts and artworks) is a form of art in which sculptures are created using welding techniques. Welding has been increasingly in sculpture after 1930, as new industrial procedures, such as electric arc welding, were adapted for aesthetic purposes. Welding techniques, including numerically controlled cutting, can be used both to cut and fuse metal. Sculpting through welding is sometimes considered a special domain.

Figure 4.1.1.1 Human – sculpture by Alexander Calder (1898-1976), created for Expo 67 on Saint Helen's Island, Jean-Drapeau Park, Montreal, Quebec.

Oftentimes, welding is performed by melting the parts to be joined and adding a filler material to form a molten pool (called the welding bath), which, upon cooling, becomes a non-removable bond. Sometimes, welding is performed solely with pressure, or by combining pressure with heat. Usually, the term welding bath refers to the active area of the welding process, roughly the size of a 10 bani coin, where the base metal has reached the melting point and is ready, if it is the case, to receive the filler material. The welding bath is essential for the success of the

welding process. After Edmund Davy discovered acetylene in 1836, in 1903, Fouché and Picard observed the welding bath for the first time during welding with the oxy-gas flame.

The welding bath must be moved steadily along the weld, maintaining a constant width and depth. The movement used to displace the welding bath has a direct effect on the quality of the weld bead. A weld that is created by forming and moving the welding, without the use of any filler material, is called autogenous welding.

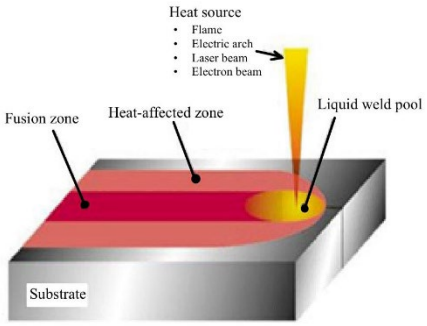

Figure 4.1.1.2 The welding bath.

Multiple different sources of energy can be used for welding, including a gas flames, electric arcs, lasers, electron beams, friction, and ultrasounds. Many times, as an industrial process, welding often be performed in various environments such as outdoors, underwater, or even in outer space. Regardless of the environment, welding can be dangerous, and therefore, safety measures must be taken to prevent burns, electric shocks, eye injuries, exposure to toxic fumes, and overexposure to ultraviolet radiation.

Until the end of the 19th century, welding processes were limited to forge welding – the method blacksmiths had used for centuries to weld iron and steel by heating and hammering.

Figure 4.1.1.3 Ornament created using forge welding.

Arc welding and oxy-gas flame welding were the techniques that developed

toward the end of the 19th century, with resistance welding emerging shortly thereafter.

Welding technology advanced rapidly at the beginning of the 20th century, with the First and Second World Wars accelerating the demand for reliable and cost-effective assembly methods. After the two world wars, several modern welding techniques were developed, including manual methods such as arc welding with a covered metal electrode, one of the most widespread welding methods today, and semiautomatic and automatic processes, such as arc welding with metallic electrode in a protective gas atmosphere, submerged arc welding (under flux), flux-cored arc welding with a consumable tubular electrode and electroslag welding. In the second half of the 20th century, innovation continued with the development of laser beam welding and electron beam welding.

The development of welding procedures continues nowadays. The welding robot is becoming an increasingly common feature in industrial processes, while researchers are actively working to develop new techniques and deepen understanding of welding.

4.1.2 Incursion in the History of Welding

The history of metal fusion through welding dates back several millennia. The earliest known examples are instances of forge welding from the Bronze Age and Iron Age, in regions such as the Middle East and Europe.

The ancient Greek historian Herodotus affirms in his *Histories* (5th century BC) that Glaucus from Chios "was the man that invented by himself the welding of iron".

Forge welding was used in the construction of the famous Iron Pillar of Delhi, India – built around 310 BC – which weighs approximately 6 tons.

Figure 4.1.2.1 The Iron Pillar of Delhi.

The Iron Pillar of Delhi (India) 7-meter-high column located within the Qutb complex, notable for the unique composition of the metal used in its construction.

The pillar, which weighs approximately 6t, is believed to have been erected during the reign of Emperor Chandragupta Vikramaditya (375-413 AD), although some historians argue that it may date as far back as 912 BC. Originally, the pillar stood at the center of a Jain temple complex consisting of twenty-seven temples. The complex was later destroyed by the Sultan Qutb-ud-din Aibak (1206-1210), and the materials from the temples were repurposed for the construction of the Qutub Minar and the Quwwat-ul-Islam Mosque.

Today, the pillar and the ruins of the surrounding temples are located within the Qutb complex. The pillar was made of forged iron with a purity of 98%, serving as a testament to the craftsmanship of ancient Indian blacksmiths. Due to its remarkable resistance to corrosion despite being exposed to the elements for over 1,600 years, the pillar has attracted significant interest from both archeologists and metallurgists.

The name of the city Delhi itself is said to be linked to a legend surrounding the tower. The Middle Ages brought progress in welding through forging, during which blacksmiths repeatedly struck heated metal with hammers until a weld was achieved. In 1540, Vannoccio Biringuccio published the work „*The Pirotechnia*", which included descriptions of the forging procedure.

„The Pirotechnia" is considered the first printed book on metallurgy published in Europe. It was written in Italian and printed in Venice in 1540, its author being Vannoccio Biringuccio, a citizen of the Italian city of Siena. In the 20th century, the chemist Cyril Stanley Smith, an important figure in Manhattan Project, and Martha Teach Gnudi translated the book in English and enriched the text with extensive annotations and footnotes. The work is illustrated with numerous reproductions after engravings.

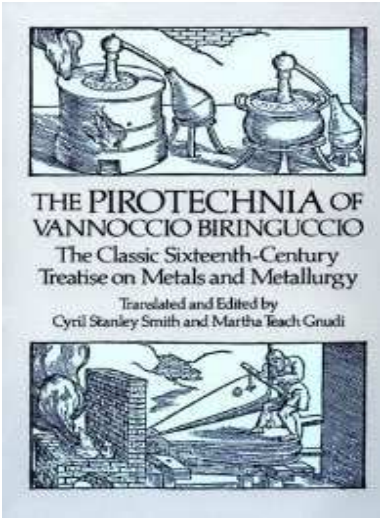
THE PIROTECHNIA OF
VANNOCCIO BIRINGUCCIO
The Classic Sixteenth-Century
Treatise on Metals and Metallurgy
Translated and Edited by
Cyril Stanley Smith and Martha Teach Gnudi

Figure 4.1.2.2 Cover of „The Pirotechnia" by Vannoccio Biringuccio.

The Renaissance handymen were skilled in the use of this procedure, and the industry, existing in an incipient form in that era, continued to develop over the following centuries. In 1802, the British scientist Sir Humphry Davy experimentally produced the electric arc by passing an electric current through two carbon rods, which initially touched at their tips and were then drawn slightly apart. Davy was the one who introduced and established the term ***electric arc***.

Figure 4.1.2.3 Vasili Petrov (19 July 1761-1834).

Figure 4.1.2.4 Humphry Davy (17 December 1778 – 29 May 1829).

Figure 4.1.2.5 The electric arc.

The closing and opening of the contacts in an electric circuit are always associated with the appearance of an electric arc between the contacts. Due to the fact that the closing speed of the contacts is higher than the speed of their opening, the thermal effect of the closing arc is smaller than that of the opening arc. The electric arc can be considered an extremely mobile conductor, whose movement is influenced by air currents and the electromagnetic field. High temperatures are present both in the arc column and at the points where the arc touches the contacts. The electric arc causes corrosion to the contacts on which it is supported.

The formation process of the electric arc during the opening of contacts develops as follows. At the moment when the two contacts separate, the thin layer of air between them is traversed by the electric current. As a result of the current passing through this gap, a very high temperature arises, giving birth to a blue flicker with a strong glow, namely, a spark. If the interrupted power is low, this breakdown of the thin air layer remains a spark. However, if the interrupted power has a significant value, the breakdown evolves into an electric arc within an interval of approximately $10^{-9}\,s$. It is important to note the corrosion of the contacts at the arc support points and the volatilization of the contact material, which is then

dispersed into the space between the contacts. The volatile nature of the contact materials greatly contributes to the formation of the electric arc.

The generated heat (according to Joule's law: $\boldsymbol{Q = R \cdot I^2 \cdot t}$) concentrates in a very small volume of material, formed at the tips of the cones where contact occurs. These cone tips are heated to very high temperatures and, eventually vaporize in an explosive manner, forming a high conductibility plasma. It is considered that the arc forms following the explosion of the contact bridges, between their remaining fragments. After the disappearance of the connection between the last elementary surfaces of the contacts, the cone tips are already heated at a temperature at which thermoelectric emissions begins. The arc appears when the voltage gradient between the contacts reaches $10^7\ V/cm$, a value at which electron auto-emission is initiated.

The electric arc is a flux of electrons and ions that contains, at its core, a very high temperature. The most intensely luminous region of the electric arc is actually its core, which exhibits the highest electric conductibility, with nearly 100% of the current passing through it. The core is surrounded by a thicker, less luminous layer called the aureole, whose properties vary due to the high temperature and the initial environment in which the arc was produced. The aureole consists of a relatively hot and luminous gas, but with a low conductibility due to its lower temperature.

The opening electric arc is an autonomous electric discharge in gas, characterized by a high current density ($10^3 \div 10^8\ A/cm^2$), high temperatures ($6000 \div 10000^{\circ}C$), elevated gas pressure, and a low breakdown voltage (with a small gradient in the arc core of approximately $10 \div 20\ V/cm$).

The main characteristic of the gas discharge lies in the fact

that, within the discharge zone, the gas – which is generally an insulator – becomes an electrical conductor. The conductivity of the gas is determined by the density of the free charge carriers and their velocity toward the two electrodes, and it varies depending on the gas density, temperature, the nature of the surrounding environment, and the intensity of the electric field.

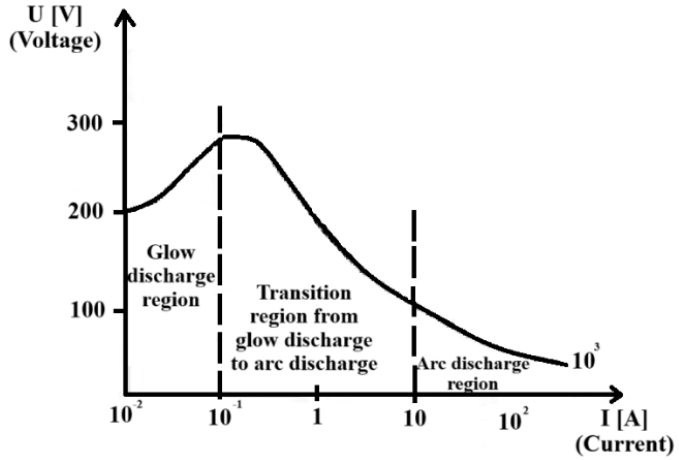

Figure 4.1.2.6 The dependency between voltage and current in gas discharges.

The figure above presents the dependency between voltage and current in gas discharges. On this curve, the electric arc occupies the place in the right extreme, characterized by a low cathode voltage drop ($10 \div 20\ V$) and a high current density ($10\ to\ 10^5\ A/cm^2$). In order to generate an arc discharge between electrodes (contacts), two conditions must be met: the voltage drop across the arc U must be greater than or equal to the cathode voltage drop, i.e., $U \geq 10 \div 20\ V$, and the circuit current must exceed $80 \div 100\ mA$. The voltage drops near the electrodes are concentrated over extremely short segments of the arc's length (approximately $10^{-4}\ cm$).

The electric arc, which is a flux of particles charged with electricity, is formed, developed and sustained through ionization processes, namely: ionization by collision,

autoelectric or thermoelectric emission, and thermal ionization.

The ionization process within the arc's core (spine) is mostly due to the high temperature of the gas; in this case, thermal ionization is fundamental and basically the only mechanism responsible for the development and maintenance of the electric arc.

The arc's spine contains equal quantities of positive and negative free charges – a state of the matter known as plasma, characterized by a high degree of gas ionization. This plasma, having a charge balance similar to that of a metal, exhibits an electrical conductivity nearly as high as that of metals. At extremely high temperatures found in the arc's core, the atoms and gas molecules attain high velocities and, therefore, high kinetic energies. Thermal ionization of gases occurs at temperatures around $8000°K$, while vaporized materials undergo ionization at approximately $4000°K$. In the formed arc, both electrons and ions (particles with opposite electrical charges) are generated as a result of high-speed collisions between molecules and electrons. The free electrons, which are always found in the space between electrodes, move rapidly toward the anode under the action of the existent electric field. Along their path, these electrons produce additional ionization by colliding with neutral particles.

In the case of the emission ionization, the emission of electrons from the surface of the cathode occurs in two ways:

- **Autoelectric emission**, which is triggered by an intense electric field in the region of the cathode, either in the initial moment after the separation of the contacts or in the final moments before the contacts close again;
- **Thermoelectric emission**, which takes place on the surface of the cathode, particularly in the area known as the cathode spot.

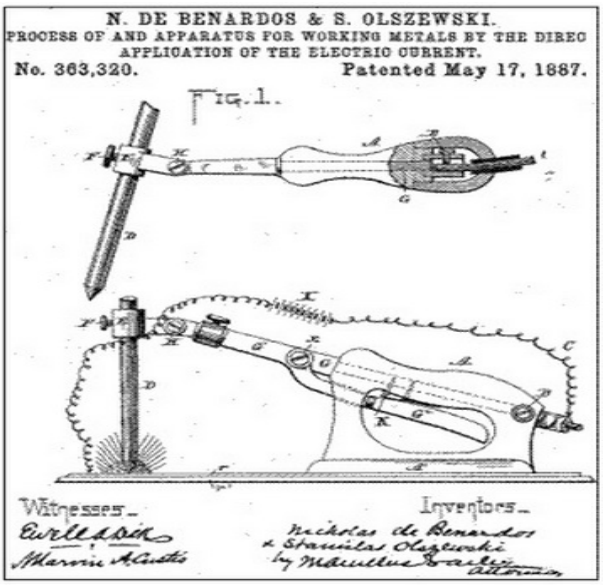

Figure 4.1.2.7 The American patent for the arc welding process called Elektogefest („Electric Hephaestus"), granted in 1887 to N. de Bernados and his sponsor S. Olszewski.

In 1881-1882, the Russian inventor Nikolai Benardos performed the first arc welding process, known as electric arc welding with a charcoal electrode. This method produces the fusion of metals by heating them with an electric arc formed between a non-consumable charcoal (graphite) electrode and the workpiece.

This was the first arc welding procedure ever used; however, it is no longer employed today, having been replaced by arc welding using a pair of charcoal (graphite) electrodes. In the charcoal electrode arc welding method, the electrode is used to generate an electric arc between itself and the metal to be fused. This arc produces temperatures exceeding 3000℃. At such temperatures, the metals melt and fuse together, forming a solid bond. Toward the end of the 19th century, progress in the field of arc welding continued with the invention of consumable (fusible) metal electrodes, by the Russian Nikolai Slavianov in 1888 and the American Charles L. Coffin in 1890.

Figure 4.1.2.8 Nikolai Slavianov.

Around 1900, A.P. Strohmenger (Great Britain) and Oscar Kjellberg (Sweden) introduced the first consumable (fusible) electrodes coated in flux, which provided a more stable electric arc. Strohmenger used a flux coating made of clay and calcium oxide to aid arc initiation, while Kjellberg dipped the electrode in mixtures of carbon and silicates to form the coating. In 1912, Strohmenger introduced an electrode with a thick flux coating, but its high cost and complex manufacturing methods prevented its widespread adoption. In 1927, the development of an extrusion process reduced the cost of flux-coated electrodes and allowed manufacturers to create more complex coating compositions. Beginning in 1950, iron powder was added to the flux composition, enabling increased welding speeds.

Figure 4.1.2.9 Charles L. Coffin.

The electric arc with a covered (in flux) consumable (fusible) metal electrode is also known as manual metal arc welding, electric welding under flux, or, more familiarly, stick welding. Thanks to the adaptable character of the process and the simplicity of the equipment and its operation, the electric arc with a flux-coated consumable metal electrode is one of the most widespread welding procedures in the world. It is a

manual arc welding process that uses a consumable electrode covered in flux to create the welding bead.

For the priming of the electric arc, the electrode is brought into contact with the workpiece, reaching the base metal easily, and then the electrode is slowly withdrawn. This maneuver initiates the arc and, in this way, leads to the melting of both the workpiece and the consumable metal electrode. As it melts, the electrode produces droplets that pass into the welding bath.

As the electrode melts, the flux coating degrades, releasing gases that create a protective shield, which protects the welding area from oxygen and other atmospheric gases. In addition, the flux produces molten slag that covers the filler material, formed by the melted drops from the electrode that entered the welding bath. The slag, which is a component of the welding bath, floats to the surface and protects it from contamination until it solidifies into the welding bead. Once hardened, the slag must be removed by chipping, revealing the finished weld bead at the surface. Because the electrode melts as the welding progresses, the welder must periodically stop the welding process to remove the remaining part of the electrode from the electrode holder and insert a new one.

This operation, along with slag removal by chipping, reduces the time during which the welder is actually forming the weld bead, making this one of the less efficient welding procedures. Generally, only about 25% of the total time required for the job is dedicated exclusively to creating the welding bead.

The welding technique used depends on the type of electrode, the composition of the workpiece, and the position in which the welding is performed. The choice of electrode and welding position determines the welding speed. Welding with overlapping joints requires at least a certain

level of skill from the welder and can be carried out using fast-melting electrodes, with the weld bead solidifying slowly. This allows for high execution speeds. Inclined, vertical, or overhead welding requires a highly skilled welder and also the use of an electrode whose molten material solidifies quickly, preventing the molten metal from leaking out of the welding bath. This generally means that the electrode melts more slowly, which increases the time required for welding.

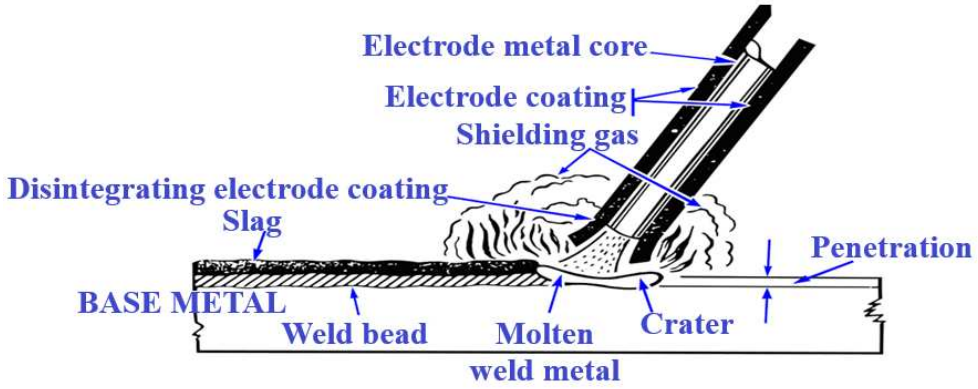

Figure 4.1.2.10 Electric arc with consumable (fusible) metal electrode covered (in flux) welding.

In 1938, K. K. Madsen described an automatic variant of electric arc welding with a flux-coated consumable metal electrode, now known as **gravitational welding**. After 1960, the procedure gained recognition due to its use in Japanese shipyards, although its applications are currently limited. Around the same time, George Hafergut (Austria) developed a lesser-known variant of the process, referred to as **Elinhafergut welding**.

The method of electric arc welding with a flux-coated consumable metal electrode remains predominant among other welding procedures used in maintenance, operation, and repair domains. Although flux-cored arc welding with tubular wire has been gaining ground, the former continues to be widely applied in the

construction of steel structures and in industrial manufacturing. Primarily, the process is used for welding steels (including stainless steels), but also for welding aluminum, nickel, and copper alloys.

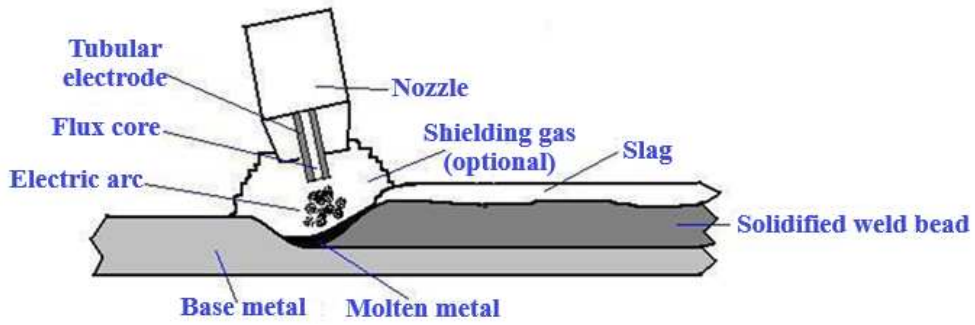

Figure 4.1.2.11 Electric arc with tubular wire filled with flux welding.

In 1905, the Russian scientist Vladimir Mitkevici proposed the usage of three-phase current for arc welding. In 1919, C. J. Holslag invented welding with alternating current, but this did not become widespread until a decade later.

Electric welding through contact resistance was developed in the final decades of the 19th century, the first invention patent act being obtained by Elihu Thomson in 1885, which led to subsequent developments over the following 15 years.

Figure 4.1.2.12 Elihu Thomson (29th of March 1853 - 13th of March 1937).

Electric welding through contact resistance refers to a group of welding procedures, such as spot welding and seam welding, which achieve fusion (assembly) on superimposed surfaces. The heat required for welding is generated by the

electrical resistance of the materials and the contact resistances between the surfaces, while force is applied to maintain the components in welding position and ensure tight contact throughout the welding process. The factors that determine the required heat and, implicitly, the welding temperature include the dimensions of the parts, the presence or absence of surface coatings, the materials from which the electrodes are made, the geometry of the electrodes, the pressure exerted by the electrodes, the welding current, and the duration of the welding process. Small molten metal baths, or nuclei, form at the points of highest electrical resistance (i.e., at the contact points), as a high-intensity current (ranging from 100 to 100,000 A) passes through the metal. In general, contact resistance welding procedures are efficient and produce low levels of pollution; however, their applications are limited to relatively small components, and the cost of welding equipment can be high. Nevertheless, in the context of mass production, depending on demand and manufacturing speed, the cost per weld can be relatively low.

Electric welding through contact resistance is a widely used technology for assembling sheet metal and metal components. Welding is achieved by passing a strong current through the fusion interface of the parts, which heats and ultimately melts the metals at a specific point (or multiple predetermined points), established through the design of the electrodes and/or the components to be welded. A constant force is applied before, during, and after the current passes, to maintain contact between the welding surfaces and, in certain applications, to forge the welded components.

Depending on the shape of the parts and the configuration of the electrodes, welding through contact resistance procedures can be classified as follows:

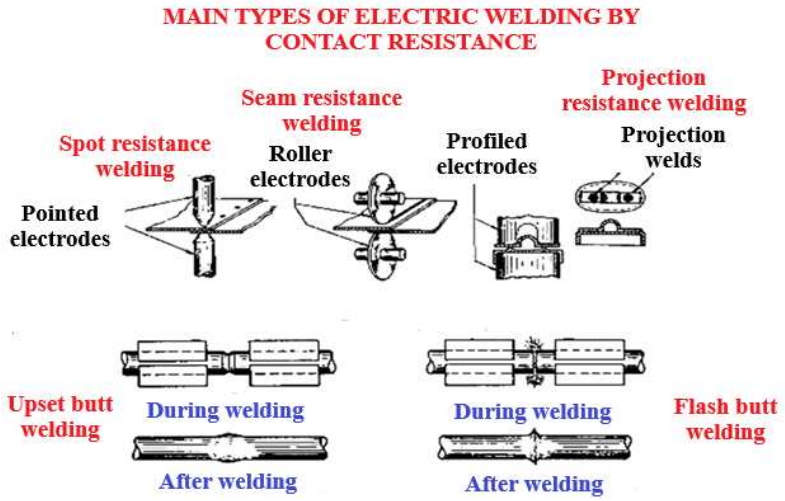

Figure 4.1.2.13 Classification of electric resistance welding.

Spot welding is a type of electric welding through contact resistance, used for the fusion of metal sheets through the direct application of opposing forces exerted by electrodes with pointed tips.

The path of the current and the heat generation are localized by the shape of the electrodes. Typically, the size of the welding nucleus formed between the sheets is determined by the contact area at the tip of the electrode.

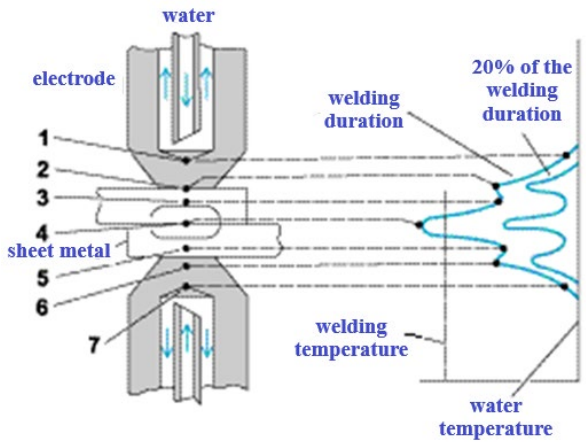

Figure 4.1.2.14 Temperature distribution during spot welding using water-cooled electrodes.

Electric spot welding is an assembly process used predominantly in the automotive industry for welding car bodies and large-scale structural components. It is also widely used in the production of apparatuses and household equipment, among other applications.

Figure 4.1.2.15 Industrial robots performing electric spot welding on automobile bodies along the production line.

Figure 4.1.2.16 Intraoral spot resistance welding – dental prosthetics (orthodontics).

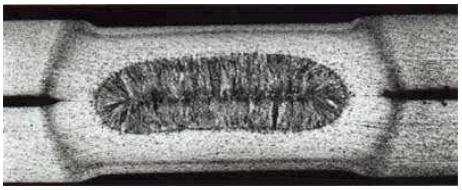

Figure 4.1.2.17 Cross-sectional detail of a spot resistance weld.

Figure 4.1.2.18 Spot resistance welding machine.

The aluminothermic welding was invented in 1893, and around the same time, another procedure was developed: oxy-gas flame welding. Acetylene was discovered in 1836 by Edmund Davy, but it was not used in practice until around 1900, when it became feasible with the invention of a suitable welding torch. Initially, oxy-gas

flame welding was one of the most widespread welding methods, due to the portability of the equipment and the relatively low costs involved. However, over time, this procedure fell into disuse in industrial applications. It was largely replaced by electric arc welding, in which the flux-coated consumable metal electrode stabilizes the arc and protects the base material from contamination, a process that has continued to evolve and improve.

The First World War led to the large-scale adoption of welding techniques, as various military powers sought to identify and apply the most efficient welding procedures. The British were the first to utilize electric arc welding extensively, even constructing a ship, the Fullagar, with a fully welded hull. During the same period, electric arc welding was also applied to the aviation industry, with some German aircraft fuselages being built using this technique.

Worthy of mention is the first road bridge in the world constructed through welding, designed by Stefan Bryła at the Warsaw University of Technology in 1927 and built in 1929 over the Słudwia River near Maurzyce, close to Łowicz, Poland. Between 1920 and 1930, significant progress was made in the field of welding technology. In 1920, automatic welding was introduced, involving the continuous feeding of a wire electrode. The concept of protective gas, which creates a controlled atmosphere in the welding zone, became a highly discussed topic, as it aimed to shield the weld from the damaging effects of oxygen and nitrogen present in the atmosphere. Porosity and brittleness of the weld seam were major challenges, leading to the adoption of hydrogen, argon, and helium to maintain controlled atmospheres during welding.

In the next decade, new developments allowed the welding of metals which react violently to oxidation, such as

aluminum and magnesium. This aspect, alongside the evolution of automatic welding and the use of alternating current and fluxes, led to a major development of electric arc welding between 1930 and 1940, and later during the Second World War. In 1930, the welding of bolts, studs, and nuts emerged, a procedure which has recently become widely used in the fields of naval construction and civil engineering. Electric arc welding under a flux layer also appeared in the same year and continues to be widely used to this day.

In 1932, a Russian, Konstantin Hrenov, successfully experimented with underwater electric arc welding. Eventually, after decades of development, electric arc welding in a protective gas environment using a wolfram non-consumable electrode was finalized in 1941, and electric arc welding in a protective gas environment using a metallic electrode followed in 1940, allowing the rapid welding of non-ferrous materials, though requiring expensive protective gases. Electric arc welding with a covered metal electrode was developed in the years following 1950, using a consumable electrode coated in a flux layer, and has quickly become the most widespread electric arc welding procedure. In 1957, an electric arc welding process using a metallic consumable tubular electrode containing flux made its debut. The flux generates a protective environment in the welding area, and the tubular wire electrode allows the use of automatic equipment, which results in high welding speeds. In the same year, plasma jet welding also emerged.

Electric arc welding under a cinder layer appeared in 1950 and was followed by a similar procedure, electric arc welding in a protective gas atmosphere, in 1961. In 1953, a Soviet scientist, N.F. Kazakov, proposed welding through diffusion. Other recent developments include, in 1958,

welding with an electron beam, which makes it possible to realize the welding cordon in a narrow and deep interstitium due to the concentrated heat source. The laser was invented in 1960, and laser beam welding had its debut a couple of decades later, proving to be particularly useful for automatic high-speed welding. In 1991, friction welding with an active rotating element was invented in Great Britain and found high-quality applications worldwide. All these three new procedures remain relatively expensive due to the high cost of the required equipment, which has limited their broader application.

4.2 Fundamental Notions

4.2.1 The Non-Removable Assembly

Non-removable assemblies are those in which the disassembly of the components requires the partial or total destruction of the assembly element or of one or more parts composing the assembly.

The procedures for achieving non-removable fixed assemblies can be classified into two categories:

- procedures in which the assembly is achieved without an assembly element;
- procedures in which the assembly is achieved with the aid of an assembly element.

The first group includes press-fit assembly procedures, while the second group includes procedures such as clinching, welding, and gluing.

4.2.2 Assembly Through Welding

Welding represents the technological process through which a non-removable assembly (fusion) between two or more components is achieved.

Contemporary welding procedures allow the non-removable assembly of a wide variety of materials, including complex alloys or materials with special properties.

Welding technologies are economical, efficient, and can significantly reduce the weight of metallic or non-metallic structures (depending on the case), while still ensuring the required reliability and strength. The welded fusion of an assembly refers to the area comprising the weld and its adjacent zones. Regardless of the welding method applied in executing the welded joints, the process must ensure both the required strength of the structure and the material continuity. In fusion welding

procedures, the welded joint is generally formed by added metal deposited in the groove, meaning in the space defined by the edges of the parts to be joined. In pressure welding procedures, the joint results from the interpenetration of the materials of the two components, either in the plastic state or in superficial molten areas.

The shapes and dimensions of the backlashes are very important for achieving high-quality welded joints; therefore, for the most commonly used industrial procedures, these backlashes are standardized. In general, the welded joint is named after the welding method, which determines the shape of the weld. When establishing the shape of the backlash, several factors are considered: the thickness and quality of the sheet material, as well as the heat input per unit of time associated with the welding procedure applied. In mechanical or automatic procedures, the weld is formed predominantly from the base metal, and in many cases—especially with thin or medium-thickness sheets—no filler metal is used. In this way, besides obtaining a more homogeneous weld in relation to the base material, several other advantages arise:

- reduced machining volume of the welded parts;
- lower filler metal consumption;
- lower cost of the joint, etc.;
- the shape of the backlashes depends on the thickness of the parts to be welded or their position after assembly.

Generally, it is economically advantageous for the backlashes to remain unprocessed, meaning the edges of the parts should remain flat.

The welding process of metals is achieved through the interaction of the marginal atoms of the welded components, forming common crystalline grains between the components as a result of recrystallization, which is

induced by the localized energy input and the intimate contact between the parts. Metal welding occurs when the temperature and pressure in the contact zone of the components reach or exceed certain critical values, enabling the formation of bonds between the crystalline lattices of the components, which together constitute the welded structure. Local cohesion during welding is established either by the contribution of thermal energy, mechanical energy, or a combination of both.

As a result of the energy input, the marginal atoms of the welding components receive the necessary energy to escape their stable equilibrium state, corresponding to a minimum energy level. Subsequently, the components bring their marginal atoms to distances equal to or smaller than the lattice parameter of the crystalline structure. At that point, the marginal atoms rearrange into crystals that are common to both components, thereby reaching a new state of energetic minimum.

It results that the welding process consists in the localized input, concentrated in both time and space, of a certain amount of energy in the welding area, with the purpose of displacing the atoms from their stable equilibrium state and bringing the marginal atoms to distances equal to or smaller than the crystalline lattice parameter, so that they can recrystallize into a common lattice corresponding to a new stable state.

This energetic mechanism is schematically illustrated in Figure 4.2.2.1.

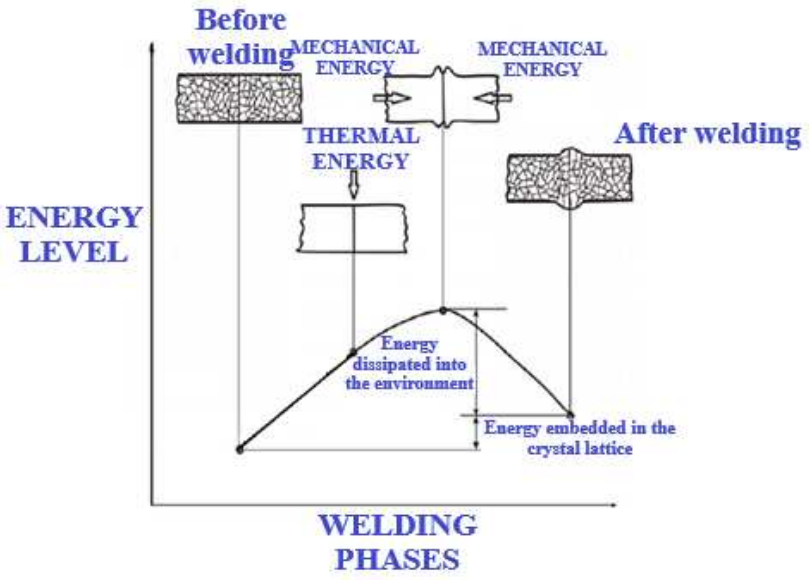

Figure 4.2.2.1 The energy mechanism of welding.

After all, through welding, the saturation of the atomic bonds located at the margins of the welding components is achieved. Welding experiments conducted in outer space have confirmed the hypothesis that the vacuum of space offers metallic components the possibility to weld through intimate contact. This situation indicates that marginal atoms have not completed all their bonds with other atoms, thus existing at an energy level higher than the minimum. When brought close together, these marginal atoms form common crystalline networks between the welding components, thereby saturating their connections.

On Earth, however, this process is not possible, because the unsaturated marginal atoms complete their bonds with gas atoms from the terrestrial atmosphere. Moreover, metal surfaces are covered by strongly cohesive layers of impurity molecules, greases, etc. All of these act as barriers between metallic atoms and prevent the interaction of the metals brought into contact.

Welding through Melting and through Pressure

To achieve the welding of a metal or an alloy, a certain amount of heat and a specific distance between the marginal atoms is required. Since thermal energy depends on the temperature T at the fusion point, and mechanical energy depends on the pressure p exerted on the contact surfaces, for each metal or alloy diagrams can be plotted in p-T coordinates (Figure 4.2.2.2).

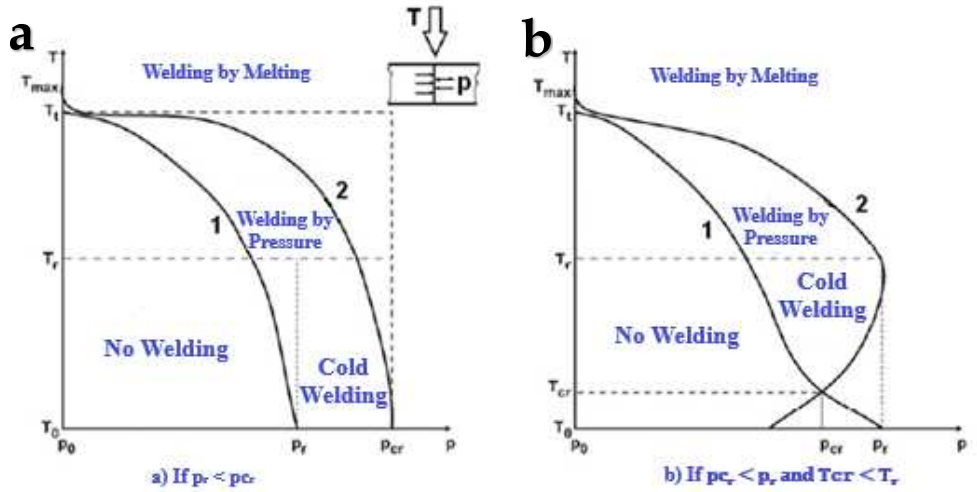

Figure 4.2.2.2 Fusion welding and pressure welding.

The atmospheric pressure is denoted by p_0, the recrystallization pressure by p_r, the critical pressure by p_{cr}, the atmospheric temperature (ambient temperature) by T_0, the recrystallization temperature by T_r, the critical temperature by T_{cr}, the melting temperature by T_t, and the maximum temperature by T_{max}.

Figure 4.2.2.2 a), in which $p_0 < p_r < p_{cr}$ and $T_0 < T_r < T_t < T_{max}$, represents the case of materials with high plasticity (such as copper, aluminum, etc.), while Figure 4.2.2.2b), in which $p_0 < p_{cr} < p_r$ and $T_0 < T_{cr} < T_r < T_t < T_{max}$, represents the case of materials with lower plasticity (e.g., steels).

In Figure 4.2.2.2 a), curve 1, which connects the point with coordinates $p = p_r$ and $T = T_0$ to the point with coordinates $p = p_0$ and $T = T_t$, separates the pressure, temperature plane into two regions. The points situated above curve 1 represent systems in which welding occurs, while the points below the curve correspond to systems in which welding does not occur. If the temperature is higher than the melting temperature T_t, and the contact pressure is at least equal to the atmospheric pressure p_0, welding through melting is achieved. In this case, the components melt, and the atoms mix within a common bath of molten metal, called the welding bath, without the need for pressure to bring the components into intimate contact.

The fusion obtained through the solidification of the welding bath is called welding through melting, and the procedure that employs this energetic mechanism is referred to as a welding through melting process.

In Figure 4.2.2.2 b), curve 2 connects the point with coordinates $p = p_{cr}$ and $T = T_0$ to the point with coordinates $p = p_0$ and $T = T_{max}$.

In the area between curves 1 and 2, situated between the melting temperature T_t and the recrystallization temperature T_r, the fusion is achieved through a combined contribution of thermal energy and mechanical energy, applied via pressure on the contact surfaces. This region corresponds to welding through pressure.

The area bounded by the abscissa $p = p_r$, the ordinate $T = T_r$, and curve 2 represents cold welding, which is typical for materials with high plasticity (such as copper, aluminum, etc.).

There are materials that cannot withstand the pressure pr required for cold welding, such that a pressure $p \geq p_{cr}$ leads to the fracture of the welded components. The cold

welding of these materials (generally steels) is performed in the area between curves 1 and 2, from the intersection point of the curves (with coordinates $p = p_{cr}$ and $T \geq T_{cr}$) up to the ordinate $T = T_r$.

- Welding through melting procedures, in which $p = p_0$ and $T \geq T_t$;
- Welding through pressure procedures, in which $p_0 < p \leq p_{cr}$ (or p_r) and $T_0 < T < T_t$.

In comparison with other assembly (fusion) procedures, metal welding presents a series of advantages, among which the following can be mentioned:

- reduction in weight compared to the cast version of the same product (e.g., car chassis, bearings);
- increase in mechanical strength and tightness compared to assemblies made with screws or rivets;
- reduction in production time and the possibility of manufacturing oversized products in a single production run or in small series;
- increase in work productivity;
- easier repair and maintenance of welded components;
- possibility of mechanization and automation.

Welding is one of the most reliable and widely used assembly procedures, being applied on a large scale in the realization of assemblies from plates and sheets of various thicknesses, profiles, bars, and wires. As previously presented, depending on the mechanism that leads to the formation of the welded joint (fusion), welding procedures are classified into two major categories:

- welding through melting, where the common crystalline structure is formed by the solidification of the molten metal resulting from the localized heating of the components to be welded;
- welding through pressure, where the common

crystalline structure is formed by the strong pressing of the components to be welded, with the welding temperature being lower than the melting point of the components. The lower the welding temperature, the greater the forces and/or pressing durations required.

The primary form of energy from which, ultimately, the thermal energy required for localized heating is derived can be mechanical, thermochemical, electrical, or radiant.

The manner in which local heating is achieved forms the basis for another classification within the field of welded assemblies. Thus, a classification can be made according to the source of the primary energy used:

- Welding using mechanical energy
  - welding through cold pressing
  - welding through forging
  - welding through friction
  - welding through percussion
  - welding through explosion
  - welding through ultrasound
- Welding with thermochemical energy
  - welding with oxy-gas flame
  - welding with thermite
- Welding using electrical energy
  - arc welding
    - with non-fusible (non-consumable) electrode
    - with fusible (consumable) electrode
  - welding through contact resistance
- Welding using radiant energy
  - with laser beam
  - with electron beam

4.3 Intraoral Electrowelding

4.3.1 The Weldability of Titanium and Its Alloys

Disregarding the technological and welding difficulties, one of the main issues encountered during the welding of titanium and its alloys is the thermal effect produced by the welding process itself, which leads to the formation of the heat-affected zone (HAZ). In relation to the welded assembly (fusion), and considering the metallurgy of titanium and its alloys, it is important to highlight the distinction between:

- *The unmodified base material*. The unmodified base material is not affected by the thermal welding cycles. In the case of commercially pure titanium and its alloys, the material that has not reached the transformation temperature is considered unmodified $\alpha \rightarrow \beta$. For the $\alpha + \beta$ or β alloys, it is recommended to consider as unmodified the area of the welded assembly (fusion) that has not exceeded the temperature of $540^{o}C$, since it is well known that above this temperature, structural modifications begin to occur.
- *The thermally modified area*. In the case of α-type alloys and commercially pure titanium, the α structure in the thermally modified zone, which transforms into β during heating, re-forms the α phase upon cooling, generally in an almost acicular configuration, depending on the cooling rate, which in turn is influenced by the material's thickness. The extent of the thermally modified area is limited due to the high transformation temperature $\alpha \rightarrow \beta$.

In the case of the $\alpha + \beta$ and β alloys, it is necessary to distinguish between the following:

- The area in which the temperature reaches the solidification point, this area

exhibiting a structure similar to that obtained through solution heat treatment (without structural modifications, but with an increase in β-phase grain size);

- The area in which the temperature exceeds 540℃, allowing a subsequent modification in the α-phase participation within the β matrix (aging process);
- The melted area. In the case of α-type alloys and commercially pure titanium, the β grains formed during solidification grow perpendicularly to the isothermal lines and transform into α grains with an almost acicular morphology. In the case of $\alpha + \beta$ alloys, the resulting structure includes martensitic formations and a β phase dispersed in an α matrix.

In the case of the β alloys, regardless of their β-phase content, the resulting structure tends to be weak and predominantly composed of a β matrix.

4.3.2 Protection Against Contamination During the Welding Operation

One of the main challenges encountered when welding titanium, which significantly influences the operating technique, is the extreme reactivity of titanium to atmospheric agents (oxygen, nitrogen, hydrogen). During the welding process, it is necessary to protect not only the molten zone but also any adjacent area where the temperature reaches or exceeds 300℃. Typically, this protection is achieved by creating an inert gas atmosphere, such as argon or helium. The inert gas envelops all the welding zones, being supplied from one or multiple sources, strategically positioned around the welding pool.

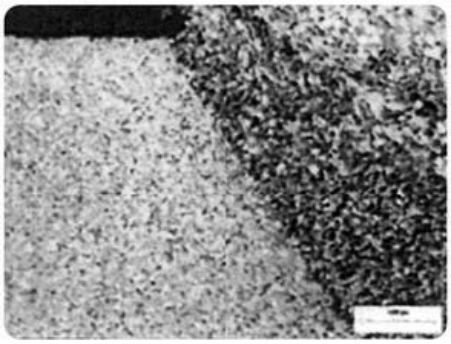

Figure 4.3.2.1 Welding of Grade 2 titanium bar in a protective gas atmosphere.

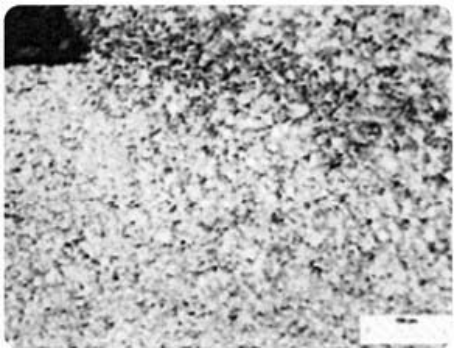

Figure 4.3.2.2 Welding of Grade 2 titanium bar without a protective gas atmosphere.

As observed in Figures 4.3.2.1 and 4.3.2.2, the appearance of the fusion obtained in a protective gas atmosphere displays a compact granulometry, preserving the initial characteristics of the welded material unchanged.

4.3.3 Electric Welding of Titanium Through Contact Resistance in Points

4.3.3.1 Electric Welding Through Resistance in Points and Syncrystallization

Electric welding through contact resistance in points is a welding procedure in which pressure is applied by electrodes onto the materials with surfaces in contact. The heat required to bring the contact surfaces to the melting or softening temperature is generated by the electrical resistance that appears during the passage of an electric current through the fusion area. Point electric welding is performed without the addition of filler metal.

Syncrystallization is the term used to describe the fusion of two metallic surfaces through atomic exchange within the crystalline lattice at the fusion interface.

Electric welding through contact resistance in points is achieved via syncrystallization in the contact surface area, which is traversed by a current of maximum intensity per unit area. As a result, the welded area is confined almost to a point, this point being referred to as the welding point.

4.3.3.2 Considerations Regarding Electric Welding Through Contact Resistance in Points

Let us consider the example illustrated in Figure 4.3.3.2.1 below. Two titanium plates are placed one over the other, between two copper electrodes connected to the output of a transformer's secondary winding.

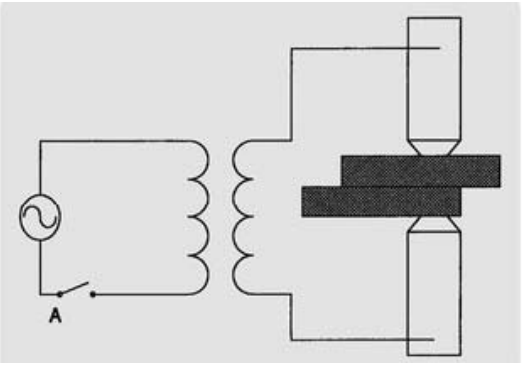

Figure 4.3.3.2.1 Operating diagram of spot resistance welding.

The upper electrode must be vertically mobile, while the lower electrode remains fixed. The upper electrode is pressed onto the plate, after which switch A is closed. The current passing through the secondary circuit generates intense heat in various parts of the circuit.

The amount of heat generated varies with the electrical resistance encountered, in accordance with Joule's Law:

$$Q = (1/J)RI^2t$$

where:

Q – the amount of heat, expressed in large calories (Cal);

J – the mechanical equivalent of the large calorie, expressed in joules per large calorie (J/Cal);

I – the current intensity, in amperes (A);

R – the electrical resistance, in ohms (Ω);

t – the time during which the current flows, in seconds (s).

We will consider, one by one, the parameters on which the heat Q depends, namely R, I, and t.

The electrical resistance R of the secondary circuit (see Figure 4.3.3.2.2) is composed of the following elements:

$\boldsymbol{R_0}$ – the resistance of the two portions of the secondary circuit up to the tips of the electrodes (excluding the two plaques to be welded), this portion of the circuit being made of copper;

$\boldsymbol{R_1}$ – the contact resistance between the upper electrode (made of copper) and the upper plaque;

$\boldsymbol{R_2}$ – the resistance of the upper plaque;

$\boldsymbol{R_3}$ – the contact resistance between the two plaques;

$\boldsymbol{R_4}$ – the resistance of the lower plaque;

$\boldsymbol{R_5}$ – the contact resistance between the lower plaque and the lower electrode (made of copper).

Because the resistances $\boldsymbol{R_0}$, $\boldsymbol{R_1}$, $\boldsymbol{R_2}$, $\boldsymbol{R_3}$, $\boldsymbol{R_4}$ *şi* $\boldsymbol{R_5}$ sunt ***are wired, the equivalent resistance*** $\boldsymbol{R}$ ***is:***

$$\boldsymbol{R_0 = R_1 + R_2 + R_3 + R_4 + R_5}.$$

In this sum:

- $\boldsymbol{R_0}$ **can be neglected**, as the electrodes are made of copper (which has higher thermal conductivity than titanium); thus, both its electrical resistance and the potential temperature rise—otherwise potentially harmful to soft tissues—can be considered negligible;
- $\boldsymbol{R_1}$ and $\boldsymbol{R_5}$ represent **the contact resistances** between the electrodes and the plaques; **their magnitude is surpassed only by** that of $\boldsymbol{R_3}$;

- $\boldsymbol{R_2}$ and $\boldsymbol{R_4}$ are **the internal resistances of the plaques** and are **relatively significant**, considering the resistivity of titanium and the fact that it naturally increases with temperature. However, **the heat generated by these two resistances is consistently lower than that generated by the contact resistances;**
- $\boldsymbol{R_3}$, the contact resistance between the two plaques, constitutes **the maximum resistance encountered in the secondary circuit.**

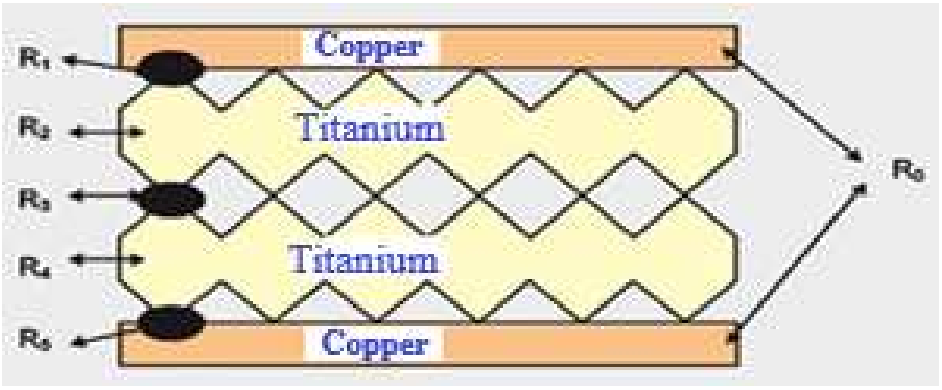

Figure 4.3.3.2.2 Schematic of resistances in the secondary circuit.

Therefore, the three contact resistances, $\boldsymbol{R_1}$, $\boldsymbol{R_3}$ and $\boldsymbol{R_5}$, play a crucial role in heat generation. Their magnitude varies depending on the nature of the metals and the condition of the surfaces, but also as a function of temperature and contact pressure. The importance of contact pressure is well established, as contact resistances are known to depend significantly on this parameter. Two metallic surfaces, even when extremely flat, always touch each other at the peaks of their microscopic roughness. When the surfaces are compressed and pressed together, the roughness peaks flatten out, effectively increasing the actual contact area, which enlarges the cross-sectional area for current flow and thereby reduces contact resistance. In short, contact resistance decreases as pressure increases.

As previously mentioned, it is necessary to apply compressive force on the pieces to be welded, in order to bring the contact pressure to an adequate level.

From this point of view, it is essential to note the following:

1. An adequate pressure reduces the contact resistances, allowing the passage of a high-energy current that produces a locally intense thermal effect within a short period of time.
2. Due to the high applied pressure, the contact resistances between the plaques ($\boldsymbol{R_1}$and$\boldsymbol{R_5}$) and the electrodes are reduced to low values, ensuring that the generated heat does not excessively heat the copper electrodes, thus preventing significant thermal deformation and unacceptable surface contamination.

The variation of temperature along the welded assembly (fusion) is illustrated in Figure 4.3.3.2.3.

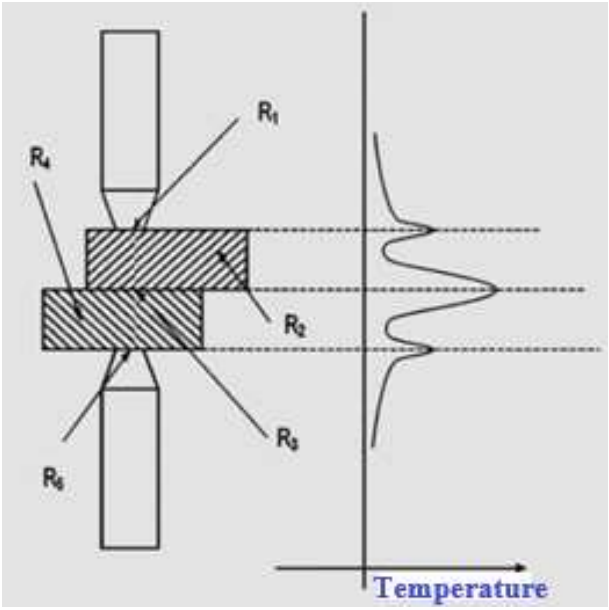

Figure 4.3.3.2.3 Temperature variation across resistances during welding.

Near the central point of the temperature graph, which corresponds to the welding point, the graph also displays, on both sides, two connection points at the electrode, plate interface. Since the electrodes are made of copper, a very good conductor of both electricity and heat, the temperatures at these points are reduced to a minimum.

In addition to the pressure that adjusts the contact resistance and allows resistance welding to occur, two other parameters that influence heating must also act appropriately. The current intensity appears squared in the Joule formula, and it is advantageous to increase it. This allows a shorter working time and also helps avoid significant heat loss in the contact area between the two plates.

This heat loss must be minimized as much as possible, considering that it not only represents wasted energy, but also leads to an increase in temperature in the areas distant from the welding point, which may cause potential harm to surrounding living tissues in our specific application. Furthermore, the spread of heat under the tips of the electrodes may result in their rapid degradation. The correct combination of heat, intensity, and time ensures the energy necessary for a long-lasting weld and the appropriate resistance of the welded assembly.

4.3.4 Parameters That Influence the Welding Process

4.3.4.1 Current Intensity

With regard to resistance, the current evolution of the procedure has led to shorter welding time intervals, which has imposed the use of very high current intensities with very low voltages. As previously shown, the heat necessary to perform spot welding is described by Joule's law. Therefore, a reduction in the time interval t requires a

corresponding increase in the current intensity I.

4.3.4.2 Other Parameters Influencing the Welding Process

The value of the current intensity depends primarily on the short time allocated to welding, and thus on the welding speed, but also on other parameters:

4.3.4.2.1 Pressure

Pressure influences the contact resistances such that higher pressures correspond to lower resistances and, consequently, allow higher current intensities. The pressure is applied for a longer duration than the current application period; the pressure cycle begins before the start of the current flow and ends after the current is switched off.

4.3.4.2.2 Contact Resistance

An inadequate surface condition, the presence of oxides, contaminants, etc., significantly increases contact resistance and, implicitly, reduces the current intensity, thus prolonging the welding time to the point where welding may become impossible. Regarding contact resistance, it is important to note that the resistance $\boldsymbol{R_3}$ between the plaques and the resistances $\boldsymbol{R_1}$ and $\boldsymbol{R_5}$ between the electrodes and plaques involve opposing requirements in terms of pressure:

- The $\boldsymbol{R_3}$ resistance should be as high as possible to facilitate local heating in the areas to be welded. Achieving this would require low pressure values; however, under such conditions, the resistance values become excessively high, leading to rapid wear of the electrode tips and overheating of the workpiece.

Therefore, there are three reasons for which a lower limit of contact pressure must be

respected, below which one should not go, in order to avoid damaging both the electrode and the workpiece, and to ensure the welding process is not compromised. On the other hand, it is evident that increasing the pressure reduces $\boldsymbol{R_1}$ and $\boldsymbol{R_5}$, potentially hindering resistance welding. Thus, it becomes necessary to identify a pressure value that maintains $\boldsymbol{R_3}$ sufficiently high to generate the required welding temperature within a short time, while also reducing $\boldsymbol{R_1}$ and $\boldsymbol{R_5}$ to acceptable levels to minimize heat at the electrode tips.

4.3.4.2.3 The Shape of the Part

The shape of the part can influence the flow of electric currents, potentially causing them to bypass the welding area.

4.3.4.2.4 Length and Distance Between the Electrodes

The length and distance between the electrodes, which are components of the secondary circuit, increase the reactance of the secondary circuit and, consequently, lead to a decrease in current intensity.

4.3.5 The Stages of the Welding Cycle

Three distinct stages can be identified in the welding cycle:

- *Pressing phase*, which involves the exclusive application of pressure, without the application of electric current;
- Welding phase, during which pressure and current are applied simultaneously;
- *Cooling phase*, in which the application of pressure continues after the electric current is interrupted.

4.3.5.1 Pressing Phase

In this phase, the pressure generated by compression brings the surfaces to be welded into very tight contact, until they meet at what will become the welding point. In cases where the parts initially come into defective contact, the compression force should be sufficient to elastically deform them until they match perfectly.

It should be understood that, in this first phase, it is useful to apply compression forces as high as possible, the required force being greater when the surfaces are less clean.

4.3.5.2 Welding Phase

During this phase, the compression force fulfills the following functions:

- It maintains the components in contact, an action easier to perform than achieving initial surface contact, so that, when current flows through the parts, they heat up and become as deformable as possible;
- It acts upon the contact resistances, enabling the passage of an appropriate welding current and localizing the heating in the area of optimal contact between the fused surfaces.

4.3.5.3 Cooling Phase

During this final phase, the pressure must maintain the parts in perfect contact throughout the entire crystallization period.

5 Devices and Materials

5.1 Introduction

The equipment presented below allows the welding of titanium components directly within the patient's oral cavity, without causing trauma or discomfort. Implantology using multiple electroweldings represents a technique aligned with modern surgical trends, which are becoming increasingly less invasive over time. This results in reduced pain and more immediate functional benefits for the patient. There is a constant concern to develop various types of implants with new shapes, lengths, and dimensions. The objective is to adapt the implant structure to the patient's anatomical characteristics, which, except in rare cases, do not require preparatory surgical interventions, such as bone harvesting from other anatomical sites.

The minimally traumatic nature of multiple electrowelding implantology has made it the most widely used technique for primary interventions, while secondary interventions, applied only in case of failure, are reserved for more invasive techniques. Moreover, in cases of short-term failure, due to the specific technical properties of Grade 2 monocorp titanium implants (T2 implants), only minor lesions of the bone structure may occur. These can be treated reparatively, allowing for the re-insertion of the implant after a short period.

The solidarization of the implants modifies the way mechanical forces are distributed within the structure. In this configuration, each implant loses its mechanical individuality and contributes to a collective support mechanism, enhancing the overall stability of the implant-supported prosthetic rehabilitation.

Figure 5.1.1 Intraoral view of electrowelded Grade 2 titanium implants, showing immediate solidarization through resistance welding, which ensures mechanical stability and allows for minimally invasive functional rehabilitation.

Figure 5.1.2 Full arch intraoral electrowelding of titanium implants (Grade 2), demonstrating simultaneous maxillary and mandibular solidarization, which enhances structural integrity and distributes functional loads uniformly across the prosthetic framework.

5.2 General Characteristics

Figure 5.2.1 Image of the intraoral electric spot-welding device used for titanium welding procedures. The unit includes the main control system, pedal trigger, and clamp electrodes, enabling precise energy delivery and syncrystallization inside the oral cavity, under safe conditions.

The technology was first introduced by Pier Luigi Mondani in 1976 and later developed and refined.

The equipment enables welding to be performed directly in the patient's oral cavity and is based on a particular phenomenon related to the crystalline lattice structure of titanium. Moreover, this application remains the only industrial use connected to this unique physical characteristic. Many colleagues

have continued to improve the device to achieve optimal clinical outcomes, among whom Dr. Lorenzon's upgraded model stands out as the most advanced and will be described below.

The welding process is electrical. The two components to be joined are positioned between the two electrodes of the spot-welding clamp. The energy previously stored in a capacitor bank is discharged through the clamp's electrodes. The current flows through the contact points of the components to be welded, thereby initiating the welding germination. Throughout the process, the junction area is protected by an argon atmosphere.

This precaution prevents titanium from reacting with atmospheric oxygen at the syncrystallization site, thus avoiding oxidation and the consequent compromise of its mechanical properties. The generated heat does not reach hazardous levels, as it is dissipated through the copper electrodes due to copper's high thermal conductivity. To ensure safety for both the patient and the operator, the device disconnects from the electrical grid during the welding phase.

The equipment integrates a microcontroller that manages the user interface, the encoder, and the display. Through the device's software, it is also possible to record a series of personalized programs (jobs) tailored to the specific types of titanium components being used.

Note: The following descriptions refer to the most technically complex model currently available on the market, a device that includes the creation of a protective argon atmosphere at the moment of syncrystallization. Other types of devices may lack this feature, based on the consensus among practitioners that the absence of argon does not significantly impair syncrystallization quality to an unacceptable degree. Of course, from a rigorous metrological standpoint, this argument does not hold; however, in clinical

practice, we prioritize outcomes first, and only afterward choose the most optimal method.

The welding cycle is divided into four distinct phases, defined as follows:

1. **Pre-welding gas (argon) supply phase** – This ensures the creation of an oxygen-free atmosphere at the welding site before the initiation of the welding process.
2. **Syncrystallization pre-welding phase** – Dependent on the energy delivered through the electrodes, this stage is essential for achieving intimate contact between the metallic components, facilitated by the softening of the materials. This benefit becomes particularly useful in welding structures with sinuous and complex curves, where the rigidity of titanium bars would otherwise pose a challenge.
3. **Post-welding gas (argon) supply phase** – This maintains an oxygen-free environment around the welding point until the temperature of the welded germination drops below the threshold at which reactions with atmospheric oxygen can occur.
4. **Final syncrystallization phase** – This is the stage in which the maximum programmed heat is delivered to complete the welding process.

The apparatus enables the customization of these four phases by assigning specific values to each stage within the 16 programmable welding settings it can store. Prior to every welding cycle, the microprocessor verifies that the electrical circuit and the appearance of the welding point meet the required parameters. Specifically, the total circuit resistance must be lower than a predefined value. Additionally, an acoustic signal alerts the operator at the beginning and completion of the welding cycle.

Figure 5.2.2 The user interface of the welding apparatus, showing the control panel and display used to program and monitor the syncrystallization phases, argon flow, and energy settings during intraoral titanium welding procedures.

The apparatus is housed in a dedicated suitcase, which facilitates transportation. The power supply cable, the foot pedal for activating the working cycle, and the spot welding claw with its connecting cables are all stored in designated compartments within the suitcase lid.

Figure 5.2.3 Transport suitcase – A robust, custom-designed case used for safely storing and transporting the welding apparatus and its components.

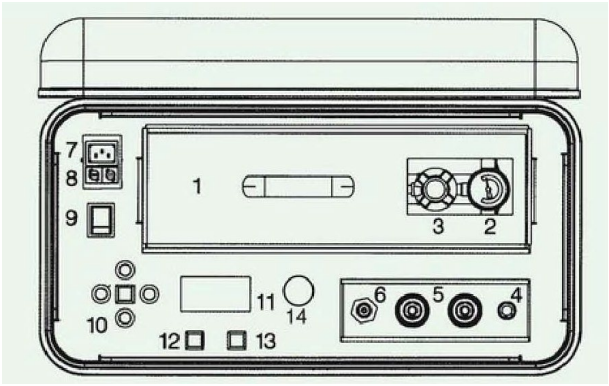

Figure 5.2.4 Interface scheme of the welding apparatus: 1. The lid of the reservoir compartment; 2. Gas pressure gauge; 3. Gas pressure adjustment knob; 4. Connector for the gas supply adapter; 5. Connector for the electrodes of the welding claw; 6. Connector for the pedal used to initiate the welding cycle; 7. VDE power supply socket; 8. Fuse: 2x250 V, 2A F (5x20 mm); 9. Power switch; 10. Navigation keypad; 11. 64x128 backlit display; 12. Programming keypad; 13. ESC key; 14. Navigation encoder.

5.3 Functioning Principle

The welding process is carried out by passing an electric current generated by a capacitor with capacity C, charged at a voltage V, delivering energy E, according to the formula:

$$E = V^2 \cdot \frac{C}{2}$$

where:

- E – energy
- V – voltage at which the capacitor is charged
- C – capacitor capacity

The current passing through the two points to be welded heats the materials and melts them together. To prevent titanium oxidation, the welding is performed in a saturated atmosphere (argon).

The welding process is influenced by several factors, primarily related to the two components to be welded. Therefore, it is necessary to experimentally determine the optimal welding parameters—specifically, the required energy and corresponding time. To this end, the equipment provides a table with 16 cycles, referred to as jobs, which allow adjustment of various welding parameters.

A user-configurable table enables the definition of energy and duration values for each memorized welding process.

In order to have the required welding energy available to the operator as quickly as possible, the capacitor C is charged as soon as the device is powered on, recharges after each welding cycle, and remains charged in standby mode. A dedicated circuit monitors the continuity of the welding circuit. If continuity is absent, the welding cannot proceed, and an appropriate signal alerts the operator to the anomaly. The SCR (Silicon Controlled Rectifier) welding activation is triggered via a dual electrical circuit, which verifies, through two independent controllers, that the microcontroller is functioning correctly.

The welding cycle consists of the following steps,

based on the parameters defined in the selected job table:

1. Pressing the foot pedal
2. Supply of inert gas
3. Disconnection of the capacitor from the charging circuit via the RL relay
4. Verification of electrical circuit continuity
5. SCR activation command

The following diagram illustrates the time sequence of the various operational cycles of the welding machine:

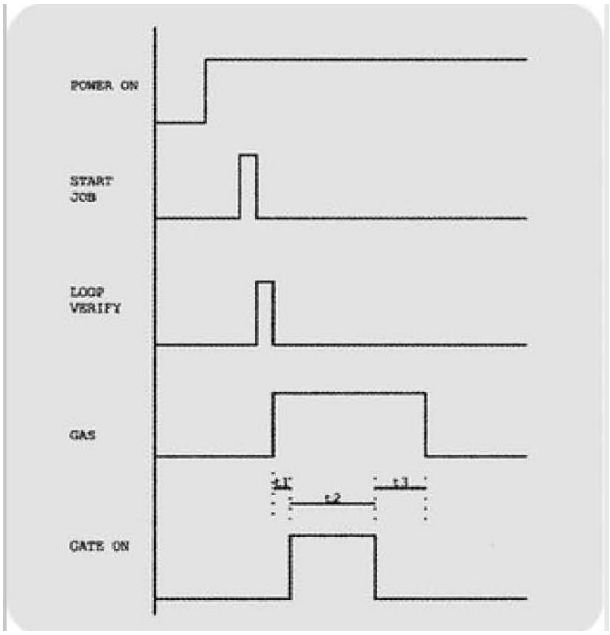

Figure 5.3.1 Temporal sequence of the machine's working cycles, illustrating the succession of operational phases: system initialization (POWER ON), job selection (START JOB), continuity verification (LOOP VERIFY), argon gas flow segmented into pre-welding (t_1), welding (t_2), and post-welding (t_3) supply phases (GAS), and the actual welding phase (GATE ON).

1. **POWER ON:** The welding unit is connected to the power supply and enters a stand-by mode.
2. **JOB START:** The machine displays the dataset corresponding to the pre-configured welding jobs.
3. **LOOP VERIFY:** The system checks, via a dedicated circuit, the continuity of the welding loop.
4. **GAS:** The welding machine introduces argon into the area where the welding is performed. In the first phase,

with an effective duration of t_1, the argon pre-welding supply takes place. In the middle phase, with a duration of t_2, the actual welding occurs, and in the final phase, with a duration of t_3, the post-welding argon supply is carried out.

5. **GATE ON:** This is the effective welding phase, during which current flows through the welding circuit. The duration of this phase corresponds to t_2.

THE ELECTRICAL INSTALLATION SCHEME

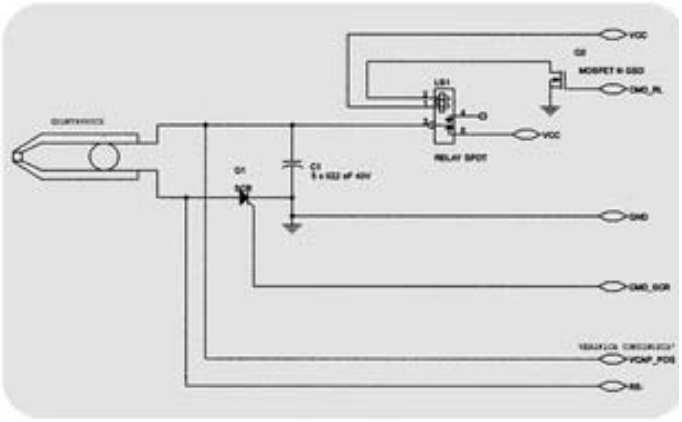

Figure 5.3.2 The electrical scheme for condenser charging–discharging and continuity control of the welding circuit.

When the welding machine is switched on, the MOSFET controls the relay, which subsequently activates the charging circuit of the condenser bank.

Once the foot pedal is actuated, the relay disconnects the condenser charging circuit. The safety circuit, powered by VCAP_POS and Rs-, ensures the integrity and continuity of the electrical circuit, which includes the electrodes and the components to be welded. If continuity is confirmed, the SCR diode is triggered, closing the circuit and initiating the discharge of the condenser. This discharge generates the current necessary for the welding process. In the absence of continuity within the electrode-to-component circuit, the SCR

does not receive the triggering signal, and an acoustic alarm alerts the operator to the malfunction.

THE SPOT WELDING RELIANCE CLAW FOR ELECTRODES

The spot welding claw – reliance for the electrodes – is an essential tool for the successful execution of a welding procedure. In fact, the pressure exerted on the two germinations is applied prior to the reduction of electrical resistance and maintains the parts in intimate contact in the area intended to be fused by current flow.

Thanks to the claw, the pressure applied to the germinations remains constant and is not subject to variation over time, as would be the case if it were applied manually by the operator. A compression spring generates the required pressure during the welding phase, so that the surgeon does not need to exert pressure manually.

Other models of syncrystallization pliers operate in a normally open state, with pressure applied through repeated compressions by the operator; the pliers remain engaged without releasing, ensuring that the operator does not influence the working pressure. At the end of the operation, the system is entirely disengaged. This technical solution is inspired by positioning claws used in industrial applications.

The two handles are insulated and equipped with interchangeable heads, as the heat generated during the welding phase leads to progressive deterioration of their properties. Additionally, each device model includes, alongside its primary components, a file or abrasive band surface that allows the assistant to remove copper oxides from the active electrode surfaces – oxides that naturally form due to environmental exposure and the action of disinfectant substances.

In the following figures, we can observe both the image and the technical diagram of the

spot welding claw with electrode support.

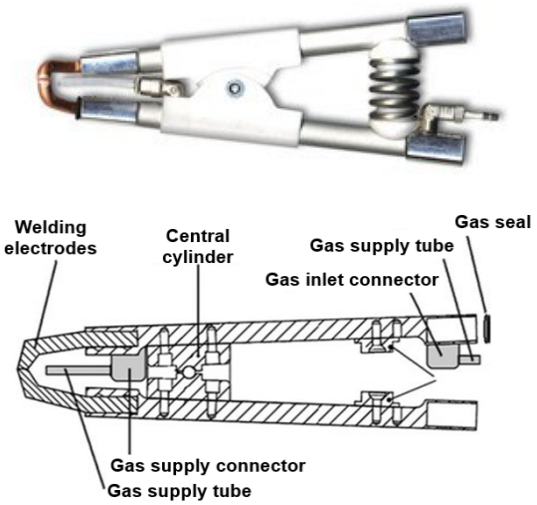

Figure 5.3.3 Image and schematic representation of the welding claw with electrode support.

5.4 The Macroscopic Test

Figure 5.4.1 presents a welded germination obtained through syncrystallization in an argon-saturated atmosphere. It appears clean and free of oxidation marks. The germination shown in Figure 5.4.2 was welded without the protection of an inert gas. It exhibits oxidation and visible welding marks.

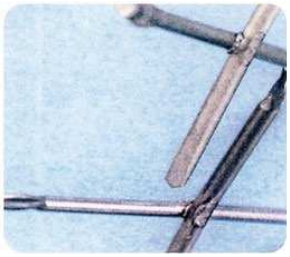

Figure 5.4.1 Germination welded in a protective argon atmosphere. The surface is clean, with no visible oxidation or burn marks, indicating an optimal syncrystallization process.

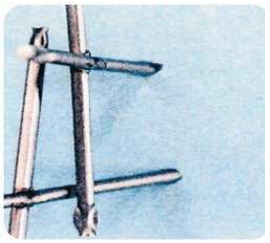

Figure 5.4.2 Germination welded without the protection of inert gas. The surface shows evident oxidation and discoloration, with visible welding marks, indicating compromised structural and aesthetic quality.

OPTICAL MICROSCOPIC TEST

The following two images were obtained using a metallographic microscope at 41x magnification. Both germinations were subjected to acid etching. The germination in Figure 5.4.3, produced using an inert protective gas, displays maximum welding penetration, which ensures the stability and strength of the joint. In contrast, the germination in Figure 5.4.4, where no protective gas was used, shows superficial welding, resulting in a structurally weaker joint.

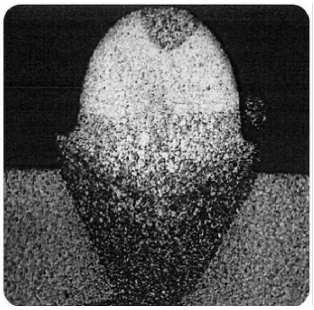

Figure 5.4.3 Welded germination in a protective gas environment – the image illustrates a deep and uniform weld, indicating proper fusion and mechanical stability, obtained with the use of an inert shielding atmosphere during the syncrystallization process.

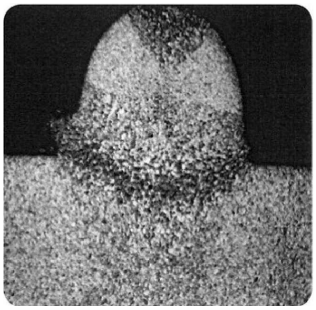

Figure 5.4.4 Welded germination without protective gas, 41x magnification – the image reveals a superficial and incomplete weld, with poor material fusion, resulting in reduced mechanical resistance. The absence of an inert shielding atmosphere has led to oxidation and compromised weld quality.

THE MACROGRAPHICS OF THE WELDING POINT

The examination of the samples was performed using a **S**canning **E**lectron **M**icroscope (SEM) LEO 420 (LEO Electron Microscope Ltd.). The main instrumental parameters employed during the analysis are displayed on the black bar at the bottom of each figure.

- EHT: Extremely High Tension of electrons
- WD: Working Distance
- Mag: Magnification

The samples were sectioned perpendicularly to the „syncrystallization" area and, without any subsequent treatment, were placed directly into the SEM analysis chamber.

Four distinct samples were examined, each corresponding to different stages or conditions of syncrystallization.

As the results obtained were highly consistent and reproducible, only the most representative images, selected from two of the samples, are presented and analyzed.

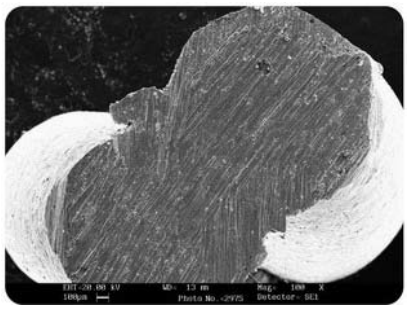

Figure 5.4.5 Microscopic image at 100x magnification showing two titanium stems joined through syncrystallization.

In this microscopic image, captured at 100x magnification to provide an overall view, we can observe a pair of titanium stems joined through syncrystallization. Even at this relatively low magnification, the connection between the two parts is clearly visible. No discontinuities or signs of contamination are evident; issues frequently encountered in metal and alloy welds produced by both traditional and modern welding techniques.

Figures 5.4.6 and 5.4.8, captured at magnifications of 500x, 1000x, and 2000x respectively, not only confirm but also emphasize the results previously observed in Figure 5.4.5. The two titanium stems appear to be firmly bonded, without any structural discontinuities.

The grooves and surface curling visible in the images are the result of cutting operations (performed to expose the internal structure of the connection area), which naturally produce such marks.

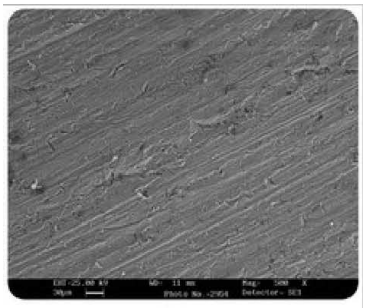

Figure 5.4.6 Microscopic image at 500x magnification showing the integrity of the syncrystallized connection. No discontinuities or contaminations are observed at the interface.

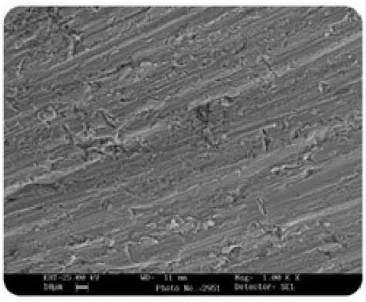

Figure 5.4.7 Microscopic image at 1000x magnification highlighting the homogeneity of the welded structure. The connection area maintains a continuous grain pattern.

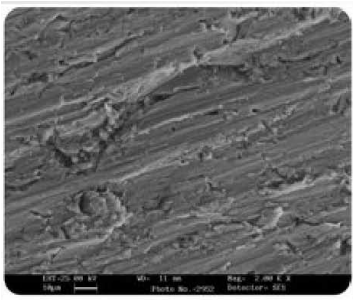

Figure 5.4.8 Microscopic image at 2000x magnification confirming the absence of microfractures or porosities. The weld appears compact and structurally stable.

Other equivalent devices are available in various technical variants and increasingly user-friendly interfaces, all respecting the same working principle and utilizing the same structural particularities of titanium.

Figure 5.4.9 The new argon control system developed by IMPLAMED ITALY.

Figure 5.4.10 The argon-free system developed by IMPLAMED ITALY.

Other syncrystallization device models are readily available, all operating based on the same fundamental principle.

Figure 5.4.11 A compact syncrystallization welding unit featuring a simplified user interface.

Figure 5.4.12 Interface detail of the syncrystallization welding unit.

Figure 5.4.13 Detail of the welding claw equipped with copper electrodes, specifically designed for syncrystallization.

We have recently noted the emergence of another intraoral welding system developed by Swiss & Wegman SRL, distinguished by its remarkable ease of use and the presence of two types of pliers: one with pre-tensioning and one with manual tensioning, both autoclavable. This system operates without the presence of argon protection in the welding area, while still adhering to the same fundamental working principles. The energy impulse can be finely adjusted, allowing for precise adaptation to various titanium bar – prosthetic element combinations.

The display and control interface are user-friendly and intuitive, enabling immediate and effortless operation.

Figure 5.4.14 Intraoral welding unit DentaWeld by Swiss & Wegman SRL, featuring an intuitive control panel and autoclavable handpieces.

Figure 5.4.15 Second view of the DentaWeld intraoral welding unit by Swiss & Wegman SRL.

Figure 5.4.16 Manual-tensioning welding pliers used in intraoral syncrystallization procedures.

A notable feature of this particular system is the use of palladium-coated pliers, which offer improved energy efficiency and reduced metallic ion release. The entire system is autoclavable.

6 Indications and clinical cases

Types of clinical situations

As previously mentioned, the general trend in modern surgery is to adopt procedures that are as minimally invasive as possible. In this regard, flapless techniques, the dental equivalent of keyhole surgery in general medicine, are considered pioneers of the minimally invasive concept. A natural question arises regarding the advantages this technique brings to implant-supported treatments. We will present the various clinical scenarios and the benefits offered by this approach.

The types of implants that allow intraoral welding are numerous. Practically any titanium component can be welded; however, what truly matters is the surface quality of the components involved. In monoblock (monocorp) implants, this concern is eliminated, as the entire body is made of titanium. In bicomponent implants, however, one may encounter situations where the insertion mount is fabricated from an alloy with inadequate physical properties for welding. For this reason, it is absolutely necessary to perform welding tests on unsterile components prior to surgery, in order to verify and calibrate the equipment.

Once these aspects are addressed, the clinical procedure can be initiated. The following clinical situations can thus be distinguished:

- 6.1 The isolated implant
- 6.2 Multiple implants in short edentulous spans
- 6.3 Multiple implants in long edentulous spans
- 6.4 Monoblock implants with ball attachments for retention of removable prosthetics
- 6.5 Special interventions

6.1 The Solo Implant

This clinical scenario, frequently encountered, especially in young patients, is also among the most challenging. The particular demands associated with isolated implants are primarily related to the patient's general characteristics, which typically include:

- Young age and high physical demands
- Normal to high masticatory forces
- Relatively intact dental arches
- The presence of compromised anterior prosthetic restorations requiring extraction, implant insertion, and immediate loading
- Rigid masticatory engrams with minimal deviations

The arch position of the replaced tooth also introduces particular challenges due to its involvement in functional guidance movements and occlusal forces during maximum intercuspation. These forces often include a lateral component, which tends to induce rotational stress on the implant. This rotational component is largely responsible for the frequent loosening of crowns on isolated implants. In order to ensure optimal stabilization during the osseointegration phase, the implant must be protected from both axial loading and rotational forces. Axial loading is minimized through established strategies such as occlusal relief (inocclusion) and progressive loading protocols.

Protection against lateral forces with unscrewing effect is ensured by applying simple anti-rotational elements, which act on the surfaces of the adjacent teeth.

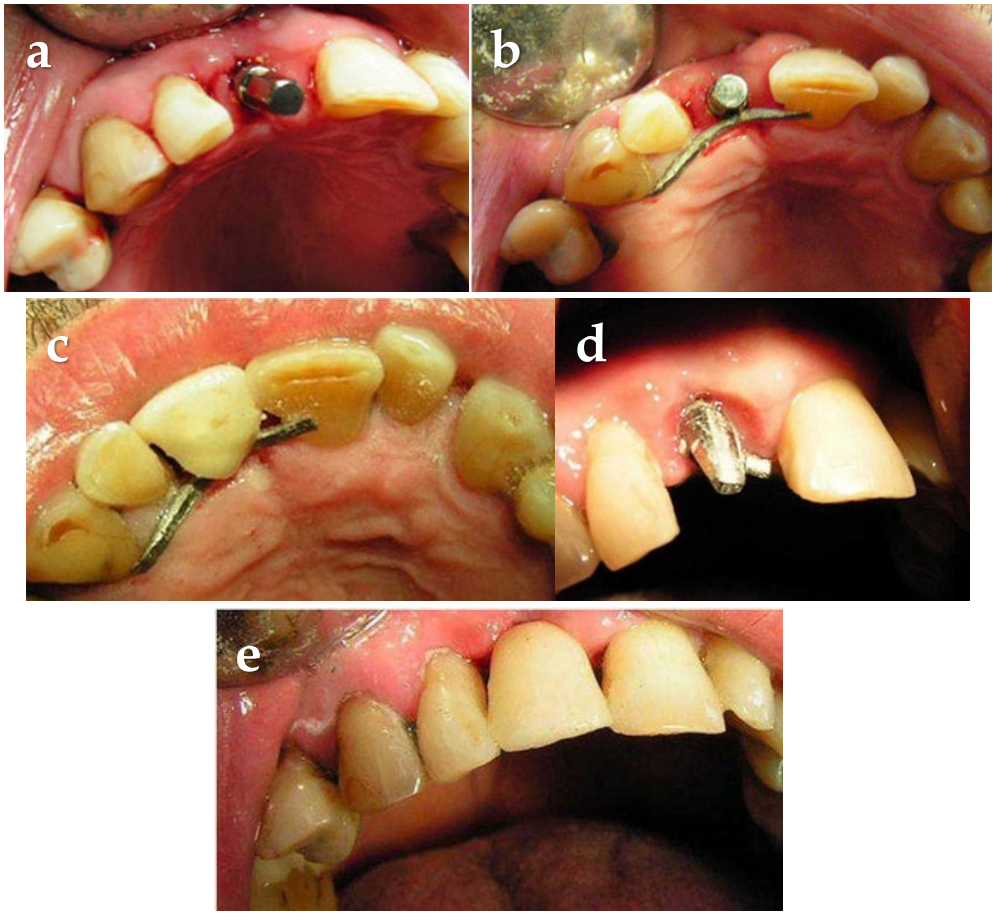

Figure 6.1.1 ***(a)*** *Intraoperative image showing a mono-corpus implant placed at the level of tooth 11.* ***(b)*** *Juxta-gingival palatal bar positioned with support on teeth 13 and 21, providing an anti-rotational effect on the implant placed on 11, followed by provisional prosthetics.* ***(c, d, e)*** *Final prosthetic restorations: palatal and frontal views.* ***Clinical case commentary:*** *Remarkable in this clinical solution is the use of a mono-corpus implant with a titanium bar (1 mm) anchored to the adjacent teeth. A solid tooth, the canine, was chosen as a support point, while the lateral incisor, showing weak implantation, was avoided. After the osseointegration period, the bio-architecture of the soft tissues can be observed, shaped by the provisional crown, which enabled a more esthetic final prosthetic. In lateral areas, masticatory forces are significantly higher and generate stronger horizontal components, thus requiring double anti-rotational anchorage, as seen in Figure 6.1.2.*

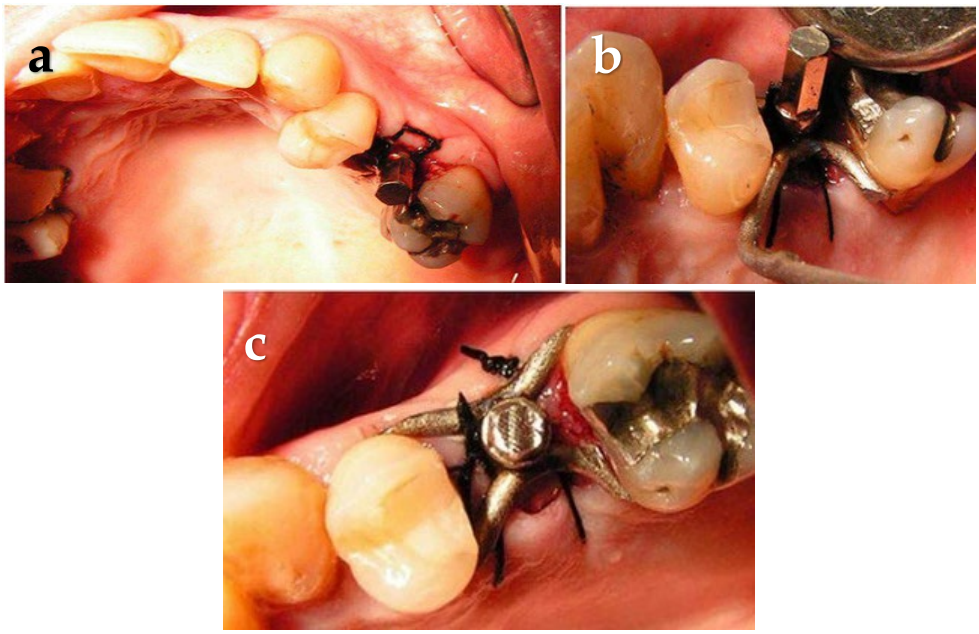

Figure 6.1.2 ***(a)*** *Post-extraction view of implant placement at the level of tooth 25.* ***(b)*** *Vestibular bar welding, followed by palatal bar welding.* ***(c)*** *The second maxillary premolar stabilized with anti-rotational effect using two welded titanium bars, positioned vestibularly and palatally in a V or X configuration.* ***Clinical case commentary:*** *This clinical approach emphasizes the need for dual-bar stabilization in posterior regions, where masticatory forces are significantly higher. The use of two bars, vestibular and palatal, arranged in a convergent (V) or crossed (X) pattern ensures enhanced anti-rotational stability of the implant, particularly crucial in single implant-supported restorations in the premolar area.*

6.2 Multiple Implants in Short Edentulous Spans

This is the most frequently encountered clinical scenario, particularly in the lateral mandibular region. The type of patient suitable for this treatment is generally:

- a patient transitioning from fixed to removable prosthetics (Kennedy Class I), who refuses the use of removable dentures;
- a wearer of removable prosthetics, maladapted to the new situation (Figure 6.2.1);
- a patient who is about to lose the lateral teeth and requests immediate functional restoration;

- a patient with an adjusted Kennedy Class I removable prosthesis, but with a predictable negative prognosis for the anterior teeth, seeking a phased transition toward an implant-supported prosthetic solution (e.g., overdenture, Toronto bridge, etc.) in two stages.

Figure 6.2 Sequence of clinical steps in the case of a patient wearing a Kennedy Class III removable partial prosthesis, maladapted, with a poor prognosis for the anterior mandibular segment and the two distal molars. The treatment plan consisted of implant-supported prosthetics for the two lateral edentulous areas, with immediate loading using a welded structure and a temporary composite prosthesis. Upon eventual anterior tooth loss, the treatment will continue with the insertion of additional implants to complete a fully fixed restoration.

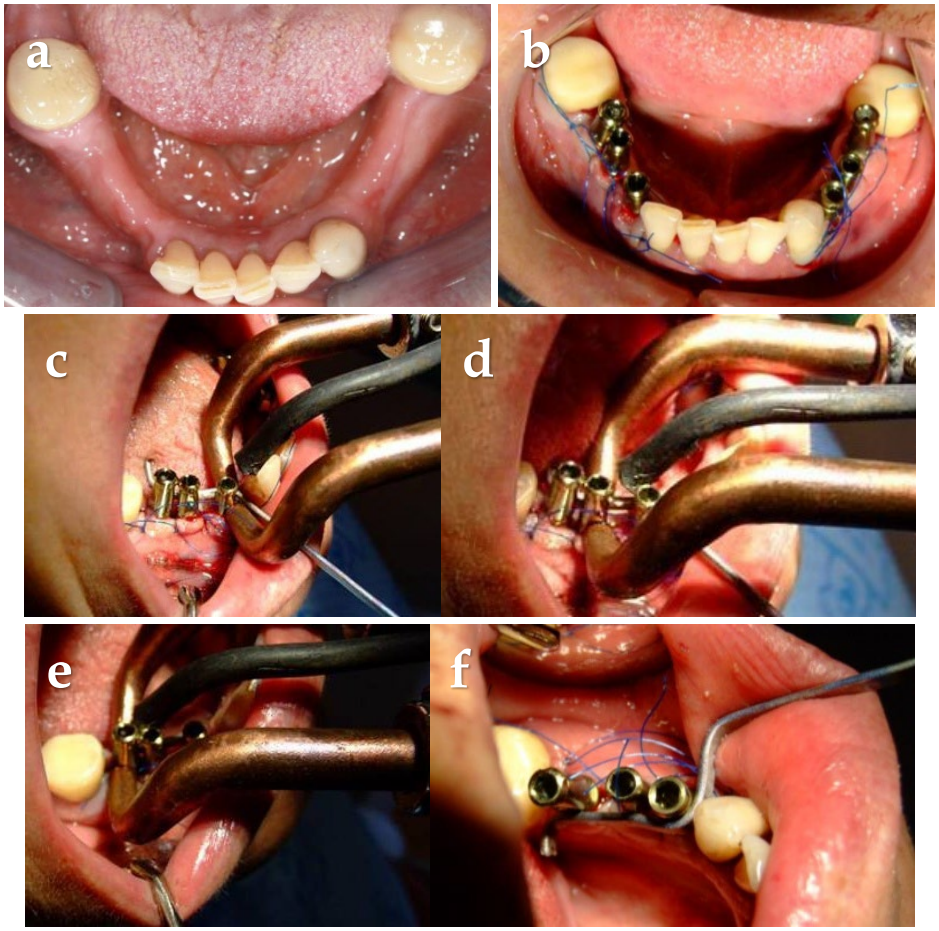

Figure 6.2.1 Clinical sequence in a patient initially wearing a Kennedy Class III removable partial denture, which was maladapted, with poor prognosis on the anterior mandibular group and bilateral distal extension edentulism. ***(a)*** *Bilateral mandibular edentulism, initially restored with a partially acrylic removable prosthesis, which the patient did not tolerate.* ***(b)*** *Insertion of bicomponent implants (WIS, Italy).* ***(c)*** *Intraoral welding phase using titanium bar.* ***(d)*** *Owing to the preconfigured immobilization tape, the welding was performed from mesial to distal.* ***(e)*** *Occlusal view showing the immobilized implant abutments during the welding procedure.* ***(f)*** *Post-welding view showing the titanium bar stabilized and the sutures in place.*

Immediately after the welding procedure, the prosthetic abutments can be sectioned under continuous cooling using the turbine spray, in order to achieve proper occlusal adjustment. This is also the moment when the torque applied to the screw connecting the prosthetic abutment to the

implant is verified using a torque wrench.

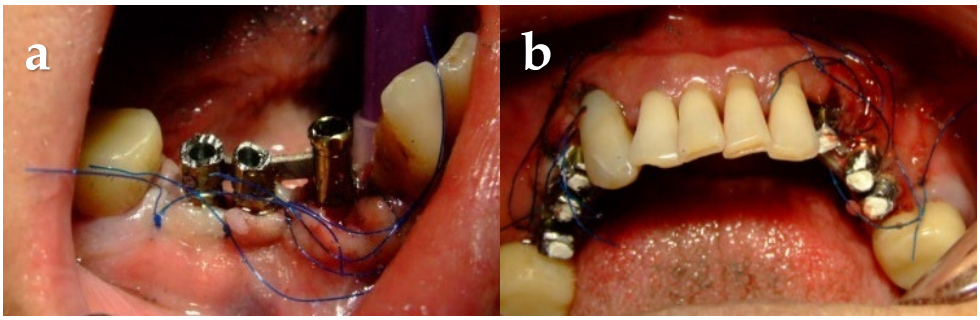

Figure 6.2.2 ***(a-b)*** *Intraoral views showing the welded prosthetic abutments after occlusal adjustment.*

The aspect of the welded abutments following occlusal adaptation, with the torque of the fixation screws perfected according to the manufacturer's specifications and sealed with provisional material.

Figure 6.2.3 Placement of the provisional prosthesis using a transparent dental guide

For the provisional prosthesis, the previously prepared elements are more easily positioned using a transparent dental guide, prior to the application of acrylic resin on the buccal aspect of the structure facing the prosthetic abutments.

The radiographic aspect at 3 months demonstrates optimal osseointegration, as illustrated in Figure 6.2.4.

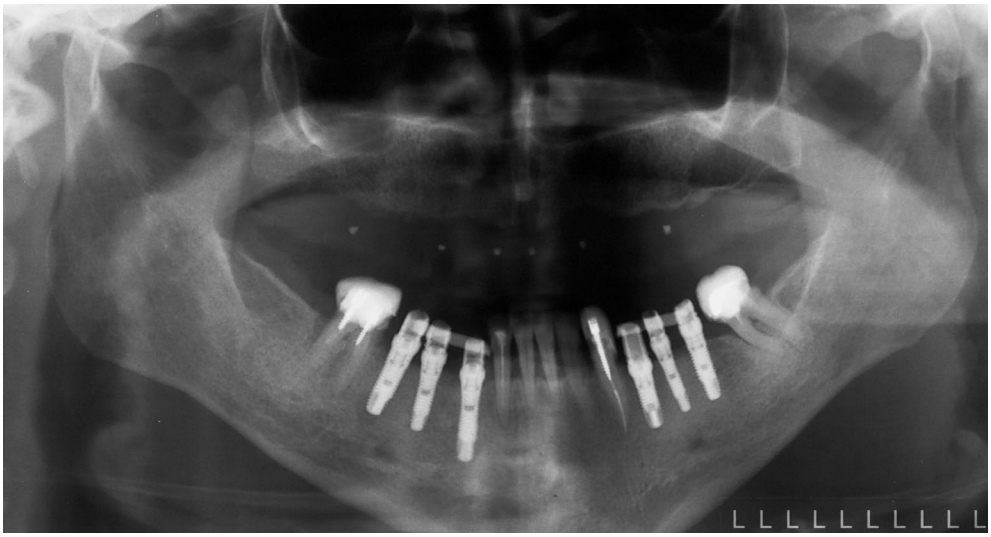

Figure 6.2.4 Panoramic radiograph at 3 months postoperatively, showing optimal osseointegration of the implants.

At the same time, the clinical aspect highlights the correct preservation of the bio-architecture of the soft tissues, progressing harmoniously with the osseointegration process.

Figure 6.2.5 Clinical view showing proper preservation of the soft tissue bio-architecture, maintained in parallel with the ongoing osseointegration process.

After removal of the welding system and unscrewing of the prosthetic abutments for impression, the compliance of the gingival fibro-mucosa to the shape of the abutments can be observed.

Figure 6.2.6 Clinical view after removal of the welding system and unscrewing of the prosthetic abutments in preparation for impression. The image reveals the adaptation of the gingival fibro-mucosa to the shape and positioning of the prosthetic abutments.

Of course, classifications can be made depending on a multitude of criteria, but the doctor always has in view the therapeutic benefit of the

patient. Besides the most frequent cases presented above, another category of clinical situations encountered is the one in which the treatment of these short edentulous spaces through implants requires significant optimization of bone support via surgical interventions, such as sinus lift procedures for increasing vertical bone height or ridge splitting to increase the bucco-oral dimension.

The benefit brought by this method in such cases consists in the possibility of using mono-corpus Ti_2 implants, taking advantage of the available bone along the patient's own anatomical axis and subsequently welding them in an optimal prosthetic position. This method has nearly 50 years of clinical validation and originates from the Italian school of dental medicine. In Romania, there has also been a strong interest in replacing missing teeth with metallic implants, with the first documented cases dating back to 1947 (The Italian Dentistry Magazine – March 1947, M.S. Formiggini, MD), followed by a generation of dentists contributing with remarkable creativity and innovation (Pasqualini, Zepponi, Tramonte, etc.).

In our country, the interventions performed by Prof. Valerian Popescu are frequently reported, followed by those of Burlibaşa and D. Vasiliu in 1969, Mărginean in 1974, and others. It is interesting to note that even at that time, there was a strong enthusiasm for experimenting with various materials for dental implants (chrome-cobalt, chrome-cobalt-molybdenum, titanium, palladium, gold, minerals such as zirconium, sapphire, ruby, etc.). Simultaneously, the distinction between the concepts of osteoacceptance and osseointegration was made with great precision, the latter still being a topic of ongoing debate (R. Chercheve).

Below we present a case of terminal mandibular edentulism, where, in order to solve it through implant-based

treatment, a sinus lift procedure would have been necessary to ensure the required bone volume for the insertion of bi-component implants. The total duration of the treatment would have extended to almost one year until the patient could have received a fixed prosthetic restoration (even a provisional one).

Figure 6.2.1 The sequence of the clinical phases in the case of a patient with sinus lift indication in quadrant I. The insertion of mono-corpus Ti_2 implants was carried out following the direction of the existing bone availability, followed by parallelization through flection, welding of a titanium bar, blocking out the undercuts of the entire structure with a common composite material, adaptation of a pre-operatively fabricated provisional bridge, and its provisional cementation.

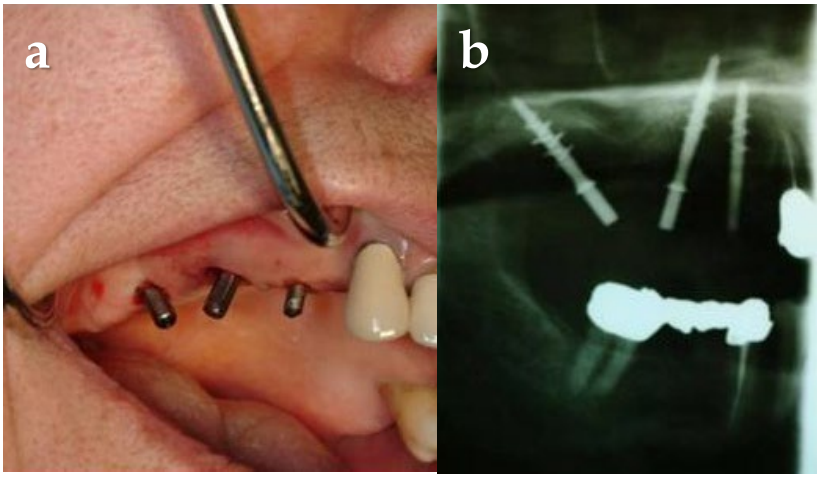

Figure 6.2.7 ***(a-b)*** *Clinical and radiographic aspects showing the insertion of mono-component implants following the axis of maximum bone availability, despite their divergent orientation.*

Both radiographic and clinical evaluation reveal that the insertion axes of the implants are markedly divergent, in accordance with the available bone anatomy (Figure 6.2.7). The clinician proceeded with implant placement along the most favorable direction dictated by the existing bone offer.

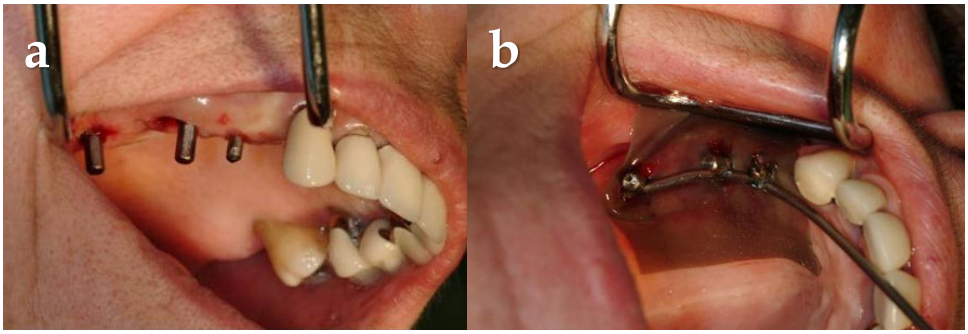

Figure 6.2.8 ***(a-b)*** *Clinical images showing the alignment of the prosthetic components of Ti2 implants by flexion, followed by intraoral welding of a titanium bar for immediate prosthetic stabilization.*

The prosthetic portions (blunts) of these Ti_2 implants are then parallelized through simple flexion, followed by welding a titanium bar over a rubber dam.

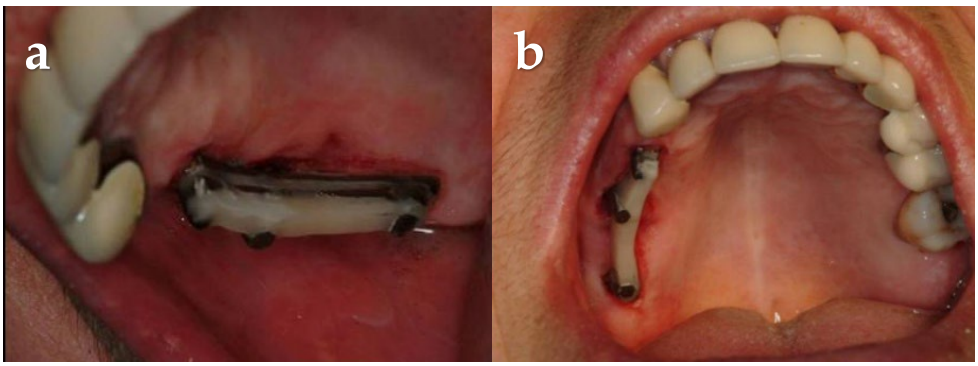

Figure 6.2.9 ***(a-b)*** *Clinical view of the suprastructure after undercut blocking with composite material, prior to finishing and adjustment using tungsten and carbide drills.*

The structure obtained through welding is then blocked out using a common composite, followed by finishing with a tungsten drill, carbide burs, and polishing composite drills.

Over this obtained mono-block, the provisional prosthetic work is applied and tested, preoperatively prepared. Normally, this is achieved by creating a significant cavity on the mucosal surface. The oral-vestibular dimension of this provisional restoration is ensured from the wax-up stage

by applying one or even two layers of wax on the oral surface to allow modeling. Then, on the finished work, drilling is performed on the inner mucosal surface until the maximum possible volume is obtained. This step is essential because the newly obtained structure in the oral cavity cannot be accurately predicted in the laboratory, and therefore, sufficient space for relining must be provided. After relining, a relatively rough acrylic block is obtained, which is subsequently reduced and finished chairside.

Figure 6.2.10 Relining of the provisional acrylic prosthetic restoration on the mono-block framework.

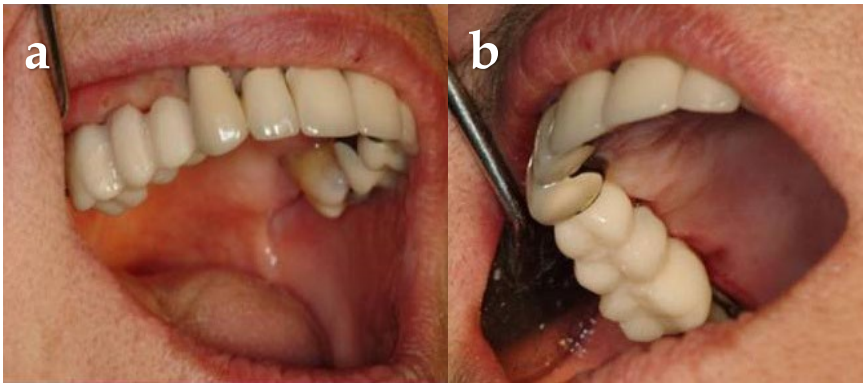

Figure 6.2.11 ***(a-b)*** *Clinical aspect of the temporary prosthetic restoration after finishing and polishing, ensuring proper adaptation, functionality, and aesthetics in the vestibular and palatal sectors.*

6.3 Multiple Implants in Long Edentulous Spans

The need for intraoral welding of implants in the case of long edentulous spans arises in three distinct clinical situations:

- The explicit request of the patient for an immediate fixed prosthesis;

- The need to guide the healing of the soft tissues using implant support;
- The necessity of a long-term provisional prosthesis to restore esthetics, function, and occlusal balance.

The primary stability of the implants, or the absence of it, directly influences the osteointegration process, especially in cases of limited bone support (critical zones). In all scenarios, the procedure must be meticulously planned so that the clinician has at their disposal a perfectly individualized provisional prosthetic work. The surgical intervention is generally more extensive and demanding for the patient, which makes it essential to reduce the total chair time. Additionally, the immediate functional loading applied by the clinician requires an absolutely flawless morphofunctional adjustment, as any compromise on the known standards inevitably leads to treatment failure.

The case presented in Figure 6.3.1 involves a 45-year-old female patient who specifically requested a fixed prosthetic restoration. The case illustrated in Figure 6.3.2 features a 68-year-old female patient whose available bone tissue did not allow for any alternative treatment without significant medical and biological costs (bone grafting, multiple interventions, variable success rates, surgical expenses, and prosthetic fabrication costs).

Figure 6.3.1 illustrates the sequence of clinical and laboratory phases for an implant-supported prosthetic rehabilitation in a case of subtotal mandibular edentulism.

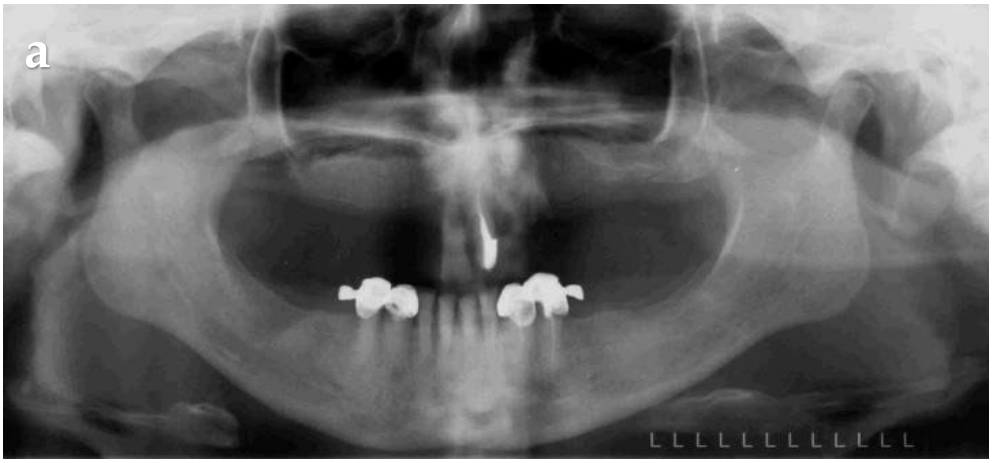

Figure 6.3.1 (a) Initial post-operative panoramic radiograph showing two implants in the mandibular interforaminal area.

Figure 6.3.1 (b) Post-operative panoramic radiograph showing multiple mandibular implants placed according to the available bone anatomy, prior to titanium bar welding.

Figure 6.3.1 (c) Clinical aspect following intraoral welding of the titanium bar and polishing of the prosthetic abutments. The final configuration ensures proper alignment, stability, and optimal support for the provisional fixed prosthesis.

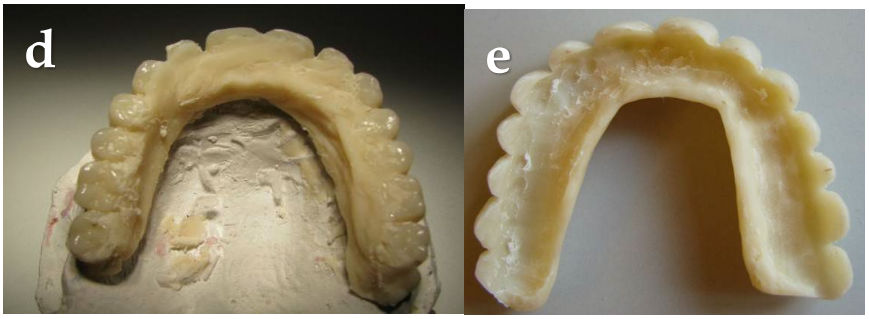

Figure 6.3.1 ***(d)*** *Initial provisional restoration showing insufficient oral-vestibular volume.* ***(e)*** *Internal view of the same restoration after the addition of autopolymerizing acrylic for further mucosal adaptation.*

The provisional restoration made preoperatively revealed that the oral-vestibular dimension was insufficient. Therefore, in the dental office, a layer of autopolymerizing acrylic was applied, followed (see next image) by the preparation of the mucosal surface.

Figure 6.3.1 ***(f-g)*** *The clinical aspect of the provisory work applied in the oral cavity.*

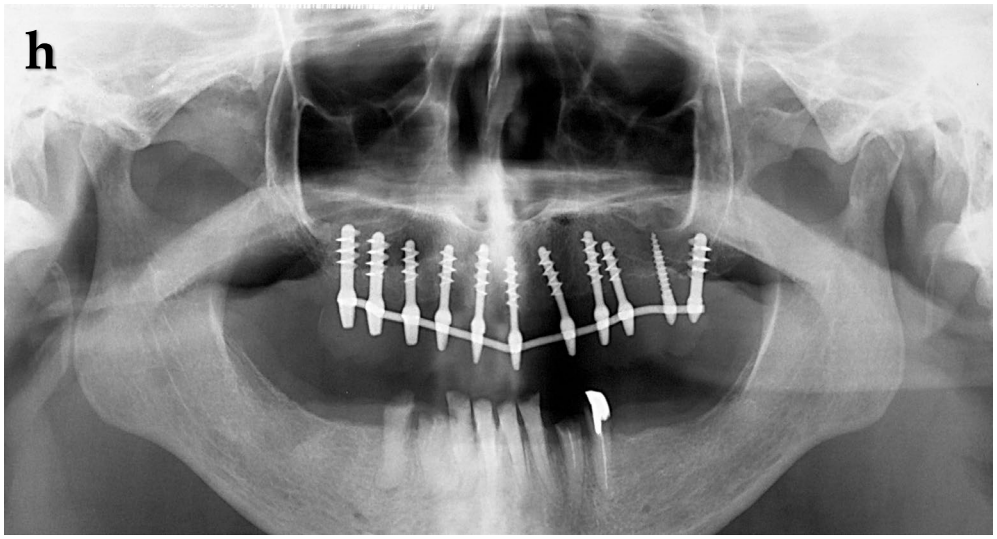

Figure 6.3.1 ***(h)*** *The radiologic aspect after the welding.*

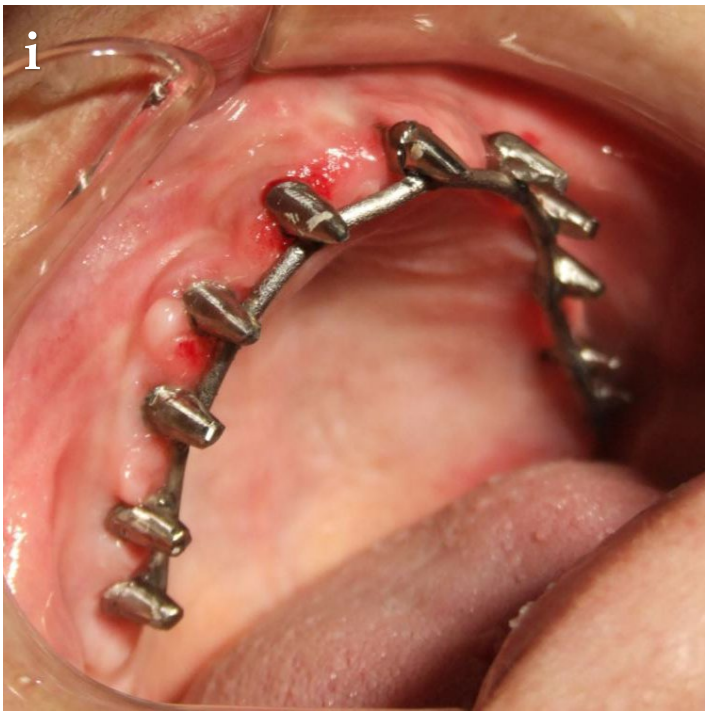

Figure 6.3.1 ***(i)*** *The clinical aspect after the welding.*

Figure 6.3.2 illustrates the sequence of clinical and laboratory steps in the restoration with worn implants of a subtotal edentulous maxilla.

Figure 6.3.2 ***(a)*** *Initial panoramic radiograph showing the clinical status of the subtotal edentulous maxilla and existing implant-supported restorations in the mandible.*

Figure 6.3.2 ***(b)*** *Frontal intraoral view showing the existing prosthetic restorations before treatment, with signs of wear, misfit, and periodontal compromise, requiring full arch rehabilitation.*

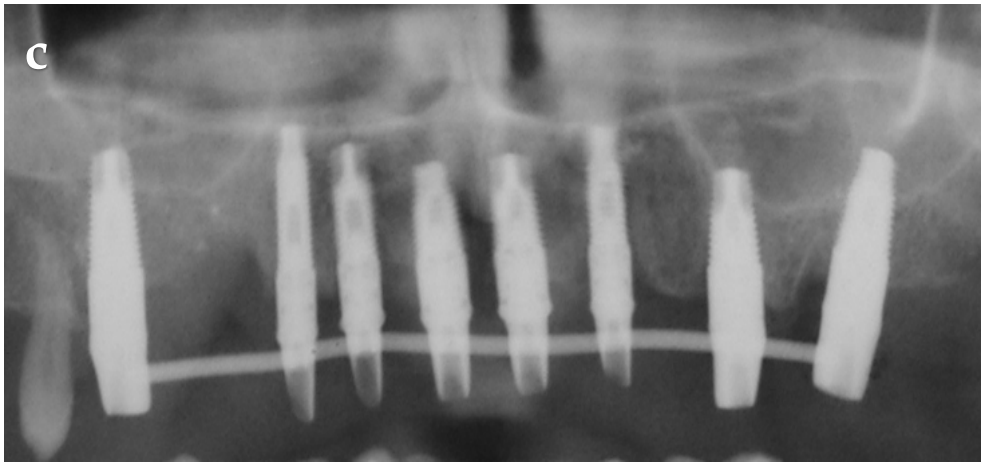

Figure 6.3.2 ***(c)*** *Radiographic view of the implant-supported structure obtained through intraoral welding, with the individualized provisional prosthetic restoration in position.*

Figure 6.3.2 ***(d)*** *The clinical view of the implant-supported structure obtained via intraoral welding, with the individualized provisional prosthetic work in place.*

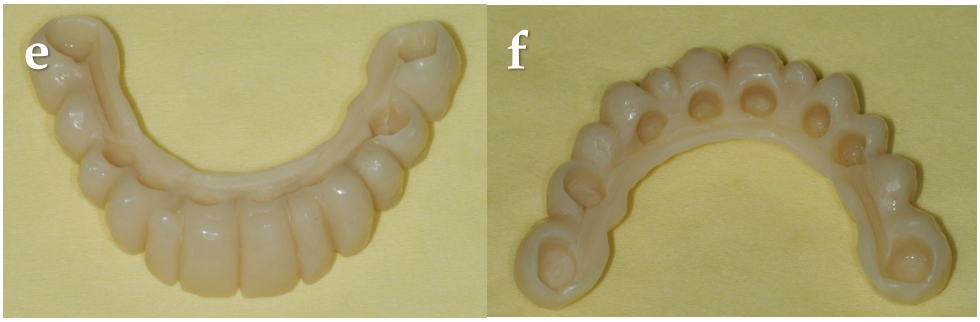

Figure 6.3.2 ***(e-f)*** *The final fixed prosthetic restoration, viewed from the vestibular and mucosal surfaces, highlighting the accurate passive fit and anatomical design.*

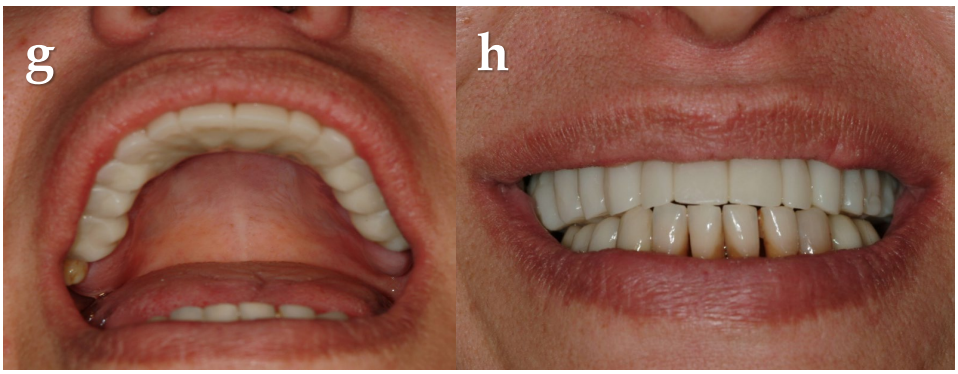

Figure 6.3.2 ***(g-h)*** *Final clinical outcome following the complete prosthetic rehabilitation on intraorally welded implants.*

6.4 Monoblock Implants with ball Attachments for Retention of Removable Prosthetics

A practical application of intraoral welding is the welding of mini-implants. In current accepted terminology, mini-implants refer to those with a maximum corpus diameter of 3 mm, predominantly cylindrical in shape, featuring self-tapping threads and lacking a connection system (mono-corpus implants). These implants are fabricated from Ti4, and the transmucosal component is designed either in the form of a prosthetic abutment or as the male element of a ball attachment system (with a retention sphere). Given that the primary function of these implants is to ensure the retention of a removable prosthesis on a prosthetic field

in the red, the dominant mechanical stresses they are subjected to are lateral traction forces, with vertical pressure being relatively rare. However, due to their mono-block structure, they are highly exposed to immediate post-operative mechanical stresses, and any accidental decoupling from the prosthetic base can compromise the mechanical protection of the freshly inserted implants.

This is precisely where immediate intraoral welding offers a significant advantage, by transforming two or more isolated implants into a unified mechanical system, capable of distributing the forces across the entire support area. Figure 6.4.1 illustrates simple clinical cases involving two or more mini-implants and immediate loading.

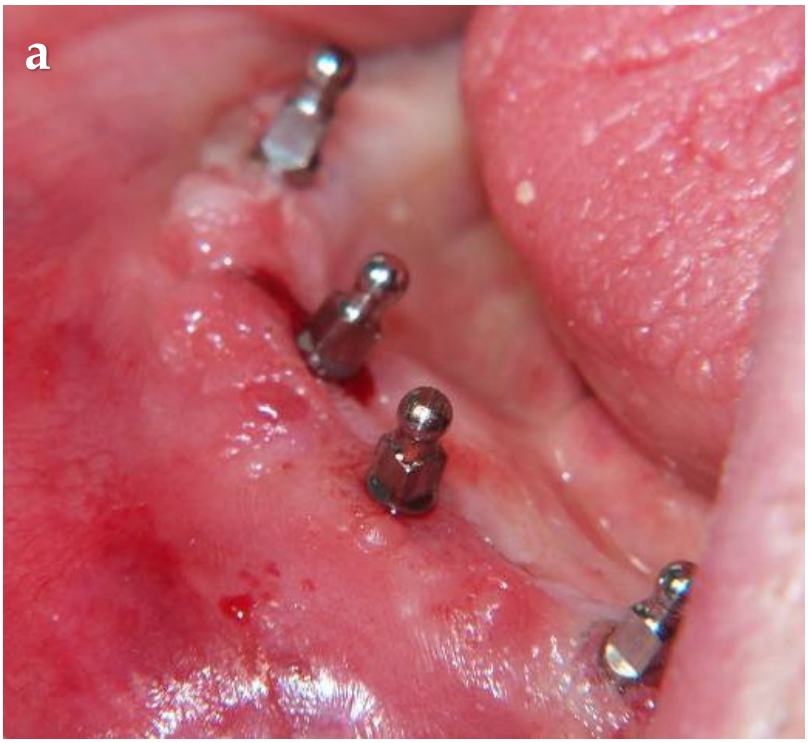

Figure 6.4.1 ***(a)*** *Mono-corpus implants with retention spheres (mini-implants), flapless inserted; immediate post-operative aspect.*

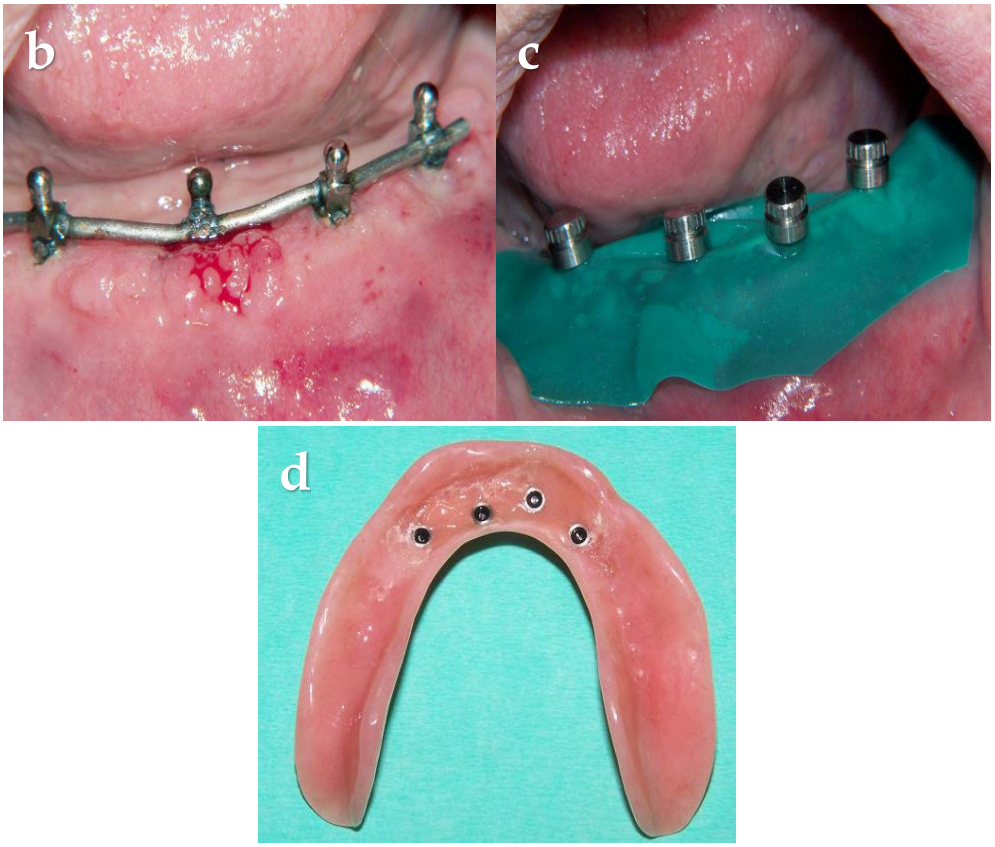

Figure 6.4.1 ***(b-d)*** *Sequence of the working phases, immediately postoperatively, illustrating the welding procedure and the insertion of the staple matrix into the acrylic prosthesis*

6.5 Special Interventions

In daily clinical practice, we frequently encounter complex cases in which treatment must be postponed to allow time for tissue regeneration, for the addition of supplementary implants to existing ones, or for implant placement in conjunction with bone defect management. Regardless of the clinical indication, intraoral welding provides an additional therapeutic option.

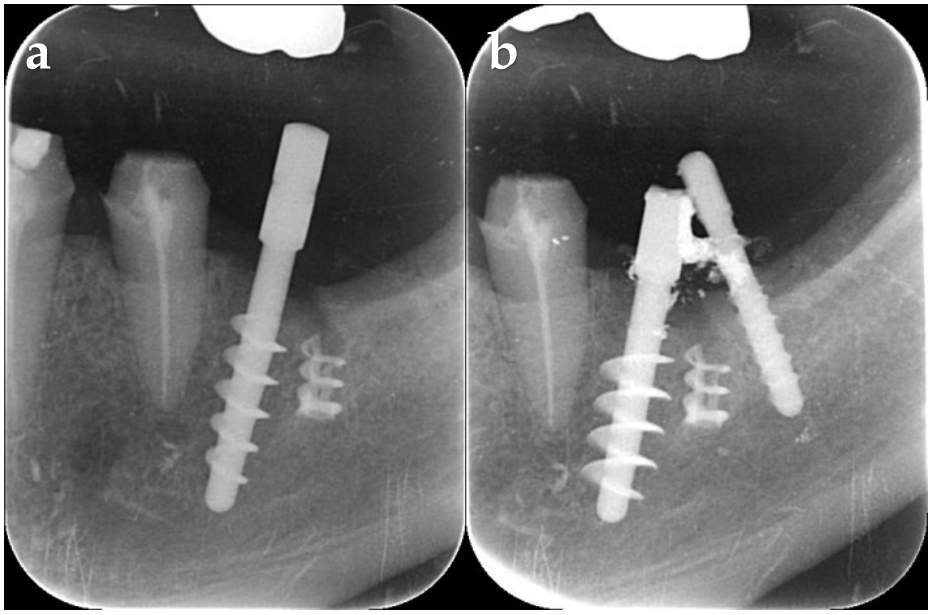

Figure 6.5.1 ***(a-b)*** *Radiographic aspect of a fractured implant that could not be completely removed from a severely atrophic ridge.*

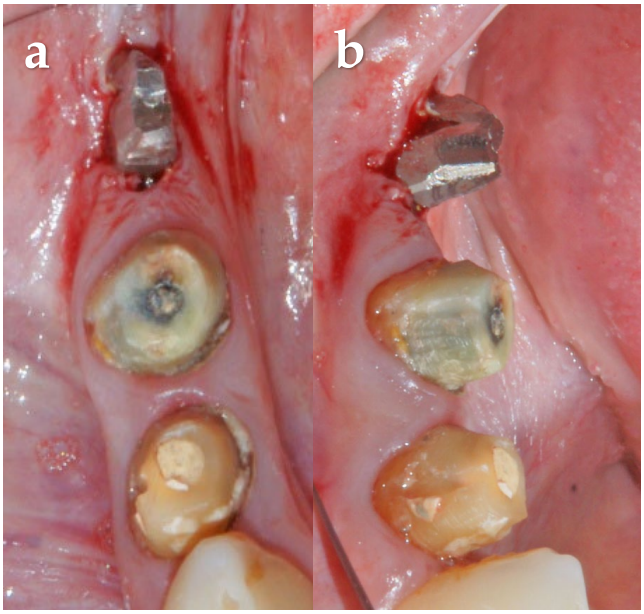

Figure 6.5.2 ***(a-b)*** *A fractured implant could not be entirely removed from a severely atrophic ridge. It was bypassed by placing two mono-corpus implants, which were then welded into a single prosthetic unit.*

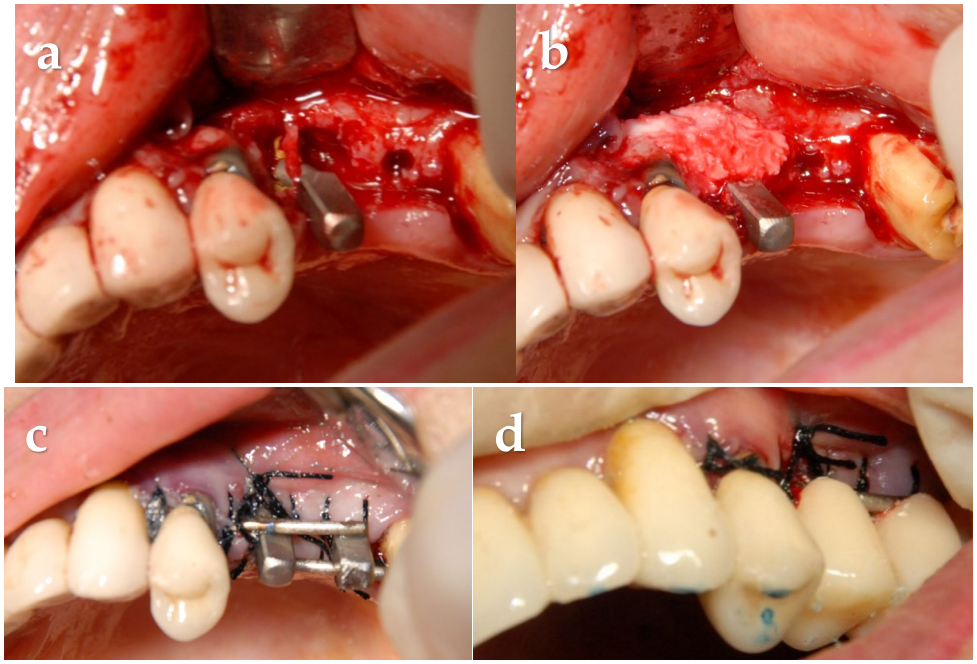

Figure 6.5.3 ***(a-d)*** *Extraction of two premolars and placement of implants in the presence of a significant bone defect. The implants were inserted following the available anatomical direction, then bent, welded, and provisionally prosthetized simultaneously with the bone defect management.*

7 The Operating Technique

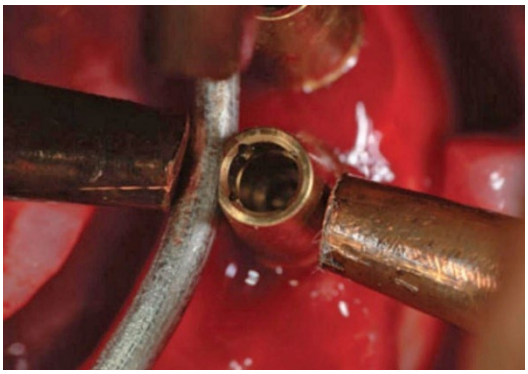

Figure 7.1 Image illustrating the components involved in the intraoral welding process.

1. The electrodes integrated in the welding forceps
2. The titanium bar
3. The prosthetic component of the implant

The welding procedure is straightforward, provided that the protocol is followed with absolute rigour. In describing the technique, I will begin by addressing a critical and well-known contraindication, patients with pacemakers. Once this aspect has been clarified during the treatment planning phase, the description of the operative technique may proceed.

7.1 Preparing the Surfaces

This step is carried out by obtaining shiny surfaces in the prefigured contact area. Both the titanium bars and the prosthetic component of the implant are covered with foreign chemical substances, such as oxides and other deposits, as well as organic materials normally present in the oral fluids and accumulated following the surgical intervention. To achieve the desired shine (i.e., exposure of the unoxidized metallic surface), standard abrasive methods with fine granulation are used. The simplest technique involves using polishing rubbers with the straight handpiece. Intraoral intervention with these is not

necessary, except in isolated cases involving mono corpus implants. In all other situations, surface preparation is carried out on the working table, directly on the bar and prosthetic abutments, which are first applied, then screwed in place, and finally welded.

The cleaning of organic elements is performed through standard cleansing of the wound area followed by decontamination of the metallic components, ending with thorough drying. The presence of residual moisture, especially inside the abutments, may lead to the occurrence of microelectric secondary discharges. While these do not affect the quality of the weld, they can be unpleasant during the operative act. Mechanical accessibility of the working field is also crucial, as the clinician must operate with complete manual comfort. The most frequent mistake or intraoperative incident is the presence of suture threads in close proximity to the abutment. These can unintentionally become interposed between the abutment and the bar, and during the electric discharge, produce a micro-flame or spark accompanied by a loud noise.

7.2 Choosing the Type of Connector

The variety of shapes and dimensions of titanium connectors available to us presents an apparently difficult choice. The main uses are as follows:

- **Bars (round profile), 0.5 mm diameter:** Highly ductile, these are used in multiple weldings in clinical situations where implants are significantly dispersed (with highly divergent axes) and where primary stability is reduced. Typically, a minimum of two bars are applied, followed by blocking out the entire structure with composite material.
- **Bars (round profile), 0.8 mm diameter:** Also used in double applications, suitable for cases with better primary

stability compared to the previous category.

- **Bars (round profile), 1.2 mm diameter:** These offer more rigid connections while occupying less space, making them suitable for application in the anterior area.
- **Bars (round profile), 1.5 mm diameter:** Provide rigid connection using a single bar, particularly indicated for the posterior regions.
- **Bars (round profile), 2.0 mm diameter:** Correspond to the Dolder bar system.

Figure 7.2.1 Double 1.2 mm bar, positioned orally and used to block out undercuts.

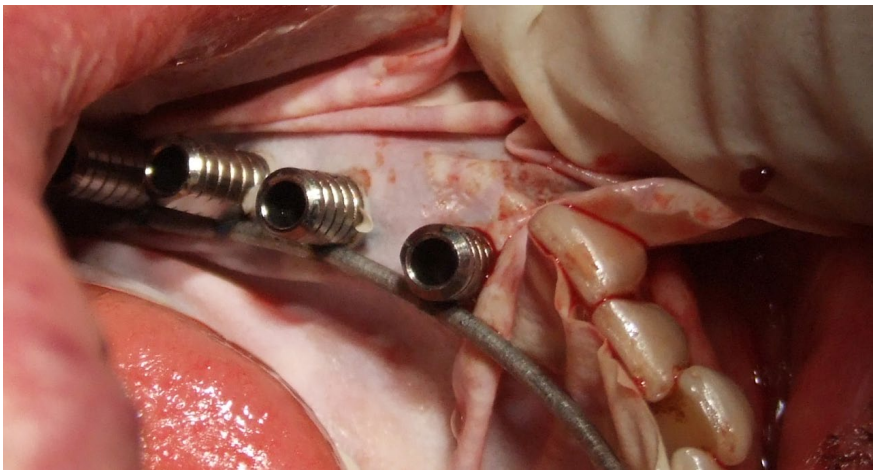

Figure 7.2.2 1.5 mm bar positioned orally. In the case of bi-component implants, the flat area of the prosthetic abutments can be utilized by placing it orally, thereby providing a greater contact surface compared to cylindrical abutments.

Figure 7.2.3 Clinical aspect after welding and removal of the rubber dam. The subsequent steps are: 1 Verification of screw torque using a dynamometric key, 2 Occlusal reduction and finishing of the sectioned bar ends, 3 Sealing the abutments with provisional material, 4 Placement of the provisional prosthesis.

Figure 7.2.4 Clinical view after removal of the prosthetic structure, highlighting the maintenance and soft tissue contouring achieved through immediate prosthetic loading.

The material from which these bars are made is predominantly grade 2 titanium, which is therefore ductile and can be easily processed. In cases involving larger diameters, even this material may be difficult to adapt intraorally to the clinical situation, thus a prior extraoral adjustment is recommended. Another form frequently used includes bars, more accurately referred to as flat bars or bars with a rectangular cross-section, where the smaller side follows

the longitudinal axis. The advantage of these flat tapes lies in the reduced oral space they occupy. However, the trade-off for this benefit is their decreased resistance to flexion in the oral–vestibular direction. To compensate for this mechanical limitation, the clinician may choose to apply an additional 0.5 mm bar on the vestibular side, if deemed necessary.

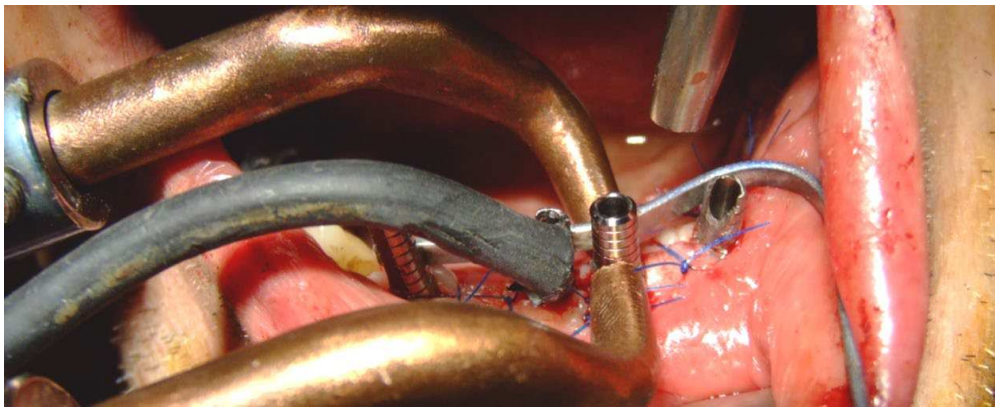

Figure 7.2.5 Welding of a titanium flat bar in the anterior mandibular region.

7.3 Preparation and Calibration of the Welding Apparatus

The variety of bar dimensions and prosthetic blunt combinations requires the adjustment of the electric impulse for each particular situation. This calibration is performed preoperatively, in a very straightforward manner, through successive trials. The device is initially activated at a minimum discharge, followed by gradual increases until a resistant weld is achieved without "burning" the welded area, an indicator of overloading. In Figure 7.3.1, the ideal appearance of the contact point can be observed.

The calibration phase is also when surface preparation is finalized, including the removal of any oxide layers on the electrode pliers. This can be done using a fine file in the case of copper electrodes, or an Arkansas stone for palladium ones.

For devices equipped with an argon gas source, this is the stage when gas pressure and flow rate are verified. Additionally, all accessories of the welding unit, particularly the rather heavy connecting cables, must be placed in optimal working positions.

Figure 7.3.1 The optimal aspect of the welding point.

7.4 Position and Direction of the Titanium Bars

The placement of the titanium bar is predominantly oral, for both aesthetic and hygienic reasons. The rationale is the following: oral placement, being relatively inconspicuous, allows for proper exposure of the welding area, thus enabling effective self-cleaning. Moreover, it ensures accessibility for routine oral hygiene measures, from toothbrushes to water picks.

Figure 7.4.1 Palatal placement of a 1.2 mm bar.

Starting from this fundamental principle, variations can be made based on clinical needs, as long as the primary objective is maintained, namely, the perfect immobilization of the implants and the even distribution of masticatory forces.

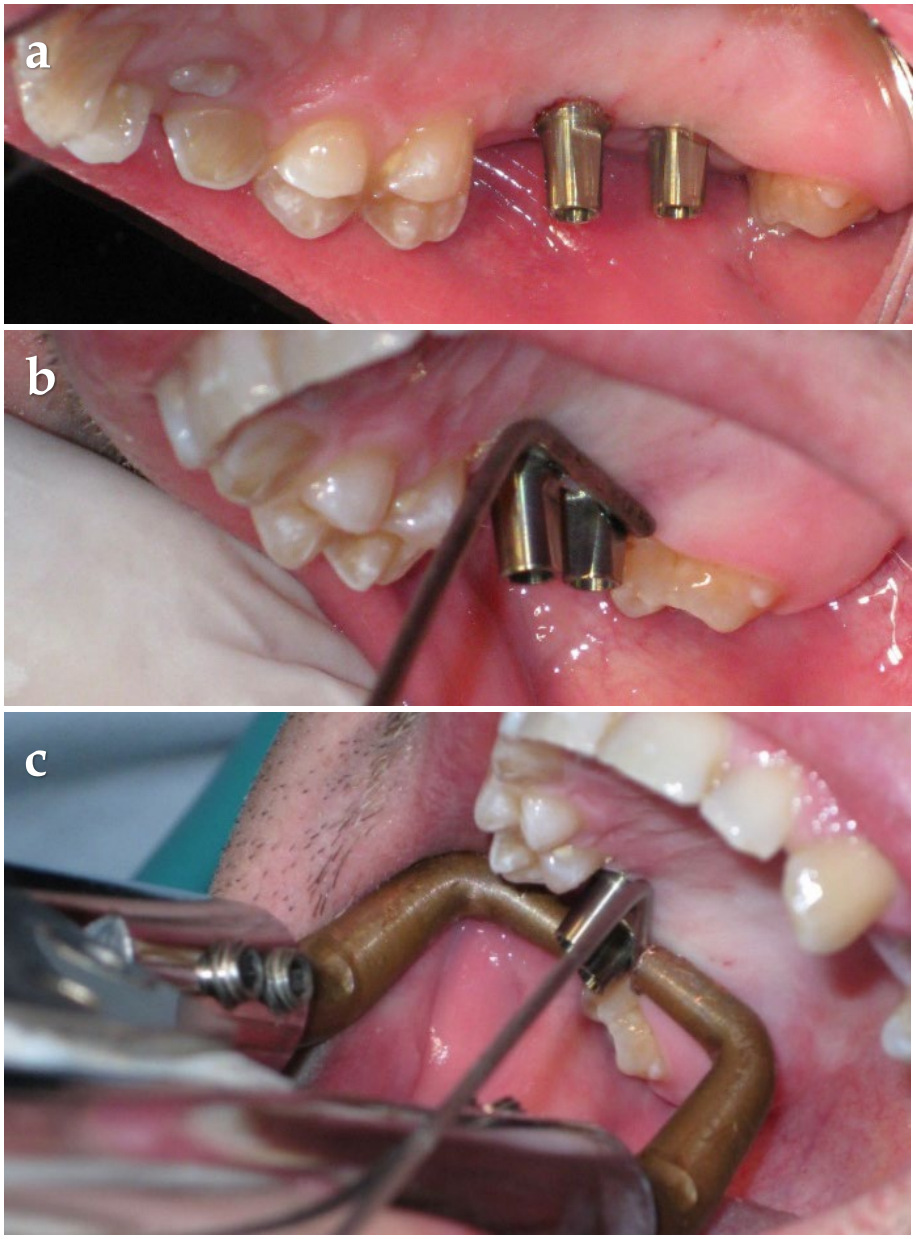

Figure 7.4.2 ***(a-c)*** *Sequence of welding phases using a 1.5 mm bar.*

Figure 7.4.5 Complete mandibular restoration with full welding using a double bar in the posterior lateral region.

Figure 7.4.6 Partial double immobilization in the region of 1.6-1.7.

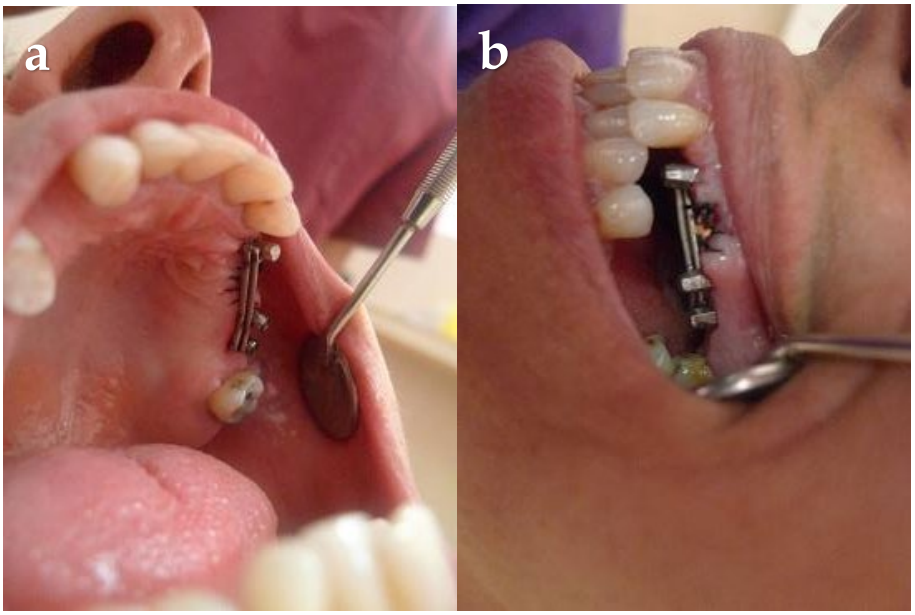

Figure 7.4.7 ***(a-b)*** *Double bar immobilization in the lateral segment using 1 mm bars.*

Figure 7.4.8 Combined oral-vestibular immobilization in the mandibular canine region (photo taken during provisional prosthesis removal, 4 months post-op).

8 Going Digital – Predictability at Its Finest *by Dr. Adam Aleksander Nowicki*

Contemporary technical skills and in-office procedures provide us today with a broader spectrum of clinical options. The following clinical cases illustrate how intraoral welding has offered us an irreplaceable advantage, allowing for the immediate immobilization of implants within minutes and at virtually no additional cost. The remainder of the prosthetic workflow was significantly enhanced through digital technologies.

Clinical Cases with Commentary

8.1 Case 1

The following case represents the treatment of a patient with severe maxillary atrophy and failing maxillary dentition.

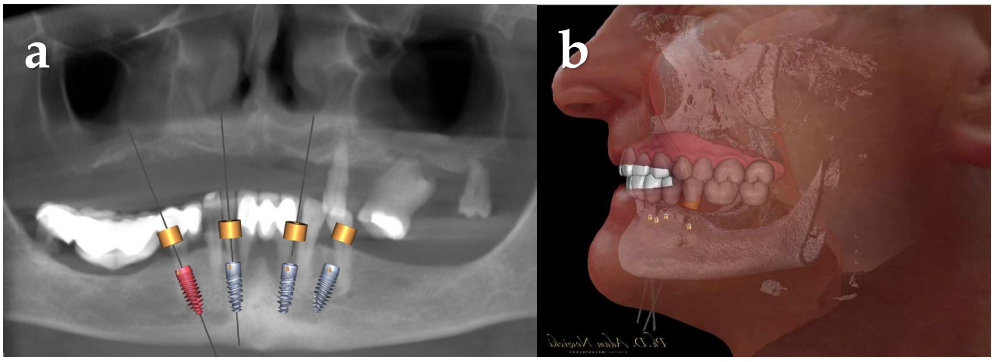

Figure 8.1.1 ***(a-b)*** *Preoperative planning integrating CBCT and facial scanning. The images demonstrate the prosthetically driven implant positioning strategy for the atrophic maxilla, guiding the trajectory of zygomatic and piriform implants in correlation with the future prosthetic design.*

The treatment plan was based on the integration of multiple digital data sources: CBCT, facial scanning, and intraoral scanning. Due to the advanced periodontal disease, the treatment was divided into three stages. The entire

procedure was conducted digitally, following the principles of prosthetically driven implantology. Additionally, all provisional prosthetic restorations were designed using digital smile design protocols.

Stage I involved the treatment of the lower arch by extracting the remaining dentition and placing four Trate Root implants (Ti grade 3) in the mandible using a pilot drill surgical guide. Intraoral welding was performed, using a 3D-printed shell retrofitted on-site, along with the delivery of an upper removable 3D-printed denture.

Stage II included the placement of two zygomatic implants, two implants anchored in the piriform rim, and one midline implant. These Medentis ICX implants (Ti grade 4) were inserted via fully guided surgery using a surgical guide. Both arches were immediately loaded by intraoral welding of multi-unit abutments with 2.0 mm Ti_2 wire and 3D-printed shells retrofitted intraorally.

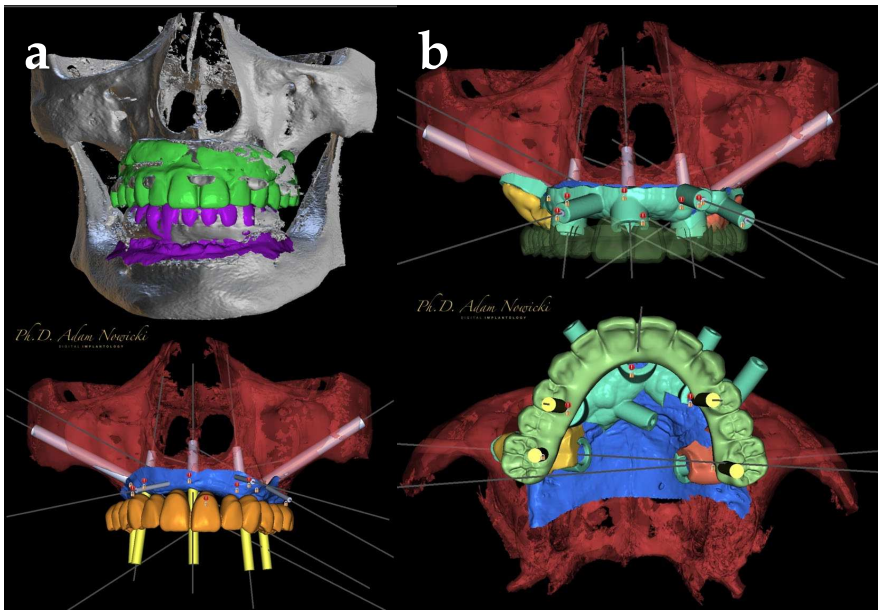

Figure 8.1.2 Surgical planning and guided procedure visualization: ***(a)*** *Digital integration of intraoral scan, bone structure, and planned prosthesis;* ***(b)*** *Navigation planning for implant placement using triple-stacked surgical guides;*

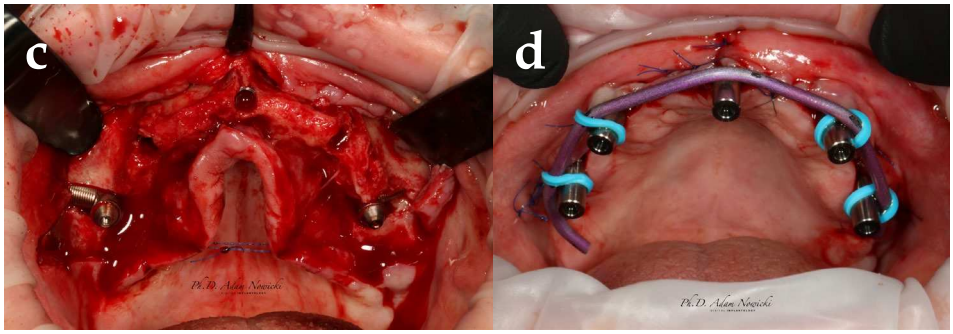

Figure 8.1.2 Surgical planning and guided procedure visualization: ***(c)*** *Intraoperative view following extractions and bone reduction;* ***(d)*** *Immediate intraoral welding of the titanium bar using elastic orthodontic connectors for stabilization.*

To ensure accurate positioning of the titanium bar during welding, elastic orthodontic connectors were employed. Following welding, the connectors for the multi-unit abutments were detached, and the entire structure was finished by the in-office dental technician.

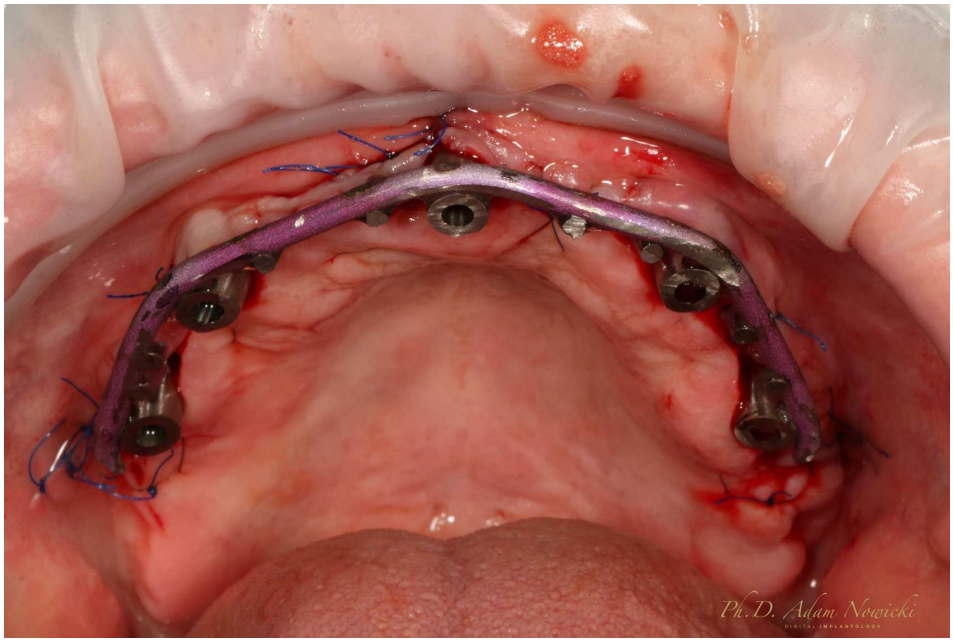

Figure 8.1.3 Postoperative clinical view showing the welded titanium framework in place, with multi-unit abutments secured and soft tissue sutured, ensuring passive fit and initial tissue adaptation.

Stage III concluded with the delivery of two milled ceramic superstructures supported by a titanium milled bar, forming the final screw-retained restorations. Intraoral scanning was performed using scan flags (horizontal scan bodies).

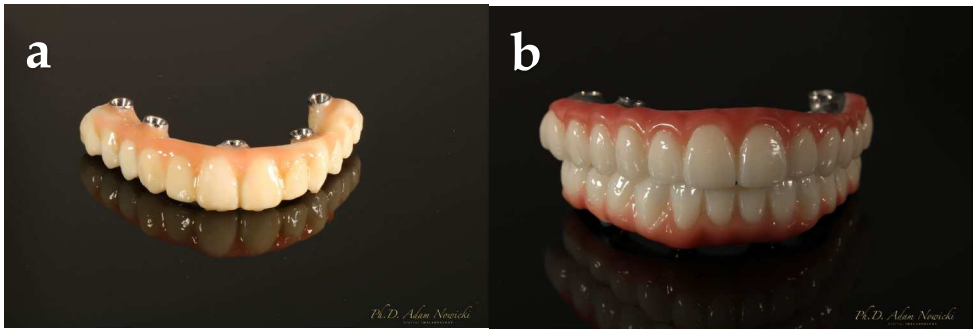

Figure 8.1.4 ***(a)*** *Final screw-retained lower arch ceramic prosthesis on a milled titanium framework;* ***(b)*** *Full-arch upper ceramic restoration demonstrating optimal aesthetic integration and occlusal design, digitally planned and fabricated.*

8.2 Case 2

This case presents the complete treatment of a patient with residual dentition and compromised aesthetics due to the Popov-Godon phenomenon, migration of natural teeth caused by the absence of opposing occlusal contacts.

The treatment planning involved facial scanning, intraoral scanning, extraoral photographs in smile, and CBCT imaging. As aesthetics were just as important to the patient as functionality, Digital Smile Design (DSD) was essential to meet these expectations.

The digitally defined ideal tooth arch position dictated the placement of Trate Root implants (six in the maxilla and four in the mandible) and highlighted the need for bone reduction. Due to the Godon phenomenon, excessive bone volume would have compromised the prosthetic restoration.

Two triple-layered, stacked surgical guides were

designed and 3D-printed from specialized resin for both the maxilla and mandible. The first guide, placed on the residual teeth, established the accurate positioning of the second guide, which was pinned to the bone and used both for alveolar bone reduction and as a base for the third guide, dedicated to fully guided implant placement.

Immediate loading was achieved through intraoral welding using 2.0 mm titanium wire (grade 2), creating a rigid frame for long-term provisional prosthetic rehabilitation.

After six months of healing, all-ceramic milled superstructures on anodized titanium bars were delivered, and occlusion was verified using a dedicated electronic device.

This case is noteworthy for its integration of Digital Smile Design, guided bone reduction, and immediate loading on a welded titanium framework, all meticulously planned from the initial diagnostic phase, leveraging the full potential of digital dentistry.

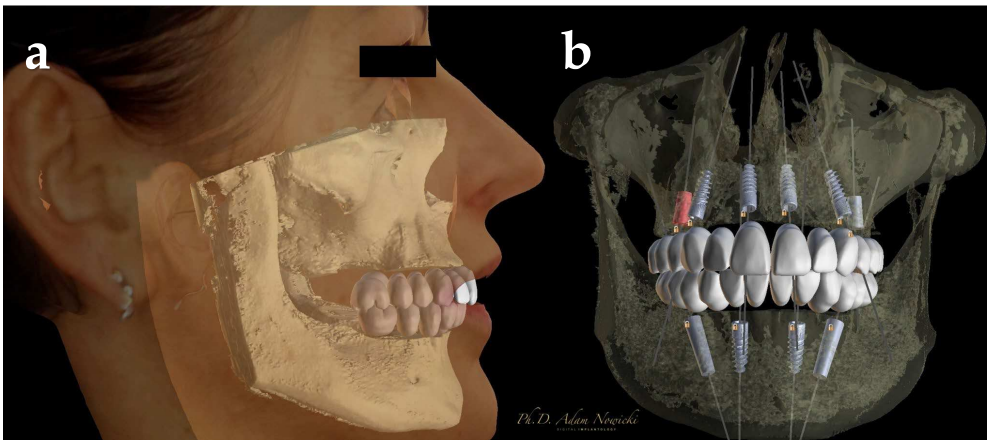

Figure 8.2.1 ***(a)*** *Facial profile rendering showing the skeletal anatomy overlaid with virtual teeth positioning.* ***(b)*** *Frontal view of the maxillary and mandibular virtual implant planning, highlighting implant angulations and prosthetically guided placement.*

Figure 8.2.2 Frontal digital simulations of the patient's smile before and after virtual prosthetic restoration, illustrating the esthetic improvements achieved through Digital Smile Design.

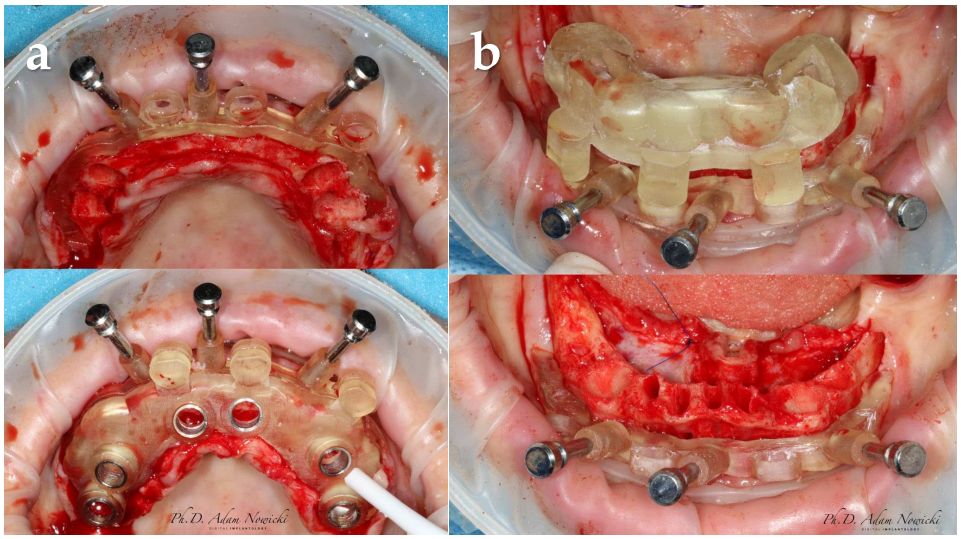

Figure 8.2.3 ***(a)*** *Initial surgical exposure of the maxilla and placement of temporary abutments.* ***(b)*** *Placement of the second surgical guide for alveolar bone reduction.* ***(c)*** *Fully pinned surgical guide in place, confirming the positions for guided implant insertion.* ***(d)*** *Final alveolar preparation completed, showing multiple implant placements guided by the surgical template.*

Figure 8.2.4 Immediate postoperative intraoral view showing the intraorally welded titanium framework secured to multi-unit abutments in both arches, ensuring immediate stabilization and occlusal support.

Figure 8.2.5 Final screw-retained ceramic restorations fabricated on anodized titanium bars, representing the definitive prosthetic outcome for both arches.

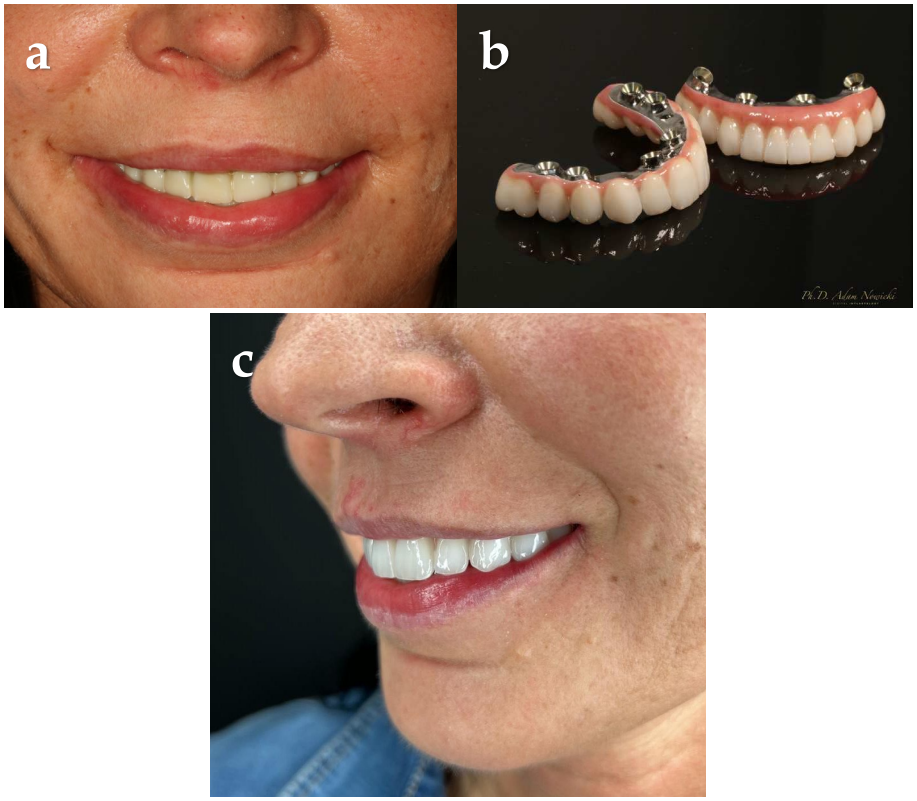

Figure 8.2.6 ***(a)*** *Frontal smile photograph of the patient with the final restorations in place.* ***(b)*** *Extraoral view of the upper and lower definitive prostheses.* ***(c)*** *Lateral view of the patient post-treatment, demonstrating the esthetic and functional harmony achieved.*

8.3 Case 3

This case presents a severely atrophied maxilla in a patient who had been wearing a removable prosthesis for over 30 years. The initial planning phase involved comprehensive data collection, including CBCT imaging, intraoral scanning, and 2D Digital Smile Design (DSD) based on dental photography. As the primary concern expressed by the patient was impaired function, particular emphasis was placed on functional rehabilitation.

Due to the vertical bone deficiency, a monoblock compressive implant system was selected to manage the case. Trate compressive implants (Ti_6Al_4V) were placed using a 3D-printed pilot drill surgical

guide. Subsequently, conometric caps were positioned on the abutments, and a 2.0 mm titanium wire was intraorally welded to create a rigid titanium framework. This framework was then adapted to a 3D-printed shell. Following mucosal ovate pontic shaping and polishing, the temporary prosthesis was immediately delivered as a long-term provisional restoration. After the healing phase, the case was finalized with a definitive prosthesis by another clinician.

Afterword:

The technologies utilized in the cases presented above can be seamlessly integrated into a single, comprehensive treatment protocol, offering enhanced predictability, esthetic excellence, and consistent clinical outcomes. All procedures were performed in a single surgical session. The synergy between digital workflows and intraoral welding provides a powerful tool for restoring both function and esthetics in patients with compromised periodontal conditions.

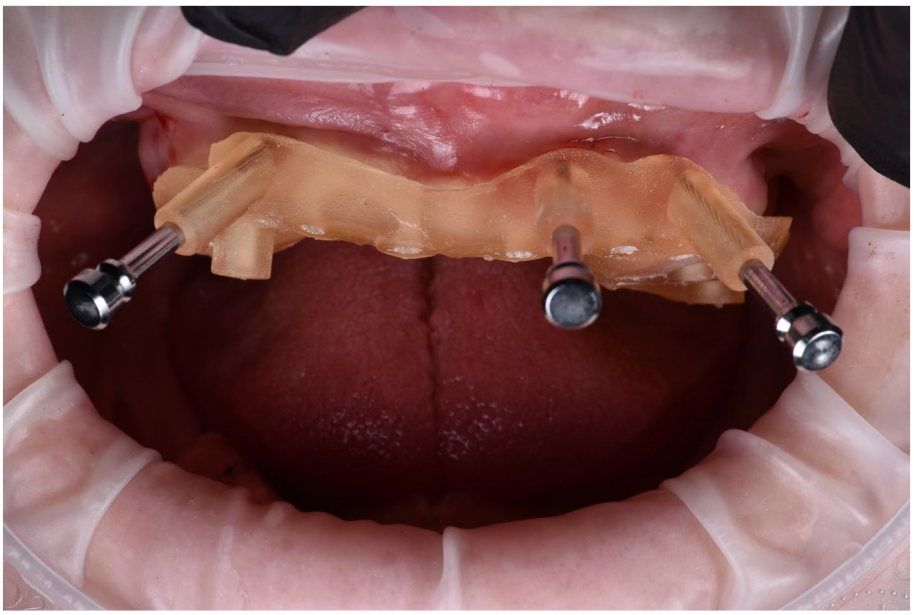

Figure 8.3.1 Surgical pilot guide stabilized in situ during implant placement. The guide was designed and 3D-printed to ensure accurate positioning of the compressive implants in the atrophic maxilla.

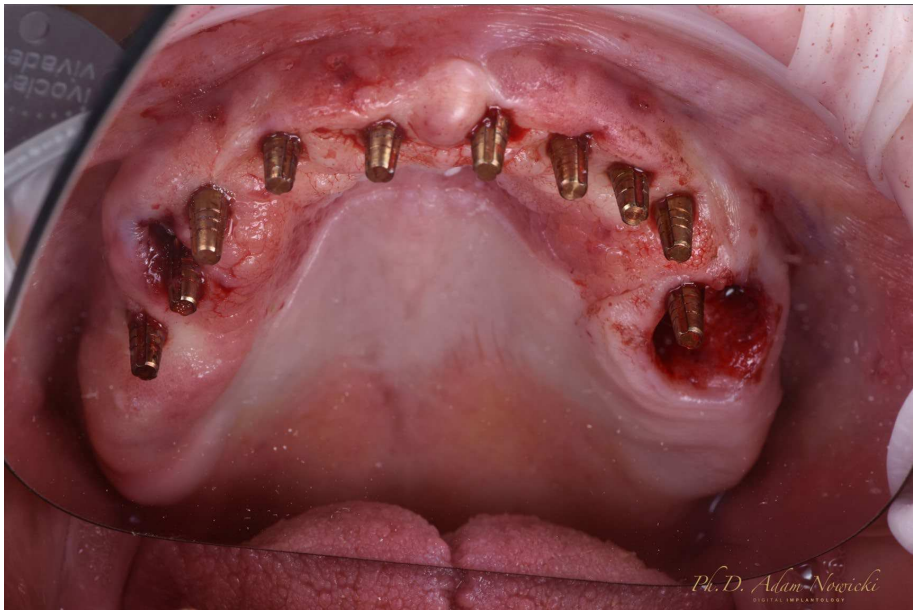

Figure 8.3.2 Palatal view following implant placement. A total of ten compressive implants (Trate Ti_6Al_4V) were successfully inserted using the guided protocol.

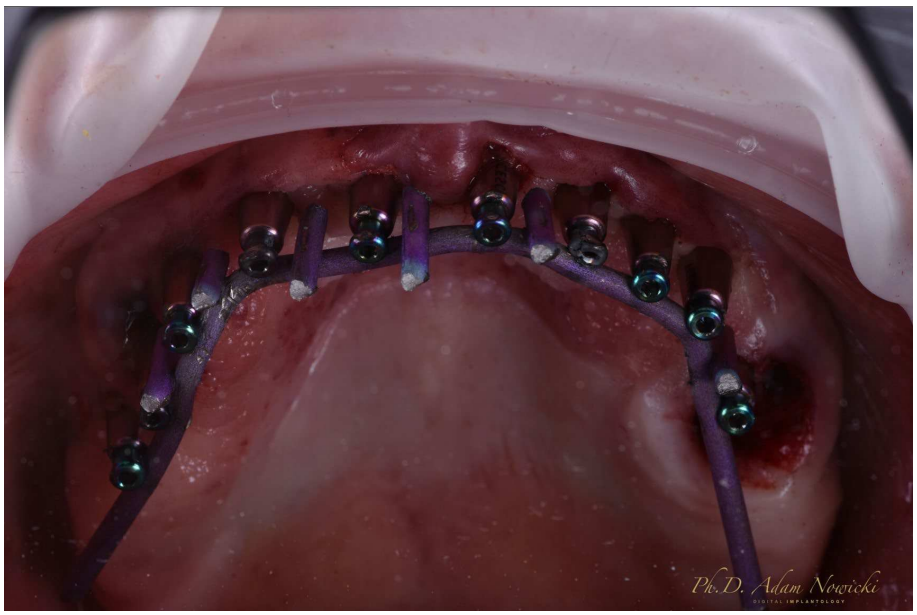

Figure 8.3.3 Intraoral welding of the 2.0 mm titanium wire to the conometric abutments. This created a rigid primary structure for the immediate temporary prosthesis.

Figure 8.3.4 Tissue side view of the 3D-printed provisional prosthesis, adapted to the welded titanium bar for immediate loading.

Figure 8.3.5 Provisional prosthesis in place immediately postoperatively. The restoration was shaped and polished for mucosal adaptation and esthetics.

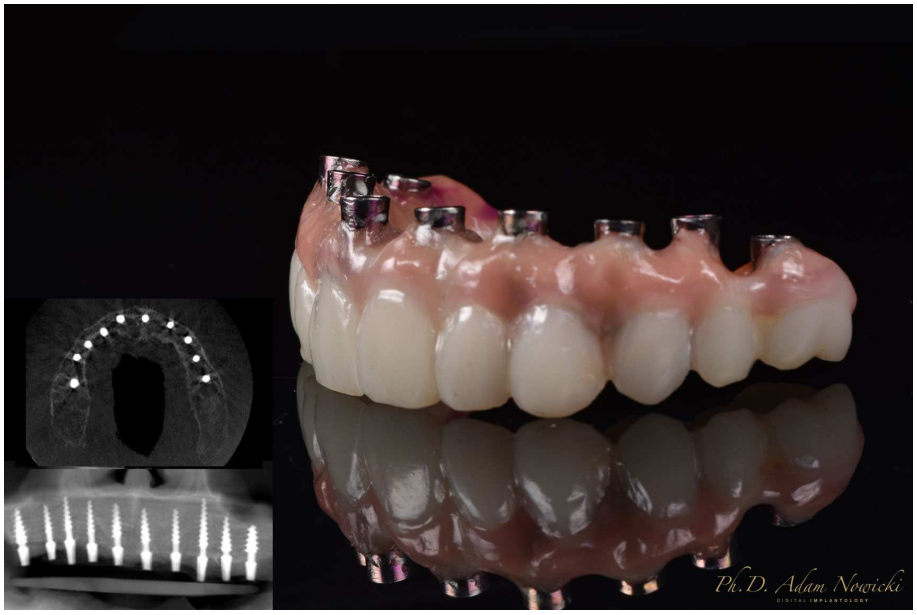

Figure 8.3.6 Definitive prosthetic restoration delivered after the healing period. Radiographic verification (CBCT and panoramic view) confirms the optimal positioning and integration of the implants and final framework.

9 Retro-Innovation and Clinical Elegance: Functional Rehabilitation with Intraoral Welding and Needle Implants *by Dr. Marco Bellina and Dr. Grigore Lăzărescu*

Everyday Procedures Every Dental Office Can Perform (With Video)

Contemporary implantology often prioritizes digital workflows, multi-stage surgeries, and increasingly complex components. Yet, real-world clinical situations, particularly involving elderly patients, limited bone volume, or economic constraints, frequently call for a return to the essentials: mechanical logic, reduced invasiveness, and speed.

This chapter revisits so-called "retro" concepts, needle-type implants such as Tramonte, Garbaccio, and Scialom, as well as intraoral welding, not as outdated relics, but as refined strategies grounded in biomechanics. These methods prioritize immediate stabilization, minimized trauma, and functional efficiency.

Rather than showcasing high-tech innovation, the following cases demonstrate clinical intelligence: the ability to adapt tried-and-tested methods to today's challenges. Simplicity, when applied with expertise, becomes a form of elegance.

9.1 Clinical Cases *by Dr. Marco Bellina*

Dr. Marco Bellina's surgical philosophy embodies a modern reinterpretation of classical implantology principles: rapid functional rehabilitation through essential biomechanics. His work centers on the use of slender, self-tapping implants (Tramonte, Garbaccio) and intraoral welding to achieve immediate stabilization, often within a single session.

What sets Bellina apart is not only his mastery of surgical minimalism, but also his strategic thinking: leveraging angulation,

bone quality, and prosthetic planning to bypass the need for regenerative techniques or extensive delays. His protocols are not merely cost effective, they are biologically considerate and time sensitive.

The following cases reveal how Bellina turns apparent clinical limitations into opportunities, combining precision and pragmatism to deliver long-term stability without overcomplicating treatment. In his hands, retro becomes revolutionary.

9.1.1 Case 1

A male patient presenting with a missing upper left canine was treated using a single **Tramonte-type implant** (4 mm diameter, 7 threads), which was stabilized in a secondary phase using a **Scialom needle**, thereby achieving a **bipod support configuration**. The two components were subsequently **intraorally welded**, the abutment was **milled to receive the prosthetic crown**, and a **provisional crown** was fitted.

The Tramonte-type implant was **angulated (bent) intraorally** to accommodate the prosthetic requirements. Once the Scialom needle was inserted, it provided the necessary additional stabilization for immediate function.

Figure 9.1.1.1 Initial intraoral situation of the maxillary left canine region. The edentulous space is bordered by heavily restored or structurally compromised neighboring teeth, emphasizing the need for a minimally invasive and immediate functional solution.

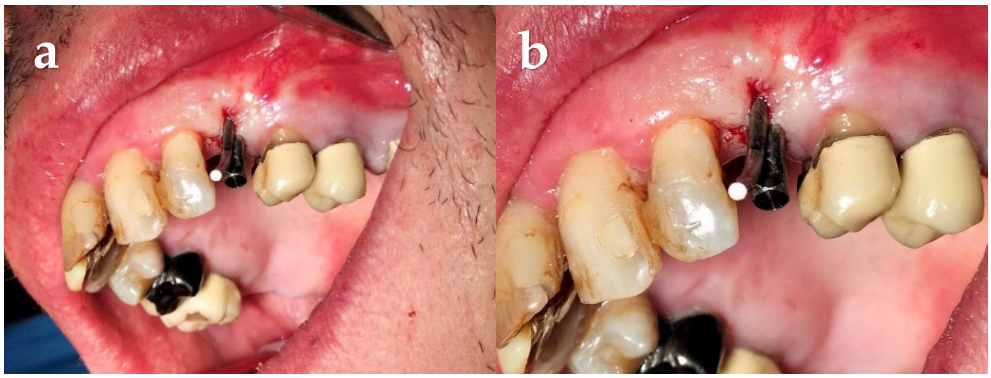

Figure 9.1.1.2 ***(a)*** *Lateral view and* ***(b)*** *close-up of the insertion of a Tramonte-type implant (4 mm diameter, 7 threads), stabilized by a Scialom needle to create a bipod support configuration. This stage sets the foundation for immediate functional rehabilitation.*

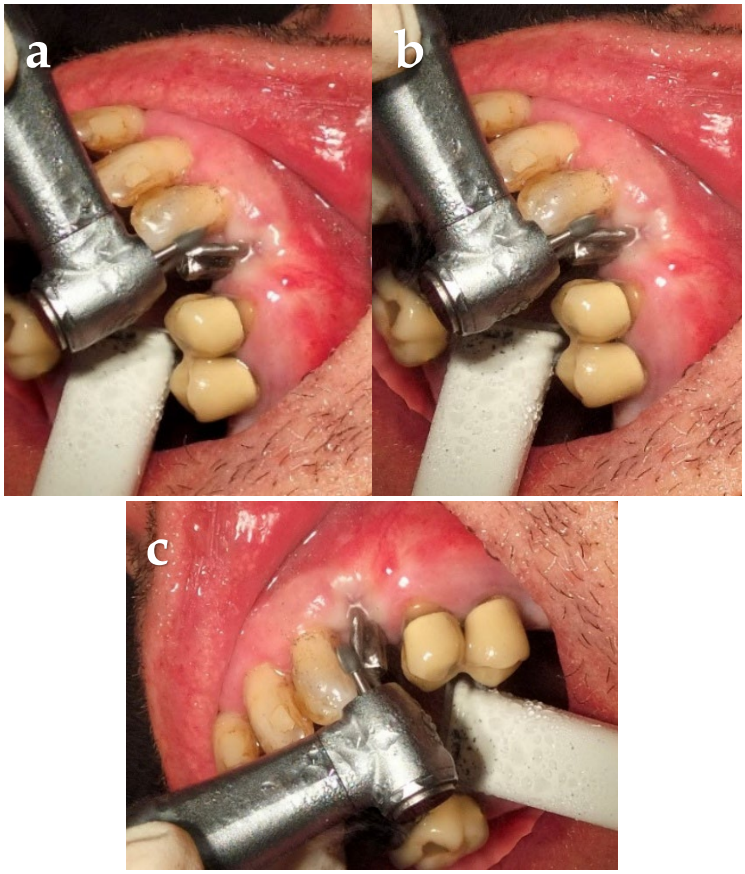

Figure 9.1.1.3 ***(a-c)*** *Intraoral adjustment of the abutment complex using rotary instrumentation after intraoral welding of the Tramonte implant to the Scialom needle. This step refines the prosthetic axis and prepares the structure for crown placement.*

Figure 9.1.1.4 Final outcome after polishing and shaping of the intraorally welded abutment complex. The prosthetic platform is now ready for provisionalization.

Figure 9.1.1.5 Provisional crown cemented immediately after implant stabilization and abutment preparation. Functional and esthetic integration is obtained within a single clinical session.

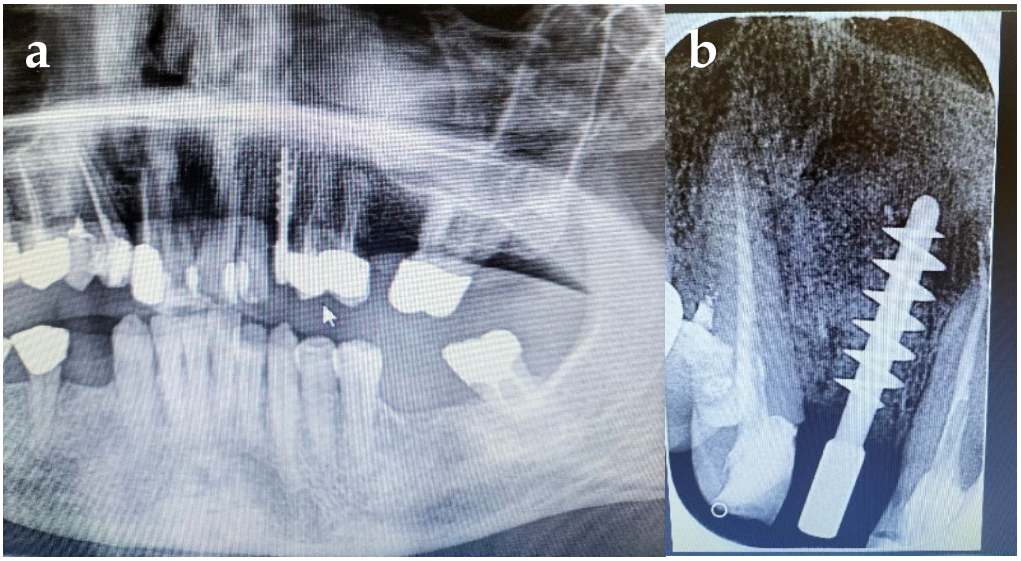

Figure 9.1.1.6 ***(a-b)*** *Postoperative radiographic evaluation confirming correct positioning of the Tramonte implant and stable peri-implant bone interface, suggestive of successful early osseointegration.*

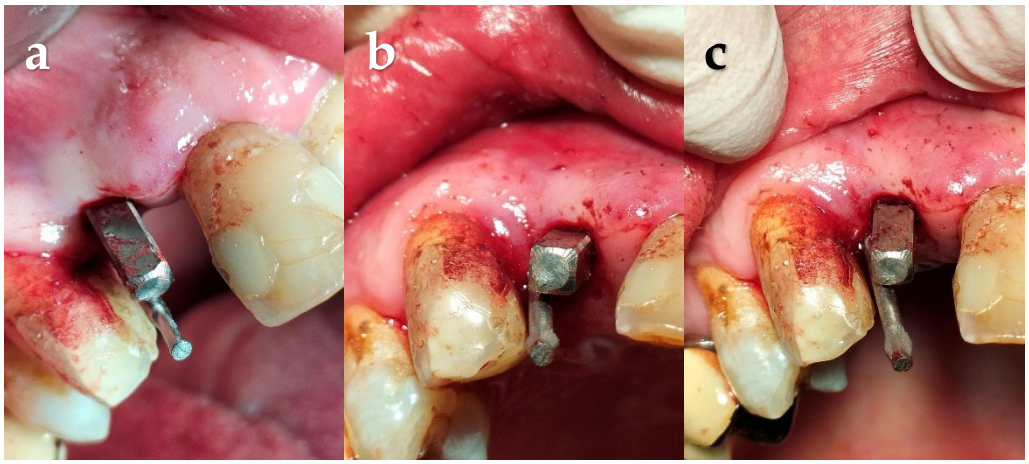

Figure 9.1.1.7 ***(a-c)*** *Multiple intraoral views of a second Tramonte-type implant placed in the right lateral incisor site, also stabilized using a Scialom needle, following the same biomechanical protocol.*

Figure 9.1.1.8 Intraoral welding of the second implant to its corresponding Scialom needle, showing a rigid metallic unit designed to resist micromovements during osseointegration.

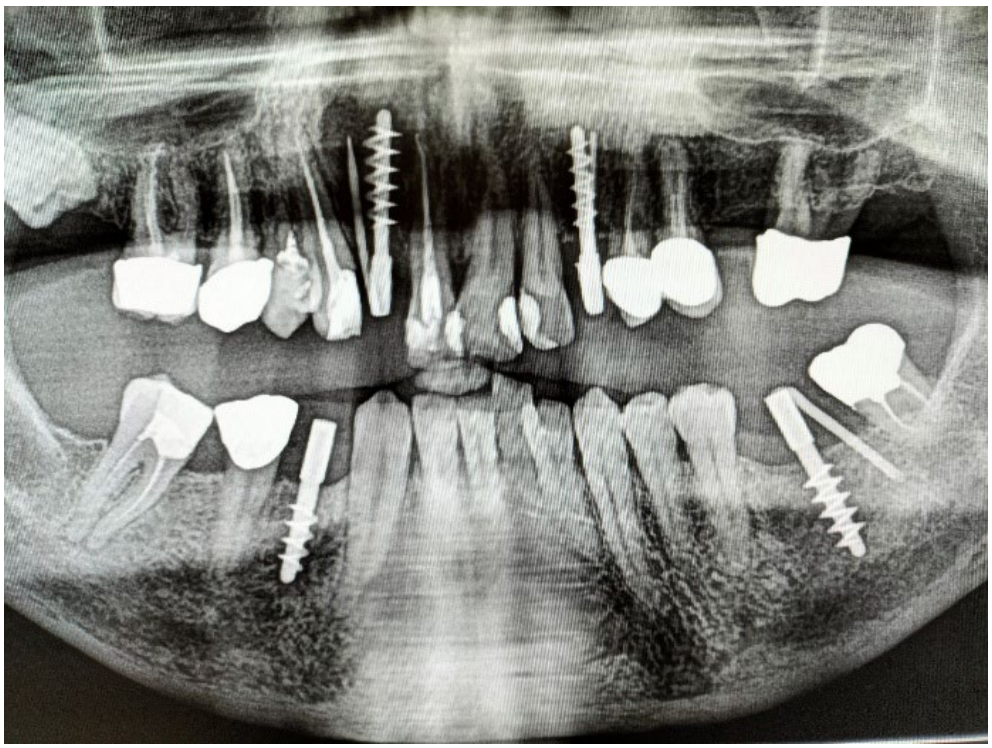

Figure 9.1.1.9 Final panoramic radiograph showing both the maxillary left and right implants, each stabilized with Scialom needles and integrated into the full arch rehabilitation plan.

9.1.2 Case 2

A patient presenting with an anterior mandibular edentulous space (in the region of the lower incisors) was treated with the insertion of two **Garbaccio-type no. 4 implants**. The implants **were joined using a 2 mm bar** and stabilized through **intraoral welding**, followed by the fitting of a **provisional acrylic bridge**.

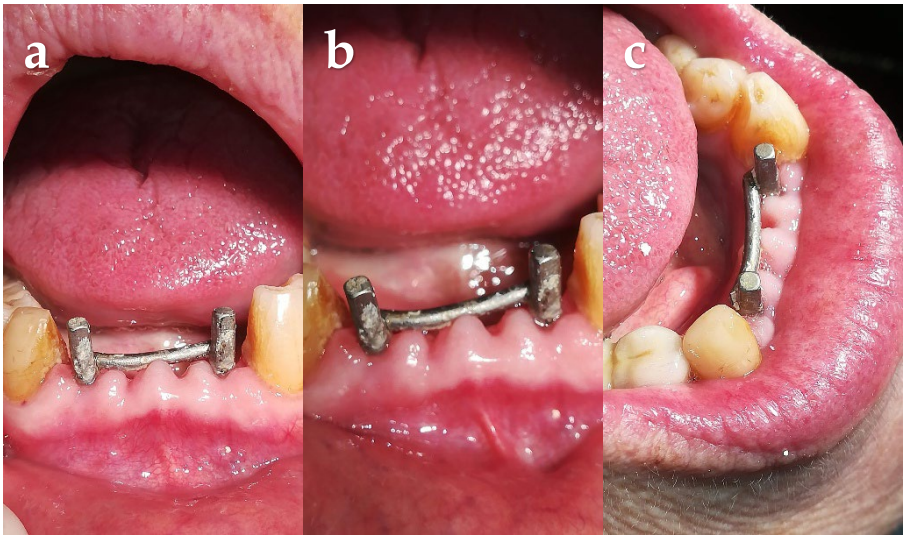

Figure 9.1.2.1 ***(a-c)*** *Intraoral view of the anterior mandibular edentulous region after placement of two Garbaccio-type no. 4 implants, stabilized with a 2 mm titanium bar through intraoral welding. The bar ensured primary splinting and immediate mechanical stability across the implants.*

Figure 9.1.2.2 Provisional acrylic bridge in place over the intraorally welded implants, ensuring functional loading and esthetic continuity during the healing phase.

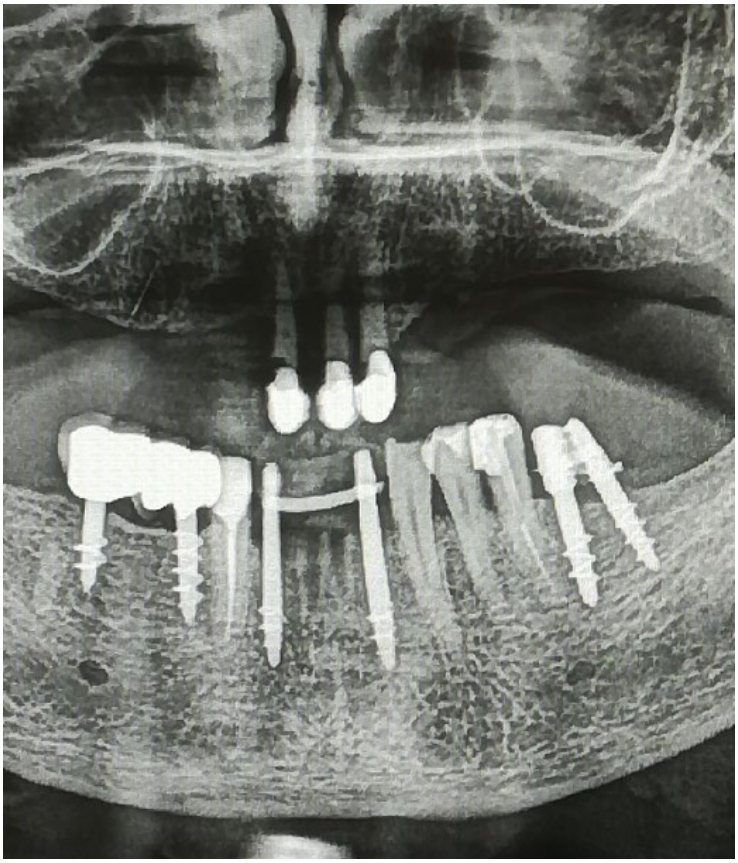

Figure 9.1.2.3 Final panoramic radiograph showing the two Garbaccio-type implants in the interforaminal region, splinted with a transverse titanium bar and supporting the provisional fixed restoration.

Watch the video here!

https://youtu.be/vaFs3RUmj3A?feature=shared

9.1.3 Case 3

Fracture of two pre-existing bi-component implants, with the apical fragments remaining deeply positioned in proximity to the **inferior alveolar nerve (IAN)**. Two **Garbaccio-type implants** were immediately placed and **intraorally welded** using a **1.5 mm vestibular bar**. The abutments were **height-adjusted and milled**, preserving the remaining structure.

After a healing period of three months, the bar was removed, the abutments were **reconditioned**, and the case was finalized with the placement of the **definitive prosthetic restoration**.

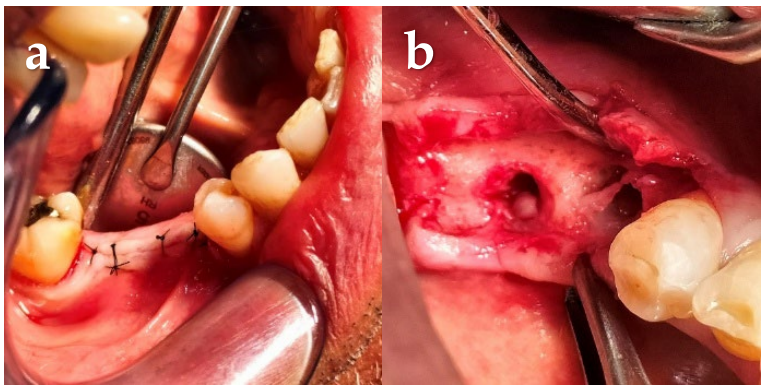

Figure 9.1.3.1 ***(a)*** *Clinical view prior to suture removal following the extraction of fractured bi-component implants;* ***(b)*** *Surgical exposure of the healed site, revealing the post-extraction bone architecture.*

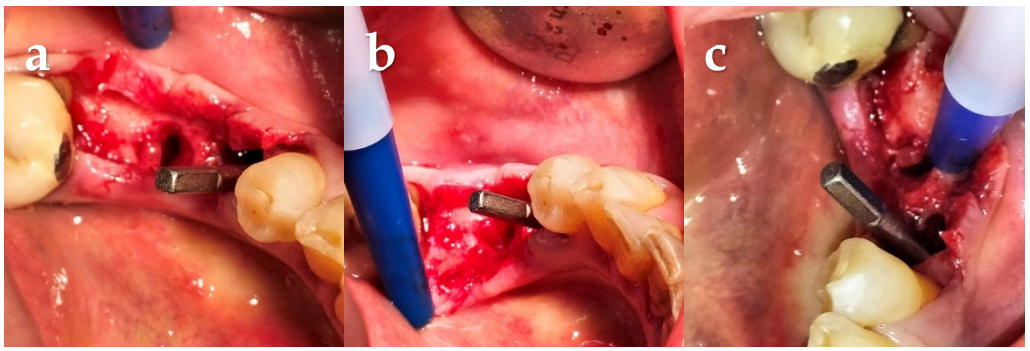

Figure 9.1.3.2 ***(a-c)*** *Implant site preparation and immediate placement of two Garbaccio-type implants in the posterior mandibular region.*

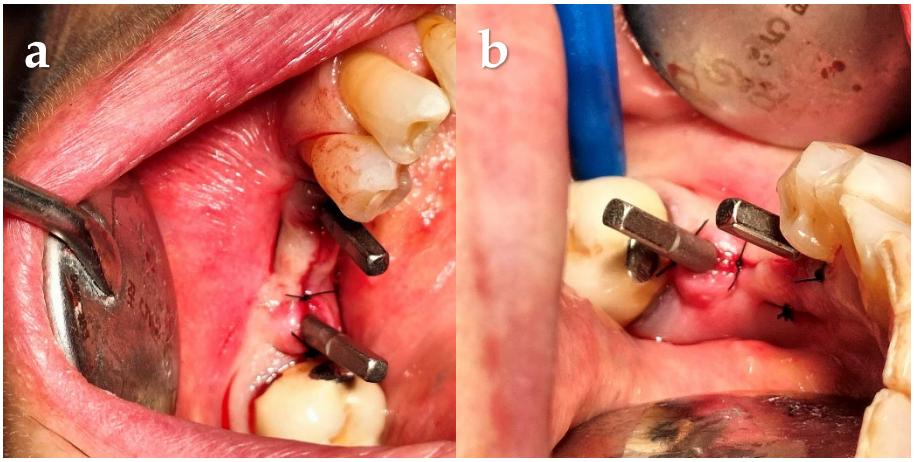

Figure 9.1.3.3 ***(a-b)*** *Primary closure of the surgical wound following implant placement, achieved through careful suture adaptation of the soft tissues.*

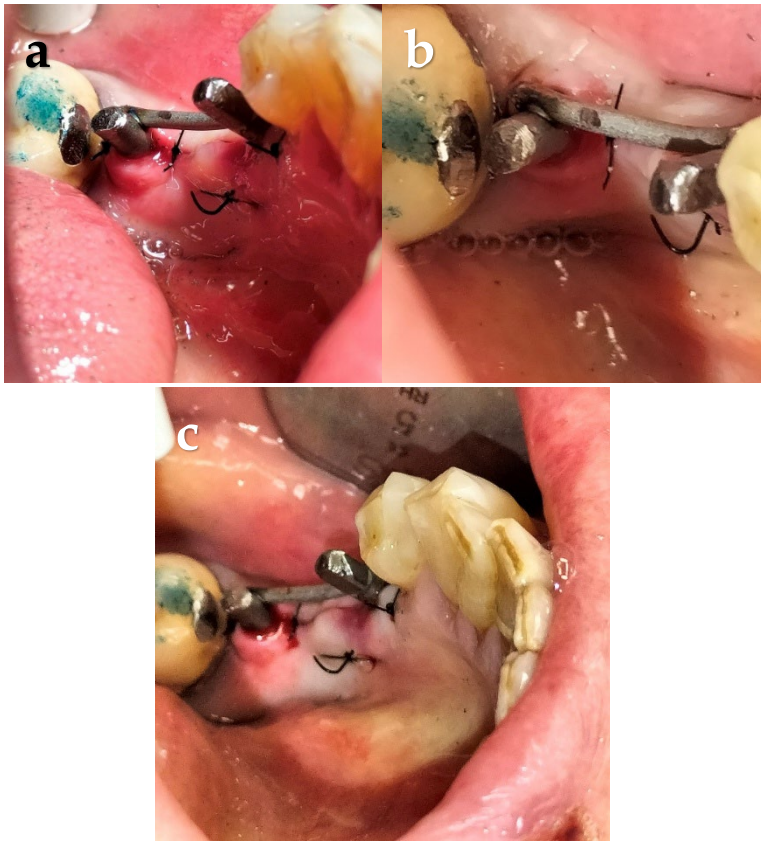

Figure 9.1.3.4 ***(a-c)*** *Intraoral welding procedure of the two Garbaccio-type implants using a 1.5 mm vestibular titanium bar, viewed from multiple angles to demonstrate the spatial orientation and stabilization.*

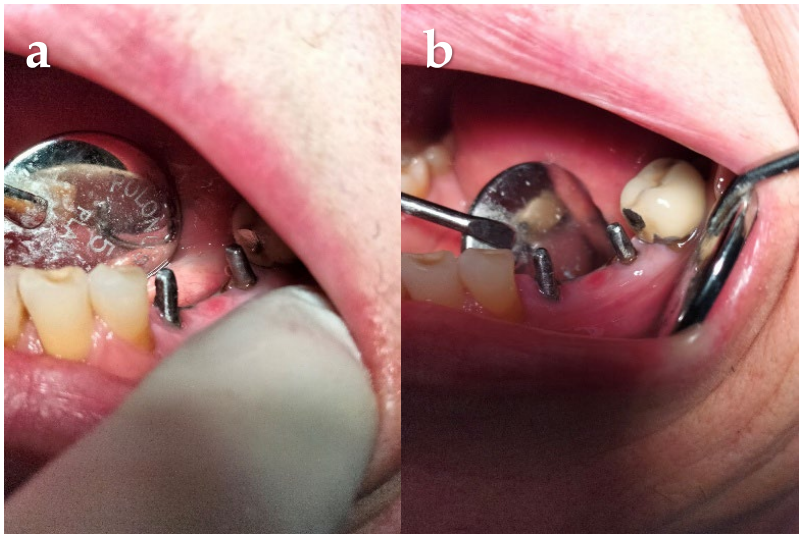

Figure 9.1.3.5 ***(a-b)*** *Post-welding intraoral images showing the Garbaccio implants after removal of the stabilization bar, with peri-implant tissue healing underway.*

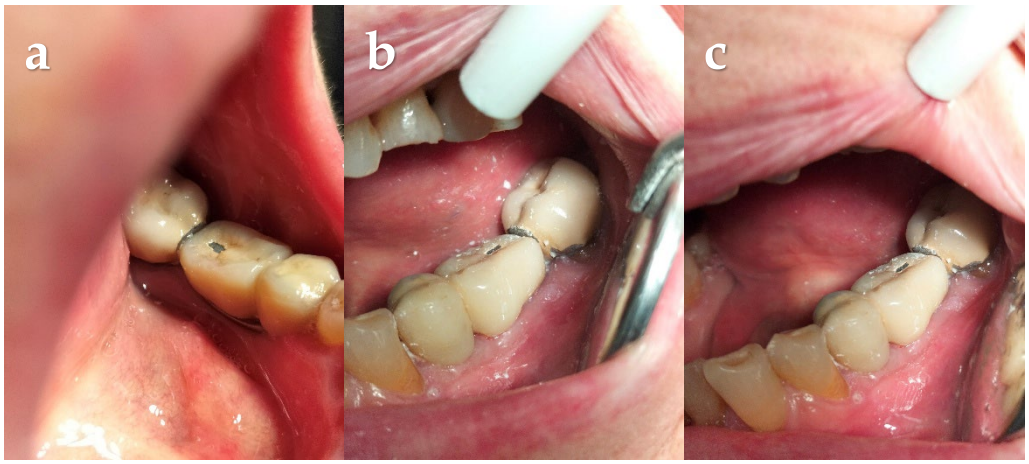

Figure 9.1.3.6 ***(a-c)*** *Provisional prosthetic restoration delivered on the healed implants, ensuring functional and aesthetic rehabilitation during the osseointegration period.*

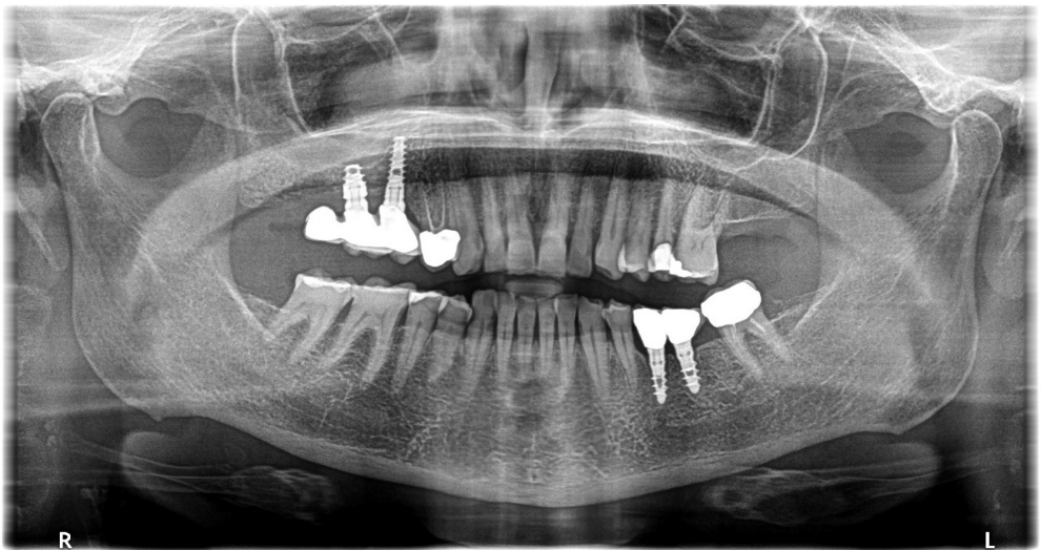

Figure 9.1.3.7 Initial panoramic radiograph showing the two bi-component implants in place, prior to fracture.

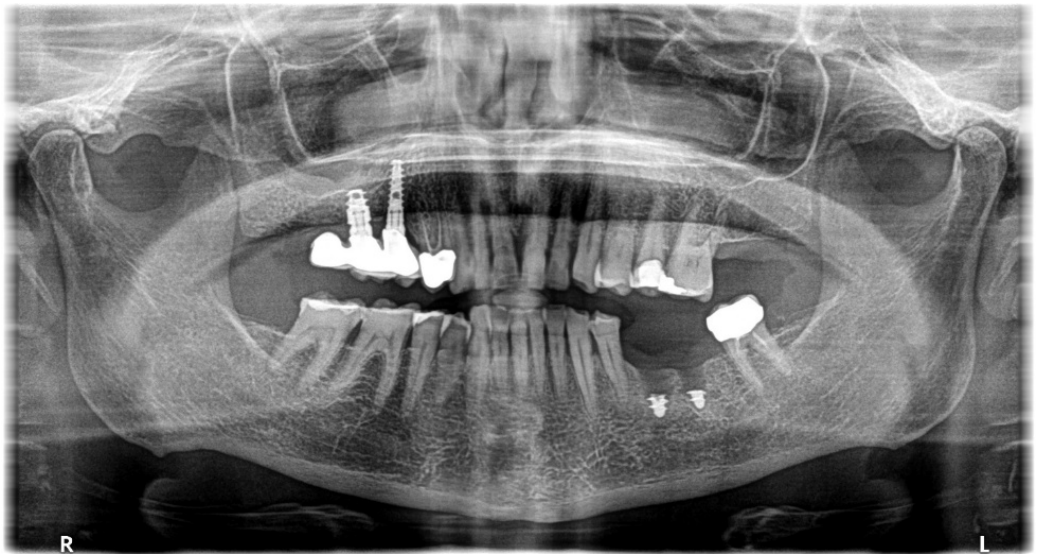

Figure 9.1.3.8 Post-fracture panoramic radiograph displaying the residual apical fragments of the broken implants, retained near the inferior alveolar nerve (IAN).

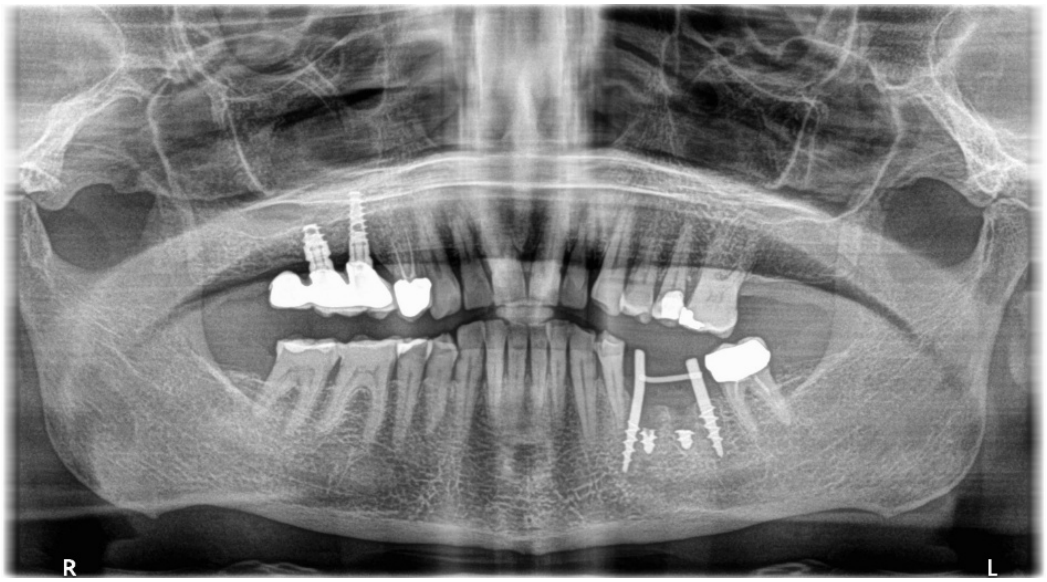

Figure 9.1.3.9 Final radiographic outcome showing the placement of the Garbaccio-type implants alongside the retained apical remnants of the previously fractured implants.

9.1.4 Case 4

An attempt was made to place three post-extraction implants; however, due to unfavorable clinical conditions, only the central **two-stage implant** could be successfully inserted at the time. Following the osteointegration period, the site was re-accessed, and two **Tramonte-type implants** were inserted, one mesial and one distal to the pre-existing implant.

In order to achieve a unified structure via **intraoral welding**, a special **welding abutment** was connected to the central bi-component implant. A **1.5 mm titanium bar** was then welded across the three implants to enhance primary stability.

Following a second healing phase, the **provisional bridge** was replaced with a **definitive ceramic prosthesis**, completing the restoration.

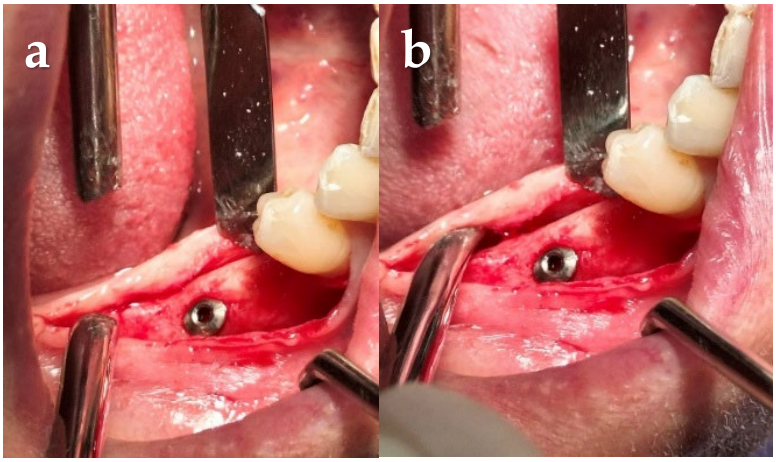

Figure 9.1.4.1 ***(a-b)*** *Re-access of the post-extraction surgical site following the osteointegration period. The central two-stage implant, previously inserted due to unfavorable initial conditions, is now visible and surrounded by well-healed soft tissues.*

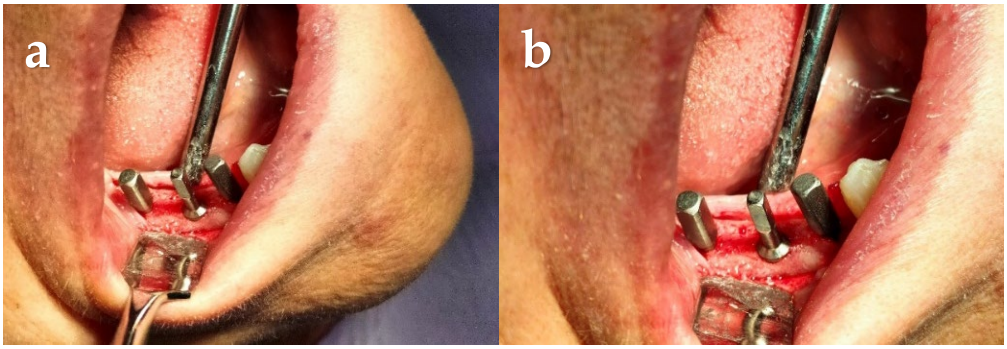

Figure 9.1.4.2 ***(a-b)*** *Insertion of two additional implants of Tramonte type: one mesially and one distally to the previously placed central implant. The bone crest is adequately exposed to ensure optimal positioning and parallelism.*

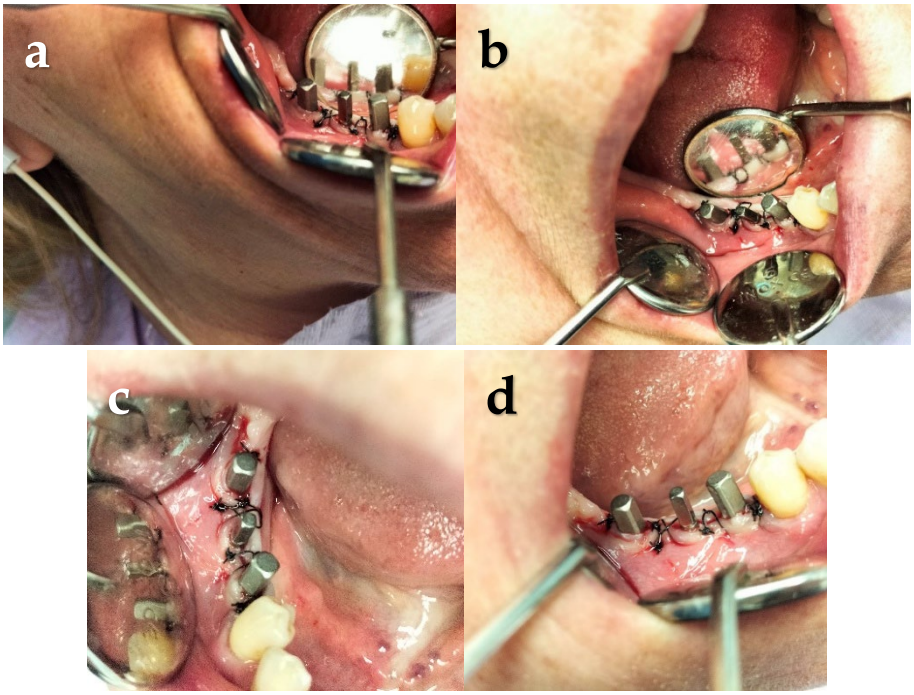

Figure 9.1.4.3 ***(a-d)*** *Clinical assessment of the suturing line following intraoral welding, focusing on tissue adaptation and proper wound closure around the implants and titanium bar.*

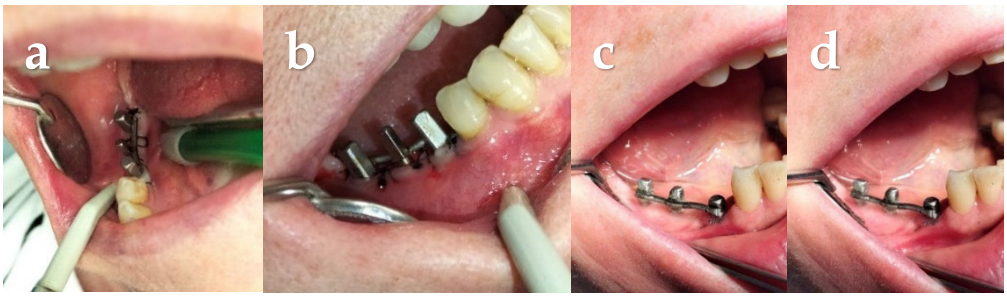

Figure 9.1.4.4 Healing following intraoral welding: ***(a-b)*** *finalization of intraoral welding after the suturing of the surgical wounds. The bar is welded in place across the implants through the mucosa, allowing for transmucosal healing;* ***(c-d)*** *the clinical aspect after suture removal, confirming uneventful healing and proper soft tissue adaptation around the implant structures.*

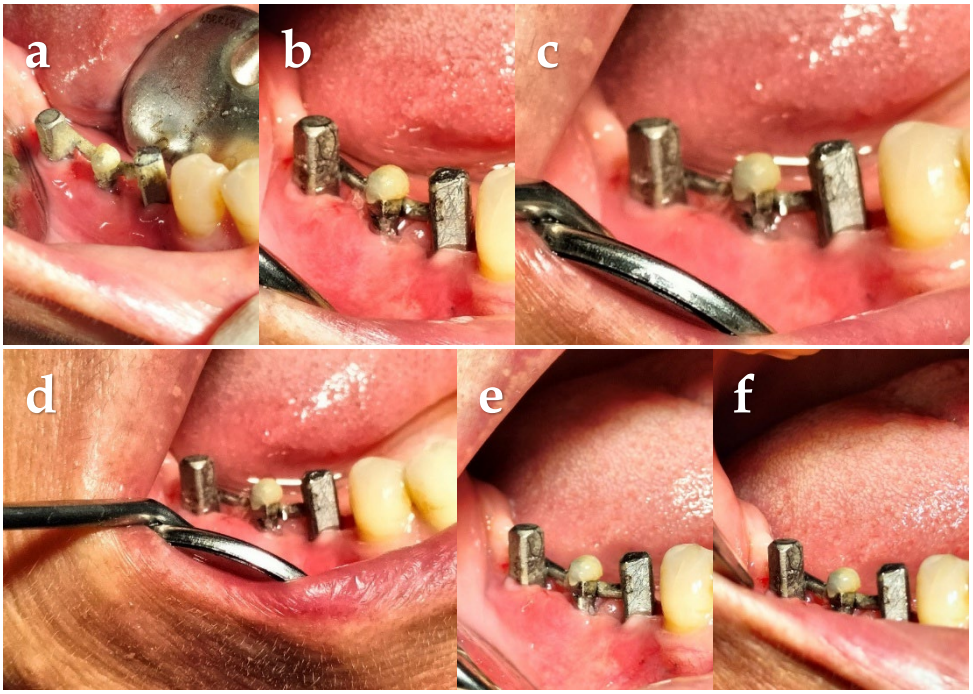

Figure 9.1.4.5 ***(a-f)*** *Postoperative follow-up during the second healing phase. Inspection of soft tissue adaptation, implant emergence profile, and bar integrity under minimal pressure stimuli.*

Figure 9.1.4.6 Shade matching procedure using a standard VITA classical guide (A3 vs. A3.5) to select the appropriate color for the definitive ceramic prosthesis. The final choice ensures harmony with adjacent dentition.

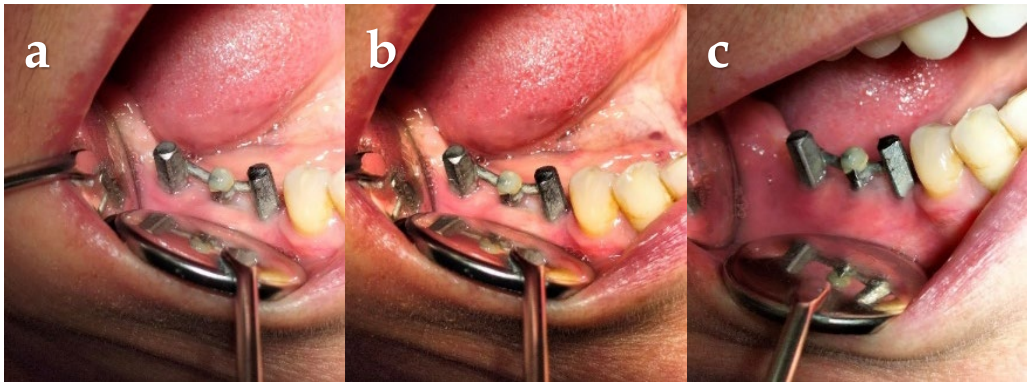

Figure 9.1.4.7 ***(a-c)*** *Removal of sutures and functional assessment of the implants prior to prosthetic phase. The healing of peri-implant tissues appears satisfactory. Evaluation of gingival contour and emergence profile.*

Figure 9.1.4.8 Postoperative panoramic radiograph confirming the successful integration of all three implants and proper positioning of the intraorally welded bar. The image verifies osseointegration and spatial orientation.

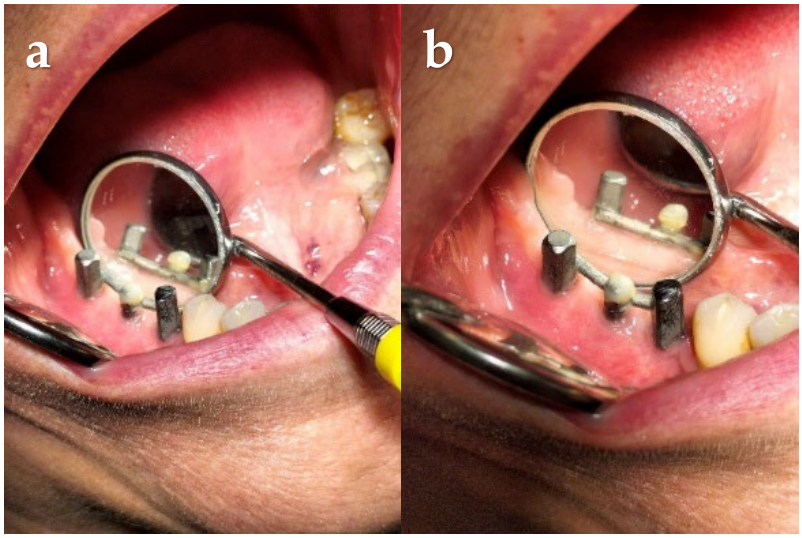

Figure 9.1.4.9 ***(a-b)*** *Clinical control of implant abutments and mucosal health using indirect vision. The emergence profile and cleanliness around the prosthetic components are adequate prior to prosthesis placement.*

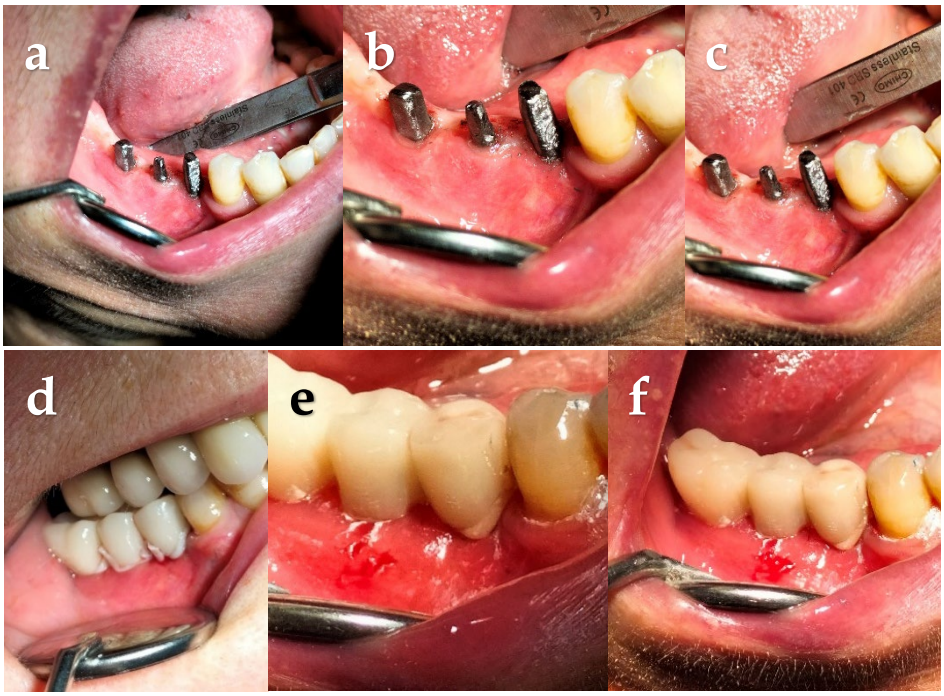

Figure 9.1.4.10 Prosthetic finalization: ***(a-c)*** *Insertion of the definitive ceramic bridge;* ***(d-e)*** *Evaluation of occlusion and aesthetic integration;* ***(f)*** *Healing post-placement and final tissue adaptation around the ceramic restoration.*

9.1.5 Case 5

Lateral mandibular edentulous space on the left side treated with the insertion of two **Tramonte-type implants, intraorally welded on the buccal side** using a **1.5 mm titanium bar**. A **provisional bridge** was initially delivered, followed by a **definitive prosthetic restoration**.

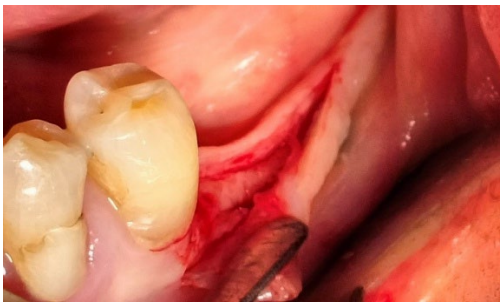

Figure 9.1.5.1 The initial clinical image illustrates the edentulous posterior mandibular region on the left side, prepared for implant insertion.

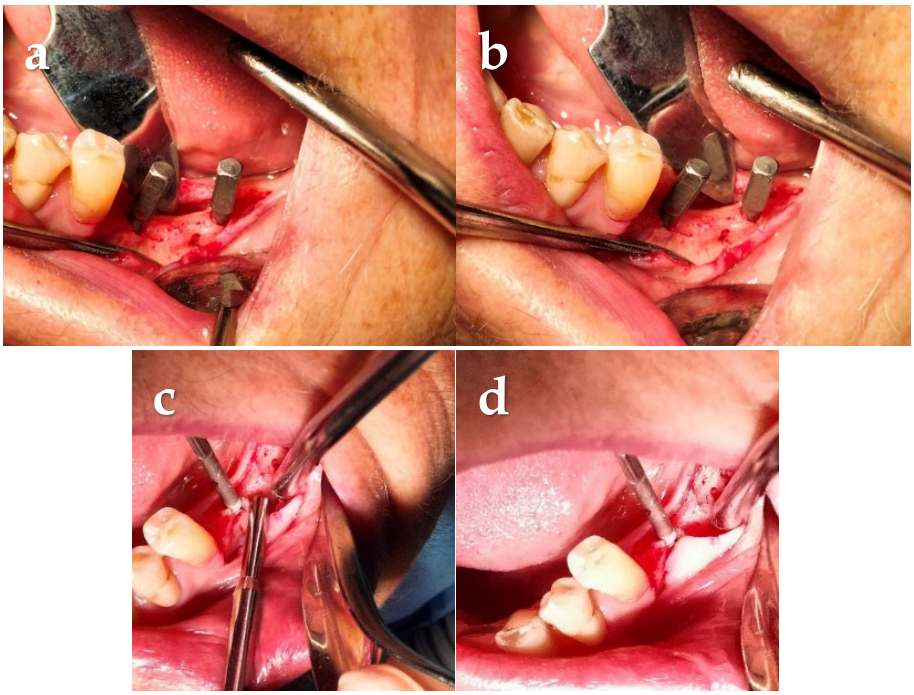

Figure 9.1.5.2 ***(a-d)*** *Two Tramonte-type implants were placed in the interradicular bone, following minimally invasive techniques. Surgical access was achieved with minimal flap elevation to preserve vascularization.*

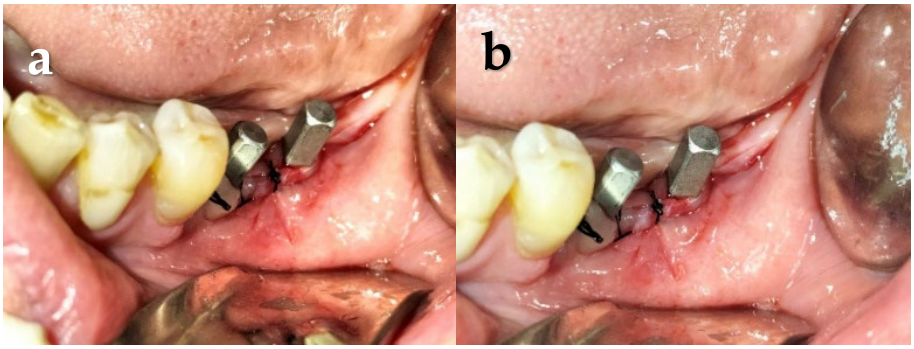

Figure 9.1.5.3 ***(a-b)*** *Immediate post-surgical view showing the sutured wound after implant placement. The two inserted implants exhibit favorable parallelism, and the soft tissues are approximated to facilitate transmucosal healing.*

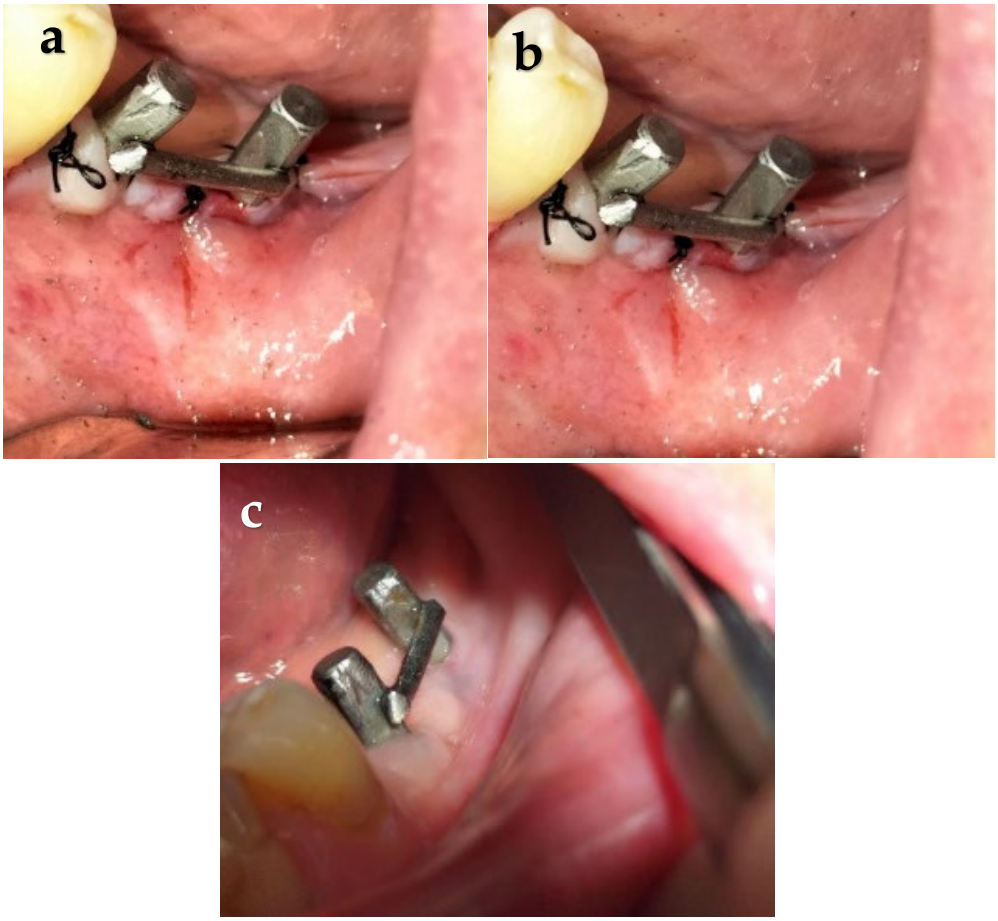

Figure 9.1.5.4 ***(a-c)*** *A 1.5 mm titanium bar was welded intraorally on the buccal side, unifying the two implants to enhance primary stability and resistance to micromovements during osseointegration.*

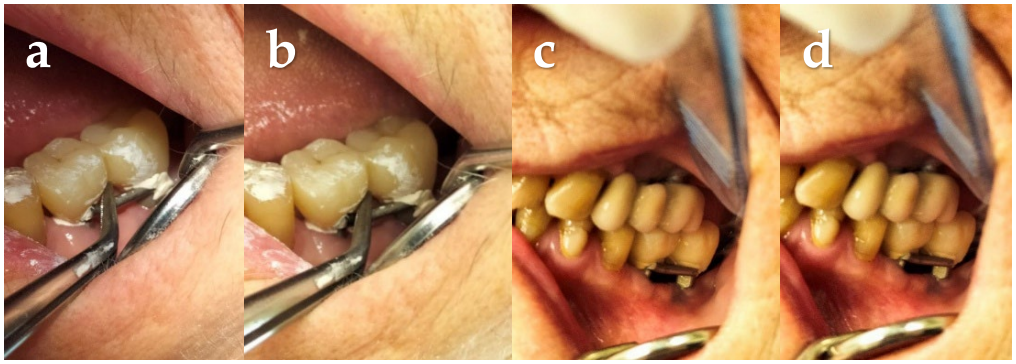

Figure 9.1.5.5 ***(a-d)*** *The images display the soft tissue closure after intraoral welding. Juxtagingival space was deliberately preserved to allow hygiene access during the healing phase.*

Please note the remaining juxtagingival space for cleaning during healing period.

Figure 9.1.5.6 Following healing, a provisional bridge was delivered to maintain occlusal function and contour the peri-implant soft tissues.

Figure 9.1.5.7 Postoperative panoramic radiograph showing the final outcome after intraoral welding. All implants appear properly positioned and integrated, confirming the success of the surgical and prosthetic protocol.

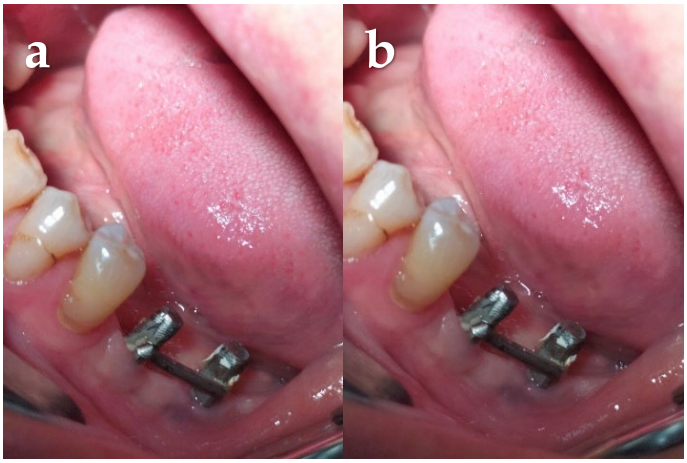

Figure 9.1.5.8 ***(a-b)*** *Connection of the welding abutment to the central bi-component implant. The surrounding soft tissues appear healthy and stable before splinting.*

Figure 9.1.5.9 Clinical view after placement of the provisional bridge. The emergence profile has been shaped to provide adequate juxtagingival space, facilitating plaque control and allowing proper hygiene maintenance during the healing phase.

Figure 9.1.5.10 The gray appearance of the structure indicates the framework at the metal try-in stage, before ceramic veneering. This step verifies passive fit and functional adaptation.

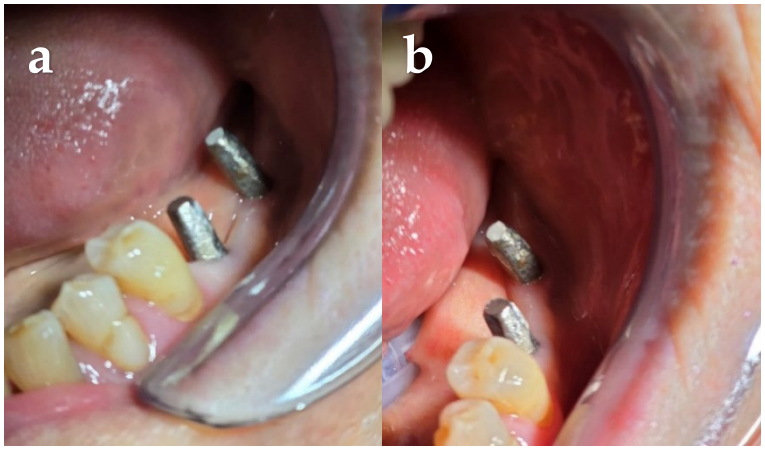

Figure 9.1.5.11 ***(a-b)*** *Early postoperative follow-up showing soft tissue healing after removal of the temporary stabilization bar. The transmucosal emergence of the implants is clearly visible and well contoured.*

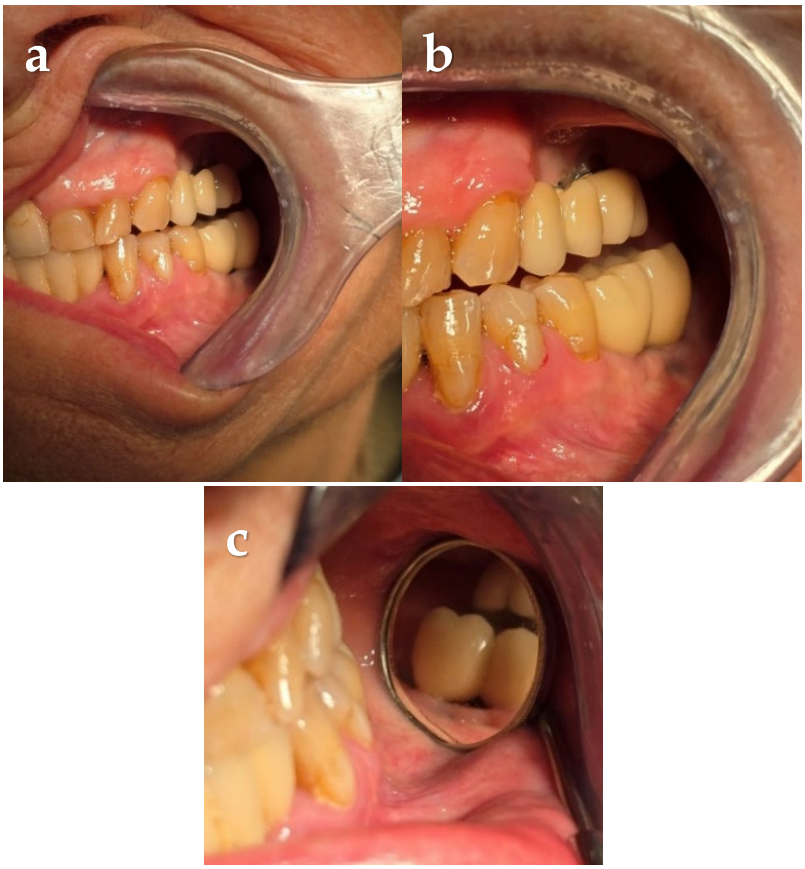

Figure 9.1.5.12 ***(a-c)*** *Final prosthetic restoration: a ceramic bridge was fabricated and cemented onto the implant abutments, ensuring appropriate occlusal loading and esthetics.*

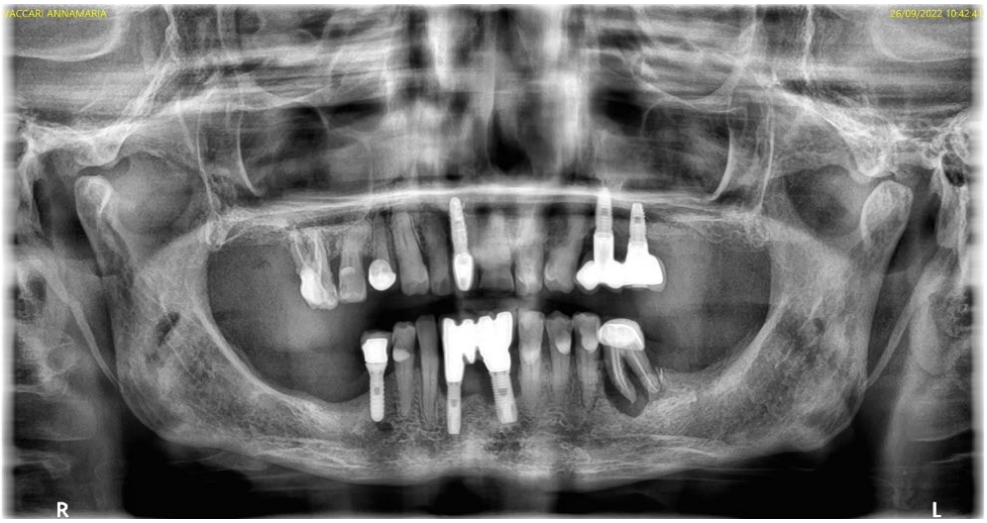

Figure 9.1.5.13 Initial radiographic control revealing a periapical radiolucency associated with the mandibular left molar. The adjacent Tramonte-type implants remain stable, but the chronic lesion indicates the need for extraction and subsequent reevaluation of local bone healing.

Figure 9.1.5.14 Follow-up panoramic image taken after removal of the molar with periapical pathology. The adjacent implants show good stability, and the alveolar bone appears to be healing adequately.

9.1.6 Case 6

Immediate post-extraction placement of implants was performed in regions 2.4 and 2.5. The patient initially refused extraction of tooth 2.3 during the same session. Consequently, the

two implants were inserted, **intraorally welded**, and **immediately loaded**, forming a temporary fixed restoration.

Six months later, the patient consented to the extraction of 2.3, which was followed by **immediate implant placement**, **immediate loading**, and **posterior welding** to integrate the new implant into the existing prosthetic structure.

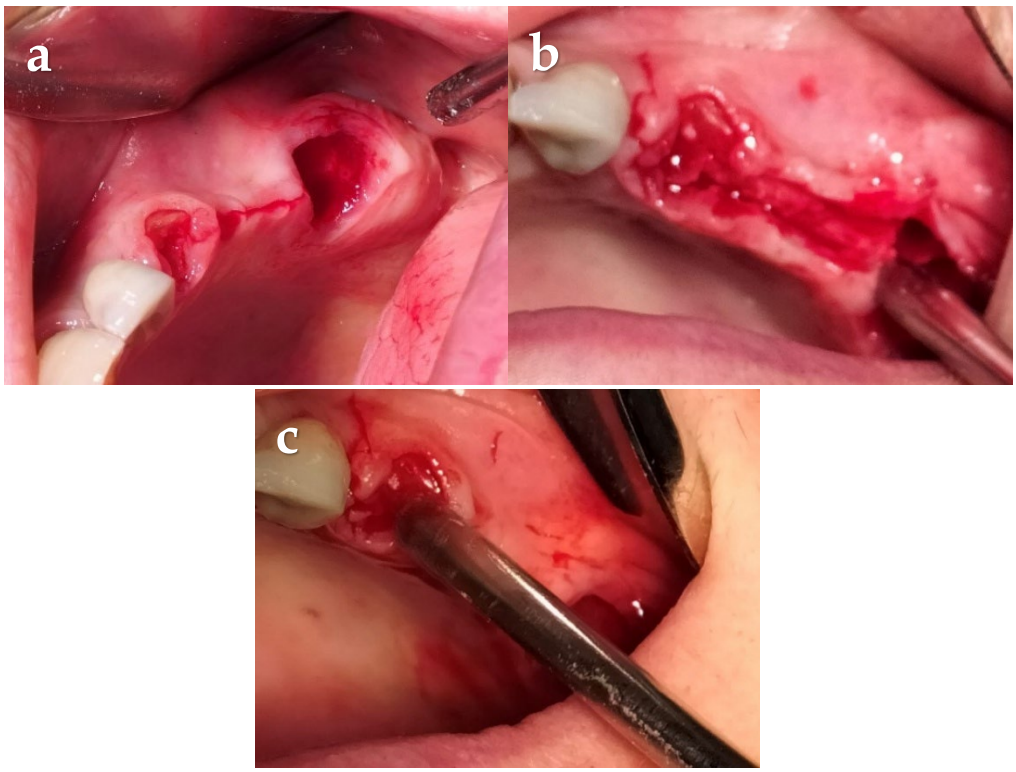

Figure 9.1.6.1 ***(a-c)*** *Initial clinical images following the extraction of teeth 2.4 and 2.5, revealing the post-extraction sockets. The soft tissue margins are clearly visible, and the alveolar crest morphology is preserved, allowing for optimal implant site preparation.*

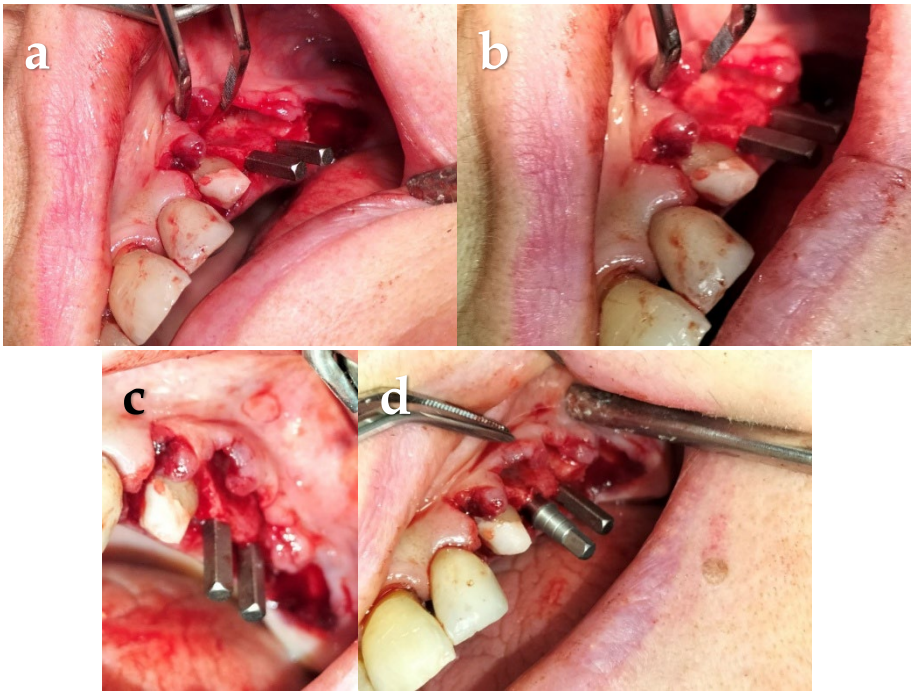

Figure 9.1.6.2 ***(a-d)*** *Intraoperative view during the insertion of two implants in regions 2.4 and 2.5. The implants were placed immediately post-extraction and intraorally welded in the same session to ensure primary stability and to support immediate prosthetic loading.*

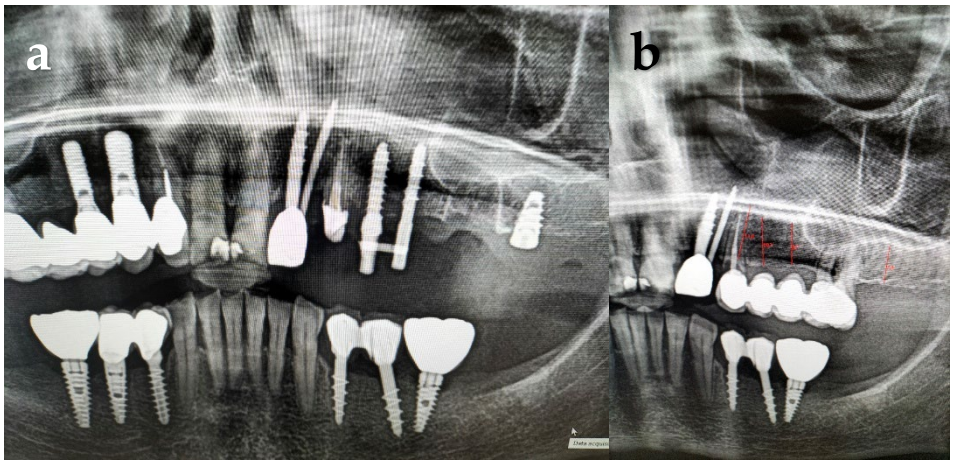

Figure 9.1.6.3 ***(a-b)*** *Panoramic radiographs illustrating the position and parallelism of the implants inserted in regions 2.4 and 2.5. The intraoral welding bar is visible, confirming prosthetic rigidity. The right image displays the fixed provisional restoration in situ and measurements for subsequent planning.*

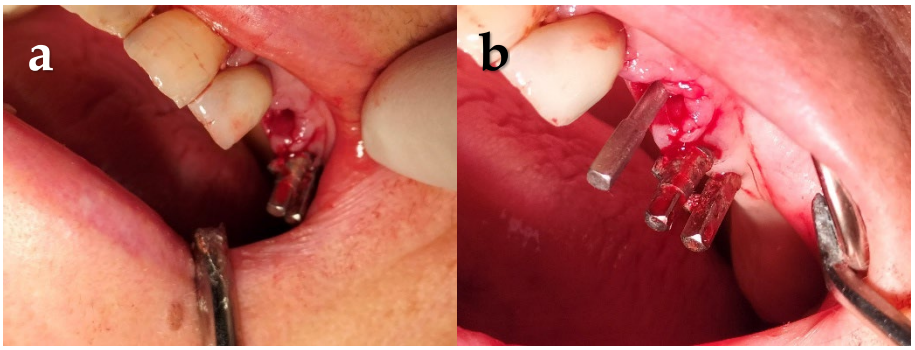

Figure 9.1.6.4 ***(a-b)*** *Clinical image at the time of the second surgical intervention, showing the extraction site of tooth 2.3. An implant has been placed immediately post-extraction, aligning with the preexisting welded structure. The prosthetic abutment was adapted for integration into the pre-existing prosthesis.*

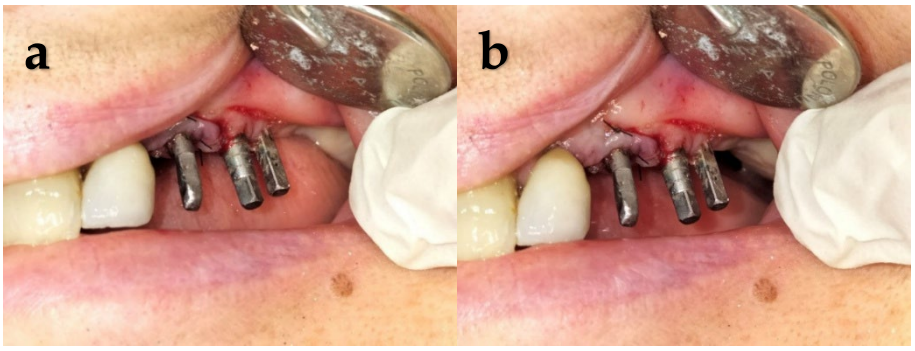

Figure 9.1.6.5 ***(a-b)*** *Postoperative images showing the healing abutments placed on all three implants (2.3, 2.4, 2.5).*

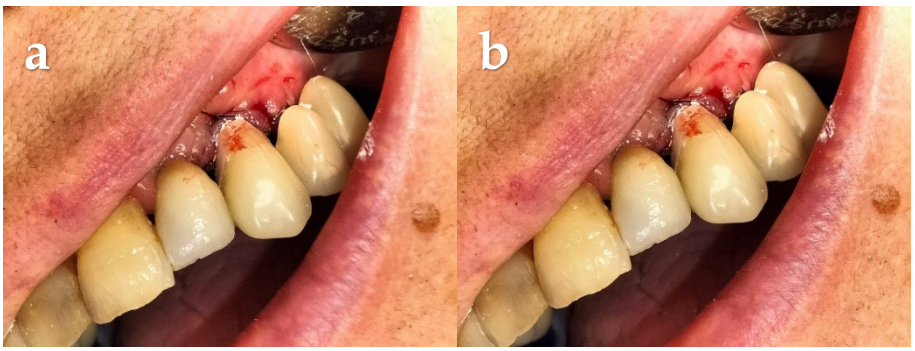

Figure 9.1.6.6 ***(a-b)*** *Provisional prosthesis adapted and reinserted after the placement of the third implant in region 2.3. Occlusal integration and soft tissue adaptation are verified.*

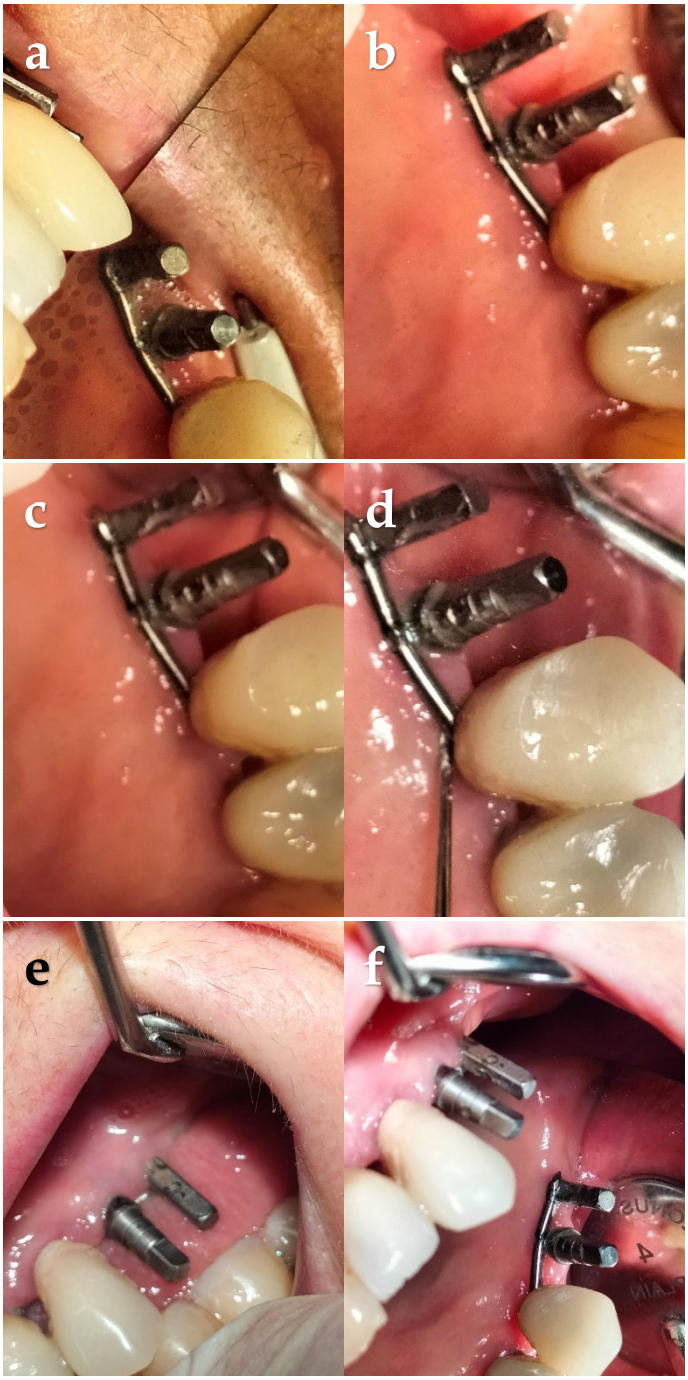

Figure 9.1.6.7 ***(a-f)*** *Follow-up clinical images at the integration stage, showing stable peri-implant mucosa and satisfactory healing of soft tissues. The intraoral welding bar remains in place, ensuring structural continuity and passive fit of the provisional prosthesis.*

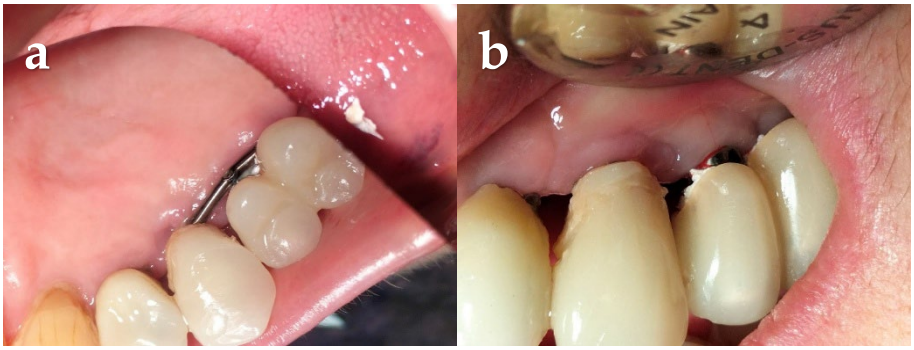

Figure 9.1.6.8 ***(a-b)*** *Clinical view of the definitive prosthetic restoration after soft tissue maturation. The emergence profiles are well-contoured, and the gingival architecture is harmonious, indicating successful functional and esthetic rehabilitation.*

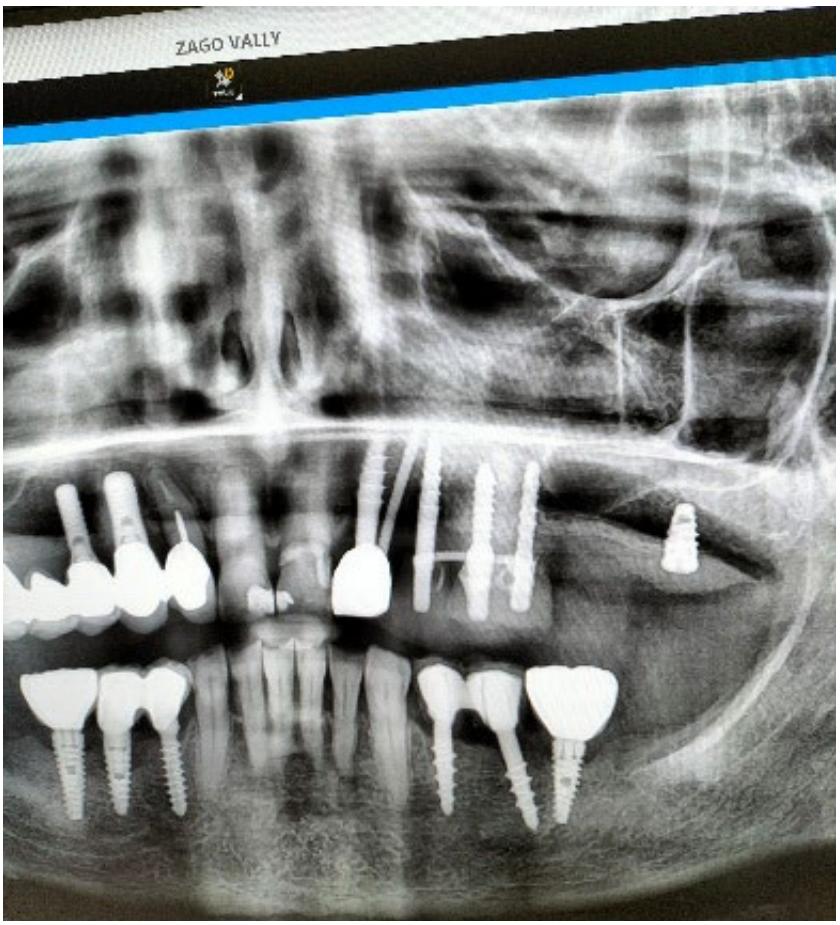

Figure 9.1.6.9 Final panoramic radiograph showing the completed prosthetic restoration supported by the three implants. Osseointegration is confirmed radiographically, and the overall alignment is stable. No signs of peri-implant bone loss are evident.

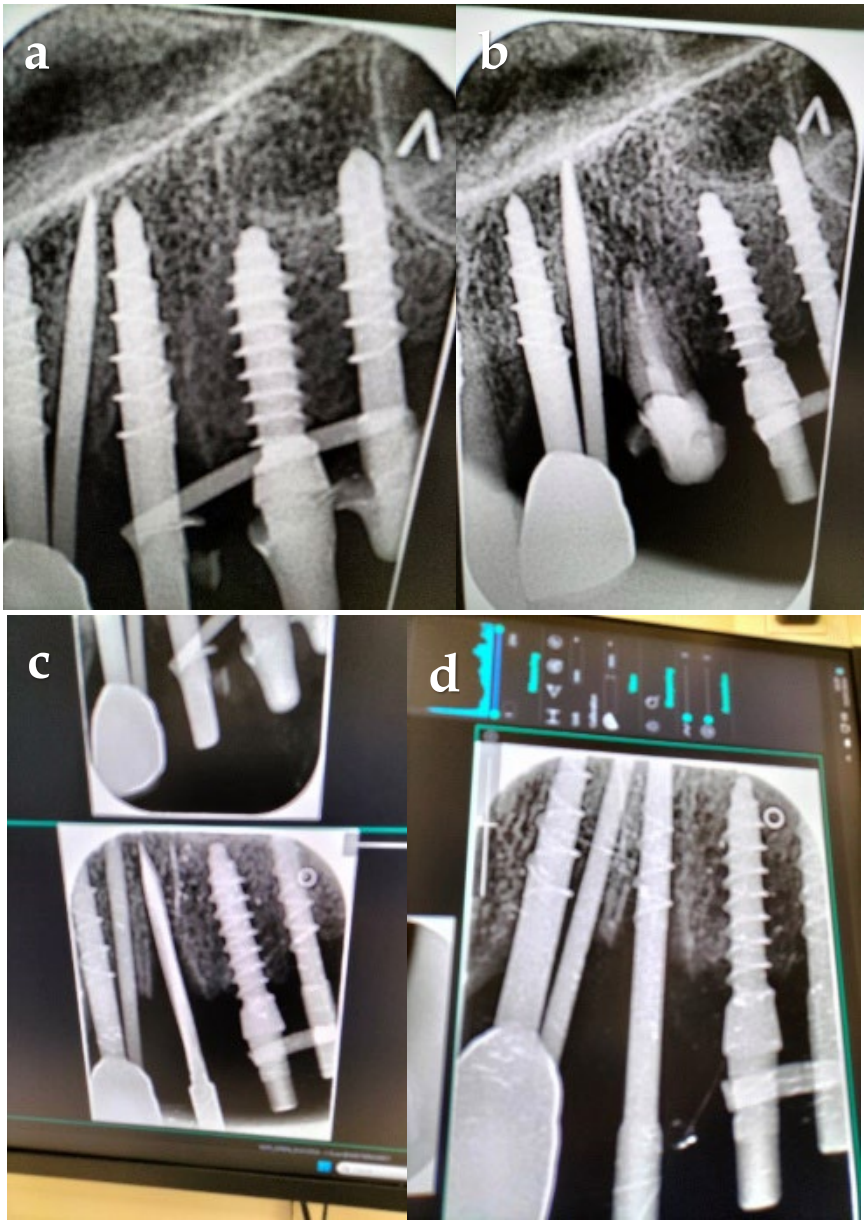

Figure 9.1.6.10 ***(a-d)*** *Periapical radiographs displaying close-up views of the implant-abutment interfaces. The welding seams and implant threads are clearly visible, confirming adequate positioning, marginal bone level preservation, and absence of radiolucency.*

9.2 Clinical Cases by Dr. Grigore Lăzărescu

9.2.1 Case 1

This case illustrates a complete mandibular arch rehabilitation using one-piece Leader Medica implants, placed through fully guided surgery and restored with immediate loading. While the workflow followed a pre-established digital and surgical plan, clinical adaptability played a crucial role, especially in retrofitting the prefabricated provisional bridge. Minor anatomical discrepancies required intraoperative modifications to achieve a passive and functional fit. The combination of a surgical guide and intraoral welding allowed for precise implant positioning, high primary stability, and rigid splinting at the time of surgery. The immediate provisionalization not only restored function and aesthetics on the same day but also supported tissue healing through strategic design and contouring of the prosthetic structure. Patient B.R.'s case demonstrates how advanced planning and pragmatic intraoperative adjustments, anchored in biomechanics and simplicity, can converge to deliver efficient and stable outcomes in full-arch implant therapy. It is a reminder that success in implantology is not defined by digital precision alone, but by the ability to adapt intelligently when the clinical reality deviates from the expected.

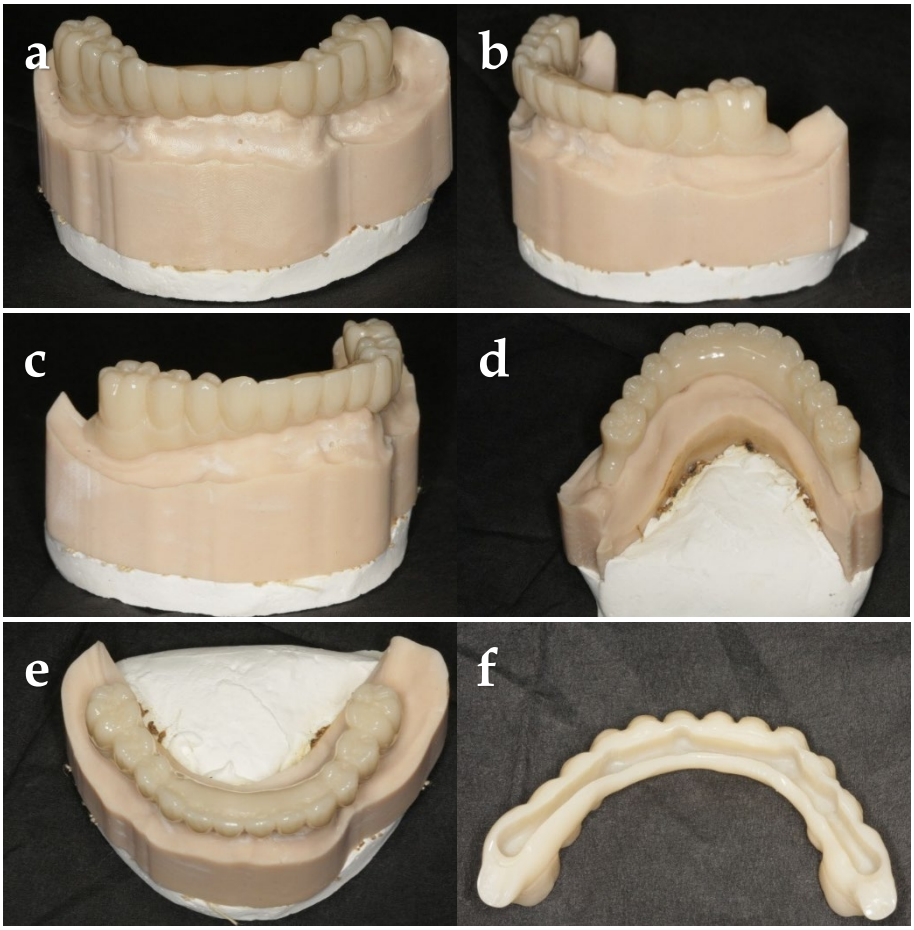

Figure 9.2.1.1 Mandibular fixed prosthetic restoration on one-piece Leader Medica implants, with intraoral welding, fabricated on a working model. ***(a)*** *Frontal view: the complete arch is shown, with aesthetic alignment and balanced crown morphology.* ***(b)*** *Left lateral view: the vestibular contour and posterior segment reconstruction are highlighted.* ***(c)*** *Right lateral view, symmetrical to the left side. The arch continuity and distal profile are visible.* ***(d)*** *Occlusal view from posterior to anterior surfaces and the adaptation of the prosthesis on the model are visible.* ***(e)*** *Superior occlusal view: the restoration covers the entire mandibular arch, displaying uniform occlusion and balanced distribution. (f) Internal view of the prosthetic restoration: the basal form is highlighted, along with screw access channels and the internal fit on the prosthetic field, useful for verifying passive adaptation on the model.*

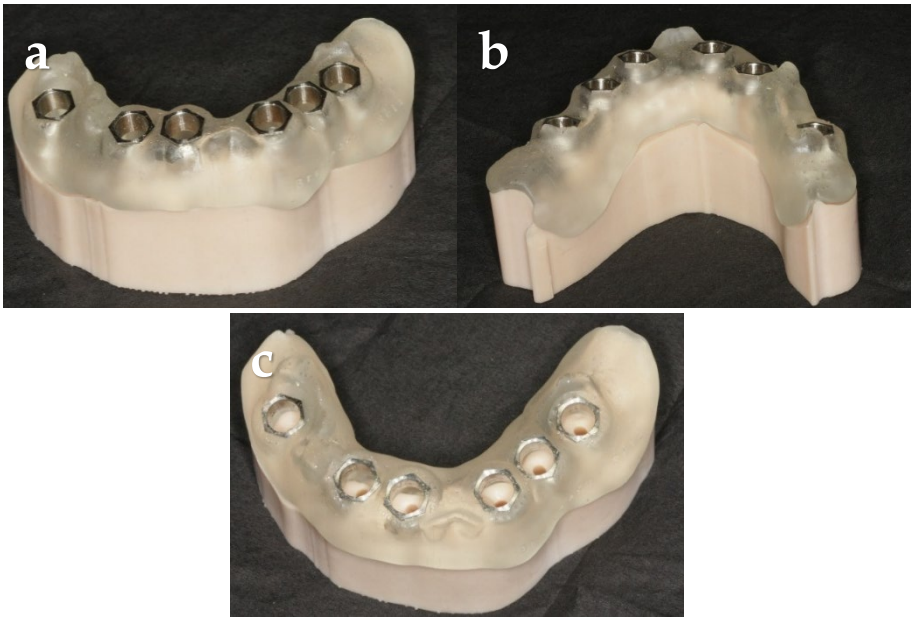

Figure 9.2.1.2 Surgical guide for one-piece Leader Medica implants, adapted on the mandibular model. Made from transparent material, the guide includes metal sleeves for the precise orientation of drills during implant insertion. ***(a)*** *Oblique vestibular view: the distribution of the 7 guide sleeves and the accurate adaptation on the model are visible.* ***(b)*** *The posterior view confirms the three-dimensional positioning and the symmetry of the guide sleeves in relation to the prosthetic field.* ***(c)*** *The occlusal view highlights the guide channels and the insertion axes of the implants.*

Figure 9.2.1.3 Original packaging of the ACTIVE one-piece implants (3P Smart Devices, Italy) used in the surgical procedure. The implant size (3.3 × 8 mm), manufacturer, and batch number are clearly indicated.

Figure 9.2.1.4 Trial placement of the surgical guide in the oral cavity, at the level of the anterior edentulous mandibular region. Passive adaptation of the guide on the alveolar ridge and the stability of its position are verified prior to drilling.

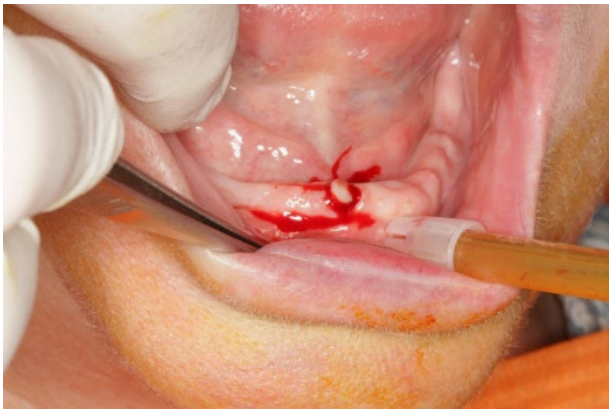

Figure 9.2.1.5 Midline mucoperiosteal incision with exposure of the alveolar ridge. This represents the initial step in the access protocol for guided implant surgery.

Figure 9.2.1.6 3P CONO-IN surgical kit, containing all drills and components required for guided insertion of one-piece implants.

Figure 9.2.1.7 Osteotomy preparation through the surgical guide using drills specific to the 3P system. The stabilization of the guide and proper irrigation are clearly observed.

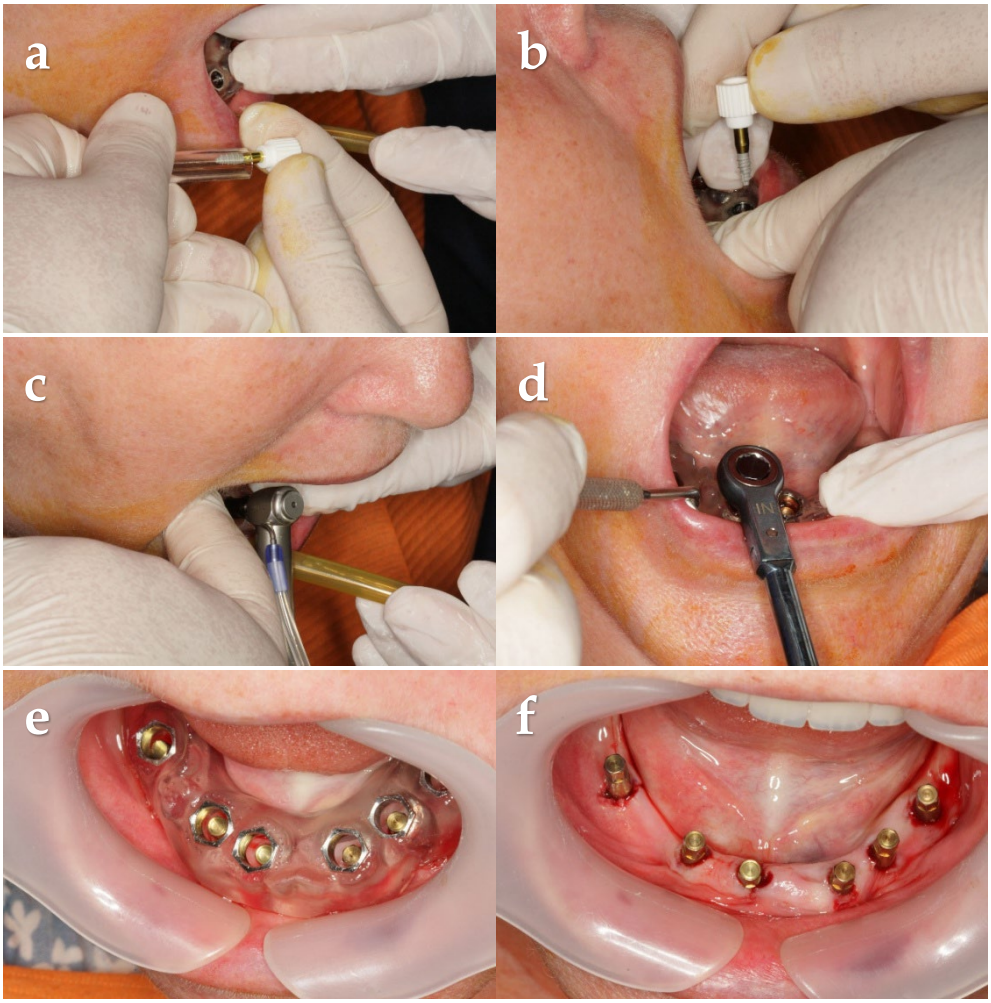

Figure 9.2.1.8 Surgical stages of multiple implant placement using a surgical guide: ***(a)*** *Retrieval of the implant directly from the sterile tube using a pre-mounted insertion device.* ***(b)*** *Introduction of the implant into the osteotomy site through the surgical guide, using the transfer device.* ***(c)*** *Continued insertion of the implant with a contra-angle handpiece under abundant irrigation, while maintaining prosthetic guidance.* ***(d)*** *Final insertion using a torque wrench for precise control of insertion torque.* ***(e)*** *Verification of implant positioning and parallelism using the transparent surgical guide.* ***(f)*** *Immediate postoperative image showing the final positioning of all six implants in the mandibular arch.*

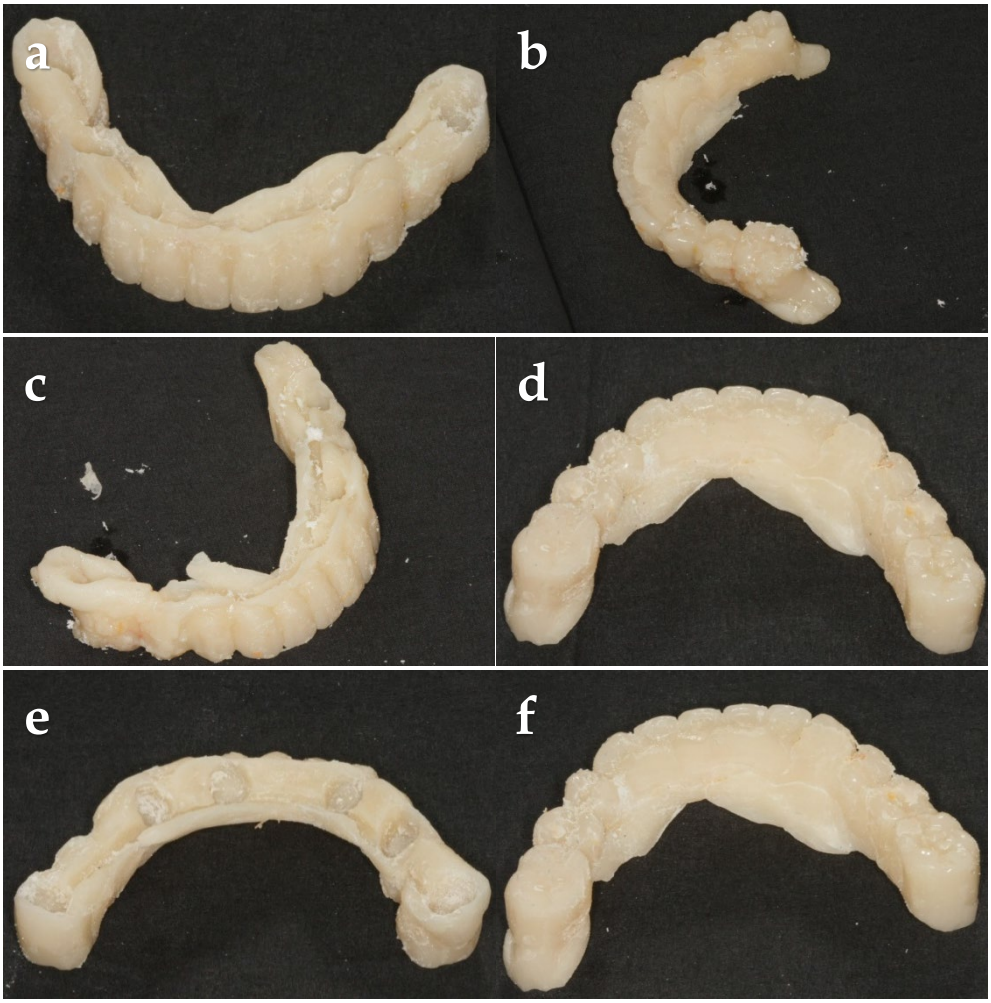

Figure 9.2.1.9 ***(a-f)*** *Individual prosthetic adjustment process prior to final fixation on the inserted implants. Individual adaptation is a key step in ensuring the functional and aesthetic success of the restoration, providing optimal fit on the prosthetic interfaces, balanced occlusal contacts, and passive insertion. Rotary instruments, mirrors, and direct visual inspection are used to check and adjust contact areas, as well as to finish the internal surfaces of the restoration.*

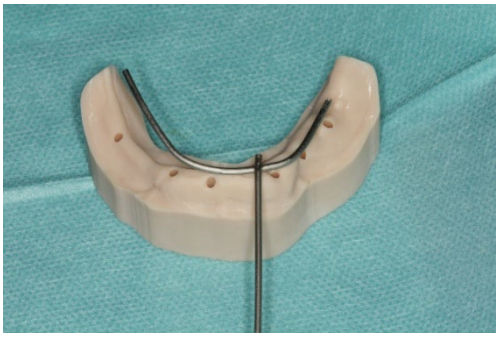

Figure 9.2.1.10 Positioning of the intraoral welding wire on the working model. The trajectory of the metal wire used for intraoral welding of the fixed mandibular prosthetic restoration is planned. The metallic guide is adapted on the working model to mark the implant positions and ensure spatial stabilization of the prosthetic framework prior to final fixation in the oral cavity. The perforations corresponding to the implant sites are highlighted in relation to the wire path.

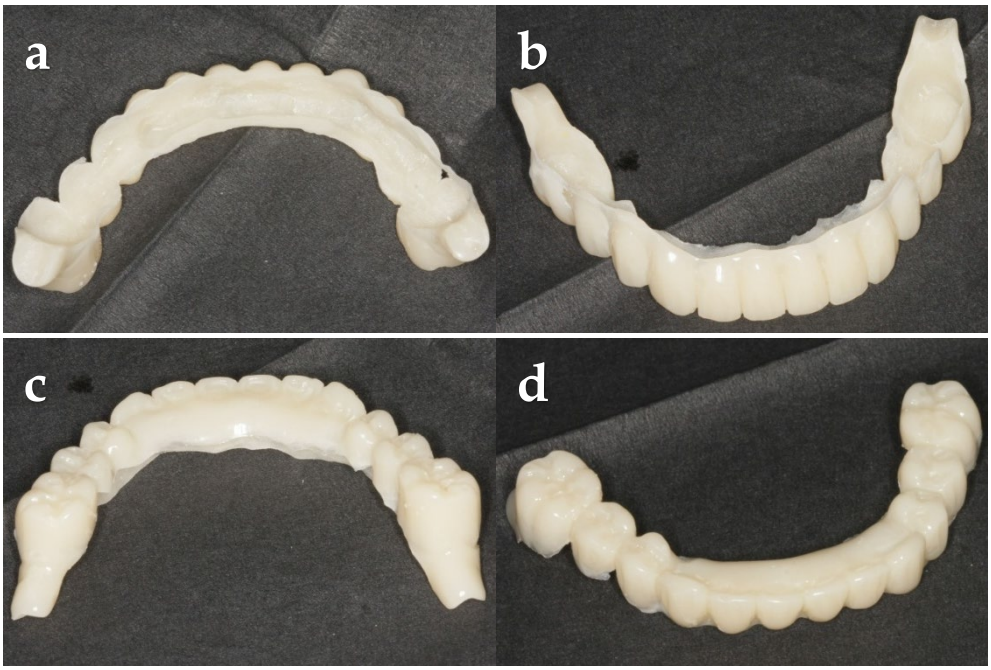

Figure 9.2.1.11 ***(a-d)*** *Final prosthetic restorations, presented from four different angles to highlight the basal adaptation, occlusal morphology, vestibular contours, and overall stability of the prosthesis. Each image reflects the level of detail and surface finishing achieved after extraoral adjustment and individual adaptation on the model, prior to final placement on the implants.*

Figure 9.2.1.12 Application of the luting agent on the internal surface of the provisional restoration. A spot-distribution technique is visible on the prosthetic surface prior to fixation onto the PMMA prosthetic components, allowing for passive insertion and potential retrievability.

9.2.2 Case 2

Sometimes, the elegance of a technique speaks better through motion than words. This video excerpt demonstrates the intraoral welding of a Ti_2 bar on a full mandibular arch, showing the intuitive workflow and ease of clinical execution.

Watch the video here!

https://youtube.com/shorts/ge7tlCc9wzY?feature=shared

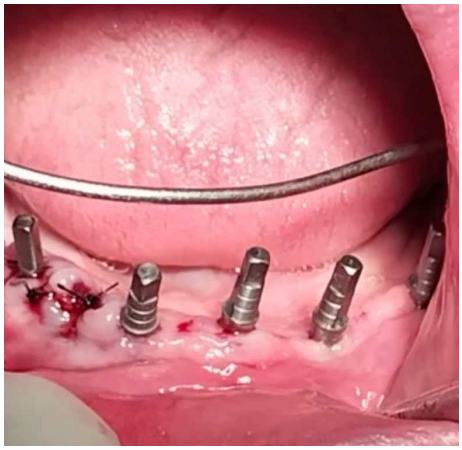

Figure 9.2.2.1 Intraoral view of the mandibular arch during intraoral welding. A titanium Grade 2 (Ti_2) bar is being positioned over the abutments of six previously inserted implants. Sutures are visible in the posterior region, indicating recent implant placement and soft tissue approximation.

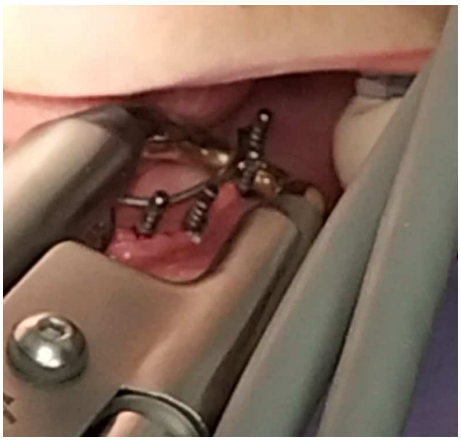

Figure 9.2.2.2 Intraoral welding in progress: a welding clamp is applied to secure the titanium bar to the implant abutments in the mandibular arch.

Figure 9.2.2.3 Intraoral finishing of the welded implant assembly using rotary tools, following the connection between the Tramonte implant and the Scialom needle. This clinical step refines the prosthetic trajectory, smooths the weld area, and optimizes the structure for subsequent crown adaptation.

About the authors

This is, indeed, a very simple but lovely chapter to write.

It is not about Dr. Grigore Lăzărescu, or Dr. Marco Bellina, or Dr. Adam Aleksander Nowicki, or even Dr. Elizabet-Zahra Sareh, the ones who actively wrote this book, but rather about the wider community of colleagues, based primarily in Italy yet extending across the globe, who have truly understood, embraced, and refined the clinical value of Intraoral Welding in daily clinical practice. Their consistent application of this technique in everyday dental practice is what gives these pages meaning. This book is, at its core, a tribute to the collective expertise, curiosity, and dedication of those who continue to prove that innovation is not always about inventing something new, but about recognizing and elevating what already works.

Dr. Grigore Lăzărescu graduated in Bucharest, Romania, in 1990, at the Carol Davila University of Medicine and Pharmacy, where he pursued an academic career until 2016, with a major interest in prosthodontics. It was back in 2000 when he first learned the Intraoral Welding technique from the beloved Dr. Lorenzo Noveri in San Remo, Italy. Step by step, piece by piece, he discovered the elegant achievements of the Italian school of implantology, studying and teaching the concepts of Tramonte and Garbaccio implants, and applying classic biomechanical principles to contemporary bi-component systems. Dr. Lăzărescu continues to explore the harmony between modern digital tools and timeless principles in functional implant dentistry.

Dr. Marco Bellina graduated in Medicine and Surgery from the Alma Mater Studiorum, University of Bologna, where he had the opportunity to study under renowned pioneers such as Pasqualini, Tramonte, Garbaccio, and Mondani. These formative encounters laid the foundation for his deep understanding of monophase implantology. Based in Milan since 1991, Dr. Bellina has practiced implant surgery since 1996 and has continuously refined his technique through advanced clinical training, including a pivotal stage with Dr. Giorgio Lorenzoni. He integrated intraoral welding into his daily workflow in 2005, equipping his own practice with welding technology. Today, he remains dedicated to promoting monophase techniques among younger clinicians while incorporating contemporary digital prosthetic protocols, embodying a unique blend of tradition and innovation.

Dr. Adam Aleksander Nowicki, DMD, Ph.D., is a distinguished implantologist and internationally recognized speaker. Bridging the gap between medicine and engineering, he conducts pioneering research in collaboration with the Department of Prosthetic Dentistry at Pomeranian Medical University and the Faculty of Mechanical Engineering at Wrocław University of Science and Technology. Dr. Nowicki has authored and co-authored numerous publications, underscoring his commitment to advancing dental science. His work consistently explores innovative frontiers, particularly in the integration of 3D printing and augmented reality (AR) technologies, revolutionizing modern implantology and prosthetic solutions.

Dr. Elizabet-Zahra Sareh is the youngest member of the team, yet brings a multidisciplinary background. She holds a degree in Dentistry from Carol Davila University of Medicine and Pharmacy in Bucharest, as well as in IT Engineering from the University Politehnica of Bucharest, and has also pursued studies at University of Agronomic

Sciences and Veterinary Medicine of Bucharest. Elizabet helped us shape an easy-going yet structured narrative about implants, Intra Oral Welding, and Immediate Loading, bringing to the table the same refreshing blend of creativity, and energy that defines her work as a passionate motorcycle content creator off the clinical track.

Dipl. Eng. Gabriel Kevorkian has provided the technical and scientific backbone of this work, establishing a strong connection between clinical common sense and evidence-based decision-making. It is to his credit that a niche discovery within the medical field has been successfully integrated into the broader context of technical and scientific inquiry.

The next author?

It should be you!

Please don't consider this a book that is closed and sealed, but rather an open invitation. Your clinical experience, your cases, your perspective, could all make a difference in a future edition. And help us all keep learning.

Don't forget to write us! We'd love to hear your feedback, questions, and even your own clinical stories.

grigore.lazarescu@thedentist.ro

Bibliography

1. Adachi M., Mackert J. R. Jr., Parry E. E., Fairhurst C. W. – Oxide Adherence and Porcelain Bonding to Titanium and Ti-6Al-4V Alloy. J Dent Res 69 (6), 1230-1235, 1990.
2. Adell R., Lekholm U., Rockler B., Branemark P.I. – A 15-year study of osteointegrated implants in the treatment of the edentulous jaw, Int. J. Oral Surg. 6, 387-416, 1981.
3. Albrektsson T. – Direct bone anchorage of dental implants. J. Prosthet Dent 50, 255-61, 1983.
4. Albrektsson T., Branemark P.I., Hansson H.A., Lindstrom J. – Osseointegrated titanium implants. Requirements for ensuring a long-lasting, direct bone-to-implant anchorage in man. Acta Ortoshop Scand. 52, 155-70, 1981.
5. Bauer H., Brauner H Titan: gefräst oder gegossen. Dtsch Zahnärztl Z 58, 165-168, 2003
6. Benedict JB, Cohen DE, Lovell S, Rohl AL, Kahr B. – What is syncrystallization? States of the pH indicator methyl red in crystals of phthalic acid.J Am Chem Soc. 128(16):5548-59, 2006.
7. Blume A., Raser G., Lenz E., Dietz W. Der – Titan-Keramik-Verbund aus experimenteller Sicht. Dtsch Zahnärztl Z 53, 718-721, 1998.
8. Böning K., Walter M. – Metall-Keramik-Verbund von gegossenem Titan. Dtsch Zahnärztl Z 46, 750-753, 1991.
9. Borelli P., Bordanaro A.C., Marzaduri E., Hruska K.L. – Immediate loading implants: a clinical report of 1301 implants.J Oral Implantol. 28(4):200-9, 2002.
10. Branemark P.I., Hansson B.O., Breine U., Lindstrom J., Hallen O., Ohman A. – Osseointegrated implants in the treatment of the edentulous jaw. Scand J. Plast Reconstr. Surgery, 16, 1-12, 1977.
11. Breustedt A. (Breustedt A., Lenz E.) – Stomatologische Keramik (Stomatologische Werkstoffkunde. LSV 2604, Bestell-Nr. 7934660, Johann Ambrosius Barth Verlag, Leipzig), 1978.
12. Brunette D.M., Kenner G.S., Gould T.R. – Grooved titanium surface orient growth and migration of cells from human gingival explants. J Dent Res. 62, 1045-8, 1983.
13. California Dental Association – Quality evaluation for dental care. Guidelines for the assessment of clinical and professional performance. California Dental Association, Los Angeles, 1977.
14. Coonaert J., Adrians P., De Boever J. Long – term clinical study of porcelain-fused-to-gold restorations. J Prosthet Dent 51, 338-342, 1984.
15. Dauskardt R. H., Marshall D. B., Ritchie R. O. – Cyclic fatigue-crack propagation in magnesia-partially-stabilized zirconia ceramics. Zitiert in

Özcan M.: Review. Fracture reasons in ceramic-fused-to-metal restorations. J Oral Rehabil 30, 265-269, 2003.
16. Degidi M, Gehrke P, Spanel A, Piattelli A Syncrystallization: a technique for temporization of immediately loaded implants with metal-reinforced acrylic resin restorations. Clin Implant Dent Relat Res. 8(3):123-34. University of Chieti, Pescara, Italy, 2006.
17. Degidi M., Nardi D., Piattelli A. – Immediate loading of the edentulous maxilla with a final restoration supported by an intraoral welded titanium bar: a case series of 20 consecutive cases.J Periodontol. 79(11):2207-13, 2008.
18. Degidi M., Gehrke P., Piattelli A. – Syncrystallization: A new Technique for Temporization of Immediately Loaded Implants14th Annual Scientific Meeting European Association for Osseointegration Munich, Germany, 2005.
19. Diaz-Arnold A. M., Schneider R. L., Aquilino S. A. – Bond strengths of intraoral porcelain repair materials. Zitiert in: Özcan M.: Review. Fracture reasons in ceramic-fused-to-metal restorations. J Oral Rehabil 30, 265-269, 2003.
20. Dorsch P. – Spannungen in metallkeramischen Systemen in Abhängigkeit von der thermischen Vorgeschichte. Zitiert in: Schwickerath H.: Der Einfluß unterschiedlicher Wärmeausdehnungskoeffizienten auf das Verhalten metallkeramischer Konstruktionen. Dtsch Zahnärztl Z 38, 554-556, 1983.
21. Eden G.T., Franklin O.M., Powel J.M., Ohta Y., Dickson G. – Fit of porcelain fused-to-metal crown and bridge castings. J Dent. Res.2360-8, 1979.
22. Eichner K. – Metallkeramik in der zahnärztlichen Prothetik: Werkstoffe, Indikation, klinische Verarbeitung. Kapitel 4: Werkstoffkundliche Untersuchungen, ISBN 3-446-12596-5, Carl Hanser Verlag München, Wien, 1979.
23. Esquivel J. F., Chai J., Wozniak W. T. – The Physical Properties of Low- Fusing Porcelains for Titanium. Int J Prosthodont 9, 563-571, 1996.
24. Evans D., Barghi N., Malloy C., Windeler S. The influence of condensation method on porosity and shade of body porcelain. J Prosthet Dent 63, 380-388, 1990.
25. Fanali S., Perrotti V., Riccardi L., Piattelli A., Piccirilli M., Ricci L., Artese L. – Inflammatory infiltrate, microvessel density, vascular endothelial growth factor, nitric oxide synthase, and proliferative activity in soft tissues below intraorally welded titanium bars.J Periodontol. 81(5):748-57, 2010.
26. Gehrke P. – The syncrystallization technique: expediting rigid splinting of immediately loaded implants. Dent Implantol Update. 17(3):17-23, 2006.
27. Gehrke P., Spanel A., Degidi M., Piattelli A., Dhom G. – FEM Analysis on Deformation and Stress Distribution in Fixed Metal-Reinforced Provisional Restorations of Immediately Loaded XiVE® Implants in the Edentulous Mandible 12th International FRIADENT Symposium Salzburg, Austria, 2006.

28. Geis-Gerstorfer J. – Titan und Titan-Legierungen. ZM 93 (7), 68-72, 2003.
29. Geis-Gerstorfer J., Lee H. R.- Calculation of the Effective Thermal Contraction Difference in Ti- and TiAl6Nb7-Ceramic Systems. IADR, 81th General Session, Abstract 3032, Göteborg (Schweden), 2003.
30. Geis-Gerstorfer J., Schille Ch., Klein P. – Geringere Oxidationsneigung unter Schutzgasatmosphäre. Dent Lab XLII, Heft 9, 1235-1236, 1994.
31. Geis-Gerstorfer J., Weber H., Simonis A., Eckhardt M., Haselberger D. – Zugfestigkeit von plasma- und lasergeschweißtem gegossenen Titan. Dtsch Zahnärztl Z 45, 545-547, 1990.
32. Gettleman L., Vrijhoef M.M.A., Uchiyama Y. – Proceedings of the International Symposium on Adhesive Prosthodontics. Academy of Dental Materials, Scheveningen, 1987.
33. Geurtsen W. – Metallische Restaurationen als Amalgamalternativen. Dtsch Zahnärztl Z 49, 853-858, 1994.
34. Gould R.L., Brunette D.M., Westbury L. – The attachment mechanism of epithelial cells to titanium in vitro, J Periodont Rest. 16, 611-6, 1981.
35. Gould R.L., Westbury L., Brunette D.M. – Ultrastructural study of the attachment of human gingiva to titanium in vivo. J Prosthet Dent. 52, 418-20, 1984.
36. Grimm W.-D., Braasch V., Schmitz I., Müller K.M. – Quantitative REMUntersuchungen zur Biofilmbildung auf Titanoberflächen. Dtsch Zahnärztl Z 57, 96-101, 2002.
37. Grotowski T., Dal Carlo L., Garbaccio D. – Carico funzionale immediato di impianti a vite bicorticale di Garbaccio post-estrattivi immediati. Studio multicentrico prospettico su oltre 15 anni di esperienza implanto-protesica ChirOrale Rivista di Chirurgia Orale, 2007.
38. Hamanaka H. – Titanium and Titanium Alloys, Dental Materials of Preference in the 21st Century. In: Proceedings of the 5th International Symposium on Titanium in Dentistry. O-1, 1-5, Chiba (Japan), 2001.
39. Hamanaka H., Yoneyama T. – Development potential of new titanium alloys in dentistry. In: Abstracts of the 4th International Symposium on Titanium in Dentistry. IL-1, 2, Geneva, 1998.
40. Hansson H.A., Albrektsson T., Branemark P.I. – Structural aspects of the interface between tissue and titanium implants.J. Prosthet Dent50, 108-12, 1983.
41. Hegenbarth E. A. – Titan und Keramik – Fortschritt oder Kompromiß (I). Quintessenz Zahntech 17, 39-46, 1991.
42. Hellwege K.-D. – Die Praxis der zahnmedizinischen Proohylaxe. Ein Leitfaden für die Individualprophylaxe, Gruppenprophylaxe und initiale Parodontaltherapie. ISBN 3-13-127186, Georg Thieme Verlag Stuttgart, New York, 2003.

43. Henning G. Die Metall/Keramik-Bindung. Dent Lab XXIV, Heft 8, 1065- 1071, 1976.
44. Hopp M. An der Titantechnologie kommt heute kein Labor mehr vorbei. Sonderdruck DZW Zahntechnik, 2-8, Ausgabe 8, 1997.
45. Hopp M. – Titan ist eine Aufgabe, der es sich zu widmen lohnt. Sonderdruck DZW Zahntechnik, 8-12, Ausgabe 9, 1997.
46. Hruska A.R. – Intraorales schweissen von reintitan. Quintessenz 35-48, 1988.
47. Hruska A.R. – Intraoral welding of pure titanium. Quintessence Int. 683-8, 1987.
48. Hruska A.R. La saldatura intraorale di fusioni in titanio. Dentista Moderna 809-19, 1986.
49. Hruska AR, Borelli P.- Quality criteria for pure titanium casting, laboratory soldering, intraoral we;66(4):561-5, 1991.
50. Hüls A., Rinke S.- Marginal fidelity of crowns produced with six different fabrication techniques, J Dent Res 74 (IADR Abstract 165), 421, 1995.
51. Hutton JE, Heath MR, Chai JY, Harnett J, Jemt T, Johns RB, and others – Factors related to success and failure rates at 3-year follow-up in a multicenter study of overdentures supported by Brånemark implants, Int J Oral Maxillofac Impl 10, 1, 33-42, 1995.
52. Huțu Em., Bodnar V., Păuna M., Constantinescu M, V, , Tâncu A.M., Epistatu D. – Tehnici curente în protetica dentară, Editura Didactică şi Pedagogică, Bucureşti, 1999.
53. Iijima D., Yoneyama T., Doi H., Hamanaka H., Kurosaki N. – Wear Resistance of Titanium and Ti-6Al-7Nb Alloy Dental Castings in a Simulated Occlusion Test. In: Proceedings of the 5th International Symposium on Titanium in Dentistry. P-61, 97, Chiba (Japan), 2001.
54. Iiyama K., Hirota K. – Fatigue Properties of T-ALLOY TOUGH (Ti-6Al-7Nb Titanium Alloy). In: Abstracts of the 4th International Symposium on Titanium in Dentistry. P-46, 25, Geneva, 1998.
55. ISO 5832-11 Chirurgische Implantate – Metallische Werkstoffe, Teil 11: Titan-Aluminium-6 Niob-7 Knetlegierung. Deutsches Institut für Normung, Beuth Verlag GmbH, Berlin 2000.
56. ISO6872 Dental Ceramic.International Organisation for Standardization1-9, 1995.
57. ISO 9693 Metal-ceramic dental restorative systems. International Standard, 1-14, 1999.
58. Jemt T, Book K. – Prothesis misfit and marginal bone loss in edentulous implant patients, Int J Oral Maxillofac Impl 11, 5, 620- 625, 1996.
59. Johns RB, Jemt T, Heath MR, Hutton JE, McKenna S, McNamara DC, and others – A multicenter study of overdentures supported by Brånemark implants, Int J Oral Maxillofac Impl 7, 4, 513-522, 1992.

60. Kappert H. F. – Titan als Werkstoff für die zahnärztliche Prothetik und Implantologie. Dtsch Zahnärztl Z 49, 573-583, 1994.
61. Kaus T., Pröbster L., Weber H. – Klinische Langzeiterfahrung mit keramisch verblendeten Titangerüsten – 3-Jahres-Ergebnisse einer prospektiven Studie. Quintessenz 47 (12), 1639-651, 7 Literaturverzeichnis 111, 1996.
62. Kerschbaum Th., Seth M., Teeuwen U. – Verweildauer von kunststoffund metallkeramisch verblendeten Kronen und Brücken. Dtsch Zahnärztl Z 52, 404-406, 1997.
63. Kobayashi E., Doi H., Yoneyama T., Hamanaka H. – Corrosion resistance of Ti-6Al-7Nb alloy dental castings. In: Abstacts of the 4th International Symposium on Titanium in Dentistry. O-12, 37, Geneva, 1998.
64. Koishi Y., Yanagida H., Matsumura H., Atsuta M., Shimoe S., Nagano K., Hamanaka H., Yoneyama T. – Application of a Ti-6Al-7Nb Alloy for Cast Restorations and Fixed Partial Dentures. In: Proceedings of the 5th International Symposium on Titanium in Dentistry. P-21, 57, Chiba (Japan), 2001.
65. Könönen M., Kivilahti J. Fusing of Dental Ceramics to Titanium. J Dent Res 80 (3), 848-854, 2001.
66. Krjukow A. Untersuchungen zum Titan-Keramik-Verbund unter Anwendung modifizierter Metalloberflächenkonditionierungen. Zahnmed Diss, Humboldt-Universität Berlin 2003.
67. Küpper H., Bachmann K. Reintitan als Alternativmetall in der restaurativen Zahnheilkunde. Quintessenz Zahntech 15, 1091-1098, 1989.
68. Lamon J., Evans A. – Statistical analysis of bending strength for brittle solids: a multiaxial fracture a problem. Zitiert in: Özcan M.: Review. Fracture reasons in ceramic-fused-to-metal restorations. J Oral Rehabil 30, 265-269, 2003.
69. Lautenschlager E. P., Monaghan P. – Titanium and titanium alloys as dental materials. Int Dent J 43, 245-253, 1993.
70. Lee H. R. – Bonding characteristics of ceramics to Ti-6Al-7Nb alloy. Zahnmed Diss, Universität Tübingen, 2003.
71. Lehmann B. Eine Implantatsuprakonstruktion aus einer modernen Titanlegierung. Quintessenz Zahntech 29 (1), 46-55, 2003.
72. Lenz E. Der Einfluß von Fluoriden auf das Korrosionsverhalten von Titan. Dtsch Zahnärztl Z 52, 351-354, 1997.
73. Lenz E., Dietz W. – Die Randschichten von Titan-Gussobjekten unter dem Einfluß verschiedener Einbettmassen. Quintessenz Zahntech 21, 633-645 1995.
74. Lenz E., Lenz U. – Studie zum Einsatz einer Titan-Aluminium-Niob-Legierung in der zahnärztlichen Prothetik. Quintessenz Zahntech 28 (2), 122-134, 2002.

75. Lenz E., Melle B., Liefeith K., Hildebrand G., Kraft D. – Der Einflußsimulierter Bedingungen des Mundhöhlenmilieus auf das In-vitro- Korrosionsverhalten metallischer Dentalwerkstoffe. Swiss Dent 16, 5-13, 1995.
76. Lenz J. Der Einfluß geometrischer Parameter auf die Größenordnung und räumliche Verteilung von Wärmespannungen in metallkeramischen Kronen. Dtsch Zahnärztl Z 38, 28-31, 1983.
77. Lindemann W. – Das Temperaturprofil in Keramik-Brennöfen. ZahntechMag 5, 620-624, 2001.
78. Lindemann W. – Elektronenmikroskopischer und röntgenographischer Nachweis der Haftoxide auf unedlen Metallen. Dtsch Zahnärztl Z 37, 285-287, 1982.
79. Lindigkeit J. – Zur Leistungsfähigkeit moderner Titankeramik: Hohe technische Qualität, einfache Verarbeitung und natürliche Ästhetik. Sonderdruck aus: DZW Spezial, Ausgabe 1, 1999.
80. Lindigkeit J. Carmen – Aspekte einer neuen Metallkermik. DSL 2, 25-27, 1996.
81. Lindstrom H, Preiskel H. – The implant supported telescopic prosthesis: a biomechanical analysis, Int J Oral Maxillo Impl 16, 1, 34-42, 2001.
82. Lorenzon G., Bignardi C., Zanetti E.M., Pertusio R. – Analisi biomeccanica dei sistemi implantari DENTAL CADMOS – Estratto, COL. 71, 10; 63-86, 2003.
83. Lubberich A. – Die Rematitan – Gießanlage – Vakuumschmelzen imZweikammer – System. Dent Lab XL, Heft 9, 1485-1488, 1992.
84. Lubberich A., Sellier A., Mythen – Fakten – Praxis Erfahrungen mit Reintitanversorgungen. Dent Lab XXXVIII, Heft 5, 677-680, 1990.
85. Makris P. – Untersuchung zur Passung und Morphologie der Fügefüge von gegossenen Titan – und Edelmetall-Teilkronen unter Berücksichtigung der Zementierungsweise in-vitro. Zahnmed Diss, Universität Marburg ; 7 Literaturverzeichnis 113, 2002.
86. Malevics N. – Subgingivale Plaqueakkumulation auf gegossenem Titan – Eine in vivo – Studie – Zahnmed Diss, Universität Witten / Herdecke, 1999.
87. Martin FW, Chan Y, and other – Treatment of the atrophic edentulous maxilla with implant-supported overdentures: a review of the literature, Int J Prosthodont 11, 7-15, 1998.
88. Mondani P.L., Mondani P.M. – The Pierluigi Mondani intraoral electric solder. Principles of development and explanation of the solder using syncrystallization. Riv Odontostomatol Implantoprotesi.(4):28-32, 1982.
89. Naert I., Quirynen M., Hooghe M., van Steenberghe D. – A comparative prospective study of splinted and unsplinted Brånemark implants in mandibular overdenture therapy: a preliminary report, J Prosthet Dent 71, 486-492, 1994.
90. Nakagawa M., Matsuya S., Udoh K., Ohta M. – Development of titanium alloys with high corrosion resistance in fluoride-containing solution. In:

Proceedings of the 5th International Symposium on Titanium in Dentistry. O-9, 16, Chiba (Japan), 2001.
91. Närhl TO, Hevinga M, Voorsmit RACA, Kalk W Maxillary overdentures retained by splinted and unsplinted implants: a retrospective study, J Oral Maxillofac Impl 16, 2001.
92. Nergiz I., Meine H.C., Niedermeier W. – Untersuchungen zur Scherverbundfestigkeit von titankeramischen Systemen. Dtsch Zahnärztl Z 54, 688-691, 1999.
93. Nilson H., Bergman B., Bessing C., Lundqvist P., Andersson M. – Titanium Copings Veneered With Procera Ceramics: A Longitudinal Clinical Study. Int J Prosthodont 7, 115-119, 1994.
94. Özcan M. Review. – Fracture reasons in ceramic-fused-to-metal restorations. J Oral Rehabil 30, 265-269, 2003.
95. Palanuwech M. – The fatigue resistance of commercially pure titanium (grade II), titanium alloy (Ti6Al7Nb) and conventional cobalt-chromium cast claps. Zahnmed Diss, Universität Tübingen, 2003.
96. Parr G.R., Gardner L.K., Toth R.W. – Titanium: the mystery metal of implant dentistry. J Prosthet Dent. 95, 410-4, 1985.
97. Pasqualini M.E., Mangini F., Colombo D., Manenti P.A., Rossi F. – Stabilizzazione di impianti emergenti a carico immediato SALDATRICE ENDORALE DENTAL CADMOS – Estratt, 2001.
98. Päßler K. – Darstellung, Prüfung und Eigenschaften von edelmetallfreien Dentallegierungen und Titan. ISBN 3-87652-997-2, Habilitationsschriften der Zahn-, Mund- und Kieferheilkunde, Quintessenz Verlags-GmbH, Berlin, 1998.
99. Päßler K. – Titan in der Zahnmedizin. In: Wirz J., Bischoff H. (Hrsg): Titan in der Zahnmedizin. ISBN 3-87652-484-9, Quintessenz Verlags-GmbH, Berlin, 1997.
100. Päßler K. – Die Weiterentwicklung des Rematitan-Systems. QuintessenzZahntech 21, 649-661, 1995.
101. Päßler K. – Der Werkstoff Titan in der zahnärztlichen Prothetik. Dent Lab XLII, Heft 7, 989-996, 1994.
102. Päßler K. – Der dentale Titanguß – Grundlagen, Technologie und werkstoffkundliche Berwertung. Quintessenz Zahntech 17, 717-726, 1991.
103. Päßler K., Bestelmeyer F., Ohnmacht P., Sernetz F. – Einflüsse auf die Qualität und Eigenschaften von dentalen Titangüssen. Dent Lab XXXIX, Heft 6, 809-815, 1991.
104. Persönliche Mitteilungen – Firma Girrbach Dental GmbH, Pforzheim 2003.
105. Pröbster L., Geis-Gerstorfer J., Simonis A., Setz J., Weber H. – Titan – zum gegenwärtigen Stand eines neuen Dentalwerkstoffs. Dent Lab XXXIX, Heft 8, 1073-1078, 1991.

106. Pröbster L., Maiwald U., Weber H. – Three-point bending strength of ceramics fused to cast titanium. Eur J Oral Sci 104, 313-319, 1996.
107. Quirynen M., Naert I., van Steenberghe D. – A study of 589 consecutive implants supporting complete fixed prostheses. Part I: periodontal aspects; Part II: prosthetic aspects, J Prosthet Dent 68, 655-663, 1992.
108. Rammelsberg P., Aschl I., Pospiech P. – Verbundfestigkeit niedrigschmelzender Keramiken zu Titan unter Berücksichtigung der Oberflächenkonditionierung. Dtsch Zahnärztl Z 53, 200-203.
109. Rateitschak K. H., Renggli H. H., Mühlemann H. R. – Parodontologie. Gesundes Parodont, Epidemiologie, Ätiologie, Diagnostik, Prophylaxe und Therapie parodontaler Erkrankungen. ISBN 3-13-387802-6, Georg Thieme Verlag Stuttgart, 1978.
110. Reppel P.-D., Walter M., Böning K. – Metallkeramischer Zahnersatz aus Titan. Dtsch Zahnärztl Z 47, 524-526, 1992.
111. Reppel P.-D., Walter M., Böning K., Freesmeyer W. B. Metallkeramischer Zahnersatz mit Gerüsten aus Reintitan und einer hochgoldhaltigen Legierung. ZWR 10, 601-605, 1997.
112. Rinke S., Schulz-Finke V., Schäfers F., Özmumcu A., Hüls A. – Vergleichende Qualitätsbeurteilung von Einzelzahnrestaurationen aus Titan und einer Edelmetall-Legierung. Dtsch Zahnärztl Z 53, 272-275, 1998.
113. Rossi F., Pasqualini M.E., Mangini F., Manenti P. Carico Immediato di Impianti Monofasici Mascellare Superirore DENTAL CADMOS – Estratto, VOL. 73, 4; 65-69, 2005.
114. Sandu Simona Andreea – Restaurări protetice pe implante endoosoase, Edit. Cartea Universitară, Bucureşti, 2003.
115. Sarinnaphakorn L., Yoneyama T., Doi H., Kobayashi E., Hamanaka H. – Elastic Property of Ti-6Al-7Nb Alloy Castings for Removable Partial Denture. In: Proceedings of the 5th International Symposium on Titanium in Dentistry. O-5, 12, Chiba (Japan), 2001.
116. Schaardt S. – Grundlagen der Titanverarbeitung in der Zahntechnik Teil 1: Werkstoff, Eigenschaften, Modellation, Einbetten. Zahntech Mag 1 (1), 2-9, 1997.
117. Schäfer R., Kappert H. F. – Die Chemische Löslichkeit von Dentalkeramiken. Dtsch Zahnärztl Z 48, 625-628, 1993.
118. Schröter W., Lautenschläger K.-H., Biebrack H. – Chemie, Fakten und Gesetze. Kapitel 23, 261-262, ISBN 3-86047-148-1, Bechtermüntz-Verlag GmbH, Augsburg, 1997.
119. Schwickerath H. Einfluß mechanischer Eigenschaften der Legierung auf die Belastbarkeit metallkeramischer Restaurationen (Teil 1). Zahnärztliche Praxis 5, 6-8, 1995.

120. Schwickerath H.- Der Einfluß unterschiedlicher Wärmeausdehnungskoeffizienten auf das Verhalten metallkeramischer Konstruktionen. Dtsch Zahnärztl Z 38, 554-556,, 1983.
121. Schwickerath H. – Prüfung der Verbundfestigkeit Metall-Keramik. Dtsch Zahnärztl Z 38, 21-25, 1983.
122. Seghi R. R., Sorensen J. A. – Relative Flexural Strength of Six New Ceramic Materials. Int J Prosthodont 8, 239-246, 1995.
123. Silness J. – Periodontal conditions in patients treated with dental bridges. J Periodontal Res 5, 60-6, 1970.
124. Smedberg J.I., Lothigius E., Bodin I., et. – Al A clinical and radiological two-year study of maxillary overdentures on osseointegrated implants, Clin Oral Impl Res 4, 39-46, 1993.
125. Sommer M. Ch., Schwickerath H., Marx R., Witt G. – Mechanische Festigkeit von Keramiken für die Verblendung von Titanrestaurationen. Dtsch Zahnärztl Z 46, 746-749, 1991.
126. Spiekermann H, Jovanovic S.A., Richter E.J. – Implant-Prosthetic Treatment Concepts for the edentulous jaw, in Laney W.; Tolman D.E., : Tissue integration in Oral, Orthopedic and Maxillofac Recons, Rochester, Minn, 1990.
127. Striezel R. Der Einfluß von fluoridhaltigen Zahnpasten auf Titanoberflächen. ZWR 103, 82-8, 1994.
128. Strub J. R., Stiffler S., Schärer P. Causes of failure following oral rehabilitation: biological versus technical factors. Quintessence Int 19, 215-222, 1988.
129. Tesch U., Päßler K., Mann E. – Untersuchungen zum Titan-Keramik-Verbund. Dent Lab XLI, Heft 1, 71-74, 1993.
130. Thull R. – Titan in der Zahnheilkunde – Grundlagen. ZM 7, 40-45, 1992.
131. Tinschert J., Marx R., Gussone R. – Struktur von Keramiken für die Titanverblendung. Dtsch Zahnärztl Z 50, 31-34, 1992.
132. Torsello F., di Torresanto V.M., Ercoli C., Cordaro L. – Evaluation of the marginal precision of one-piece complete arch titanium frameworks fabricated using five different methods for implant-supported restorations.Clin Oral Implants Res.19(8):772-9, 2008.
133. Toth R.W., Parr G.R., Gardner L.K., – Soft tissue response to endosseous titanium oral implants, J Prosthet Dent.58, 564-7, 1985.
134. Villavecchia I., Eigemann G. – Nuovo dizionario di mercerlogia e chimica applicata. Milan, Hoepli ed. Vol 7, 1983.
135. Watson R.M., Jemt T., Chai J., Harnett J., and others – Prosthodontic treatment, patient response, and the need for maintenance of complete implant-supported overdentures: an appraisal of 5 years of prospective study, J Prosthodont 10, 345-354, 1997.

136. Weber H., Pröbster L., Geis-Gerstorfer J. – Titan als prothetischer Werkstoff. Dtsch Zahnärzl Z 47, 473-481, 1992.
137. Wehnert L., Moormann A., Freesmeyer W. B.- Simulationsrechnungen zur Thermodynamik des konventionellen Titan-Keramik-Verbundes und zum Einfluß des verbundverbessernden Ionenimplantationsverfahrens. Quintessenz Zahntech 24 (10), 1027-1037, 1998.
138. Wiedmann O. – In letzter Zeit hat sich im Bereich der Technologie Titan und Keramik viel getan. Sonderdruck aus: DZW Zahntechnik, Ausgabe 3, 2000.
139. Wikidal M., Geis-Gerstorfer J. – In-vitro-Bürstversuche zur Wirkung fluoridhaltiger Präparate auf Legierungsoberflächen. Dtsch Zahnärztl Z 54, 171-175, 1999.
140. Wirz J. – Auswirkungen restaurativer Werkstoffe auf die Mundschleimhaut. ZM 92 (22), 64-69, 2002.
141. Wirz J. – Titan – ein Werkstoff der modernen Prothetik. Quintessenz 45, 731-739, 1994.
142. Wirz J., Jäger K., Grande V. – Kronen und Brücken mit Titangerüsten. Quintessenz 45, 849-860, 1994.
143. Wirz J., Schmidli F., Steinemann S., Wall R. – Aufbrennlegierungen im spaltkorrosionstest. Schweiz Monatsschr Zahnmed, 571-90, 1987.
144. Wolf B., Päßler K., Schmidt A., Walter M. – Gießtechnische Verarbeitung von Titanlegierungen. Dent Lab L, Heft 3, 367-371, 2002.
145. Wolinsky L.E., de Camargo P.M., Erard J.C., Newman M.G.- A study of in vitro attachment of Streptococcis sanguis and Actinomyces viscosus to saliva-treated titanium, Int J. Oral Maxillofac Implants, 27-31, 1989.
146. Yilmaz H., Usanmaz A., Yaluğ S. – Die keramischen Massen für die Titanverblendung und ihre physikalischen Eigenschaften. Quintessenz Zahntech 25 (9), 995-1002, 1999.
147. Yoshitani Y., Niinomi M., Fukunaga K., Kuroda D., Fukui H., Takeuchi T., Katsura S. – Mechanical Properties of Biocompatible Titanium Alloy Castings Made by Dental Precision Casting Method. In: Proceedings of the 5th International Symposium on Titanium in Dentistry. P-71, 107, Chiba(Japan), 2001.
148. Zertifikat In vitro Zytotoxizitäts Tests der Titan-Legierung giroTAN LN (Ti Rest Al6 Nb7). Prüfung nach ISO 10993-5:1999 „Biological evaluation of medical devices – Tests for in vitro cytotoxicity". Zentrum für Zahn-, Mundund Kieferheilkunde der Universität Tübingen, 2001.
149. Zertifikat Prüfung der Korrosionsbeständigkeit der Titan Legierung giroTAN LN (Ti Rest Al6 Nb7). Prüfung gemäß der internationalen Norm ISO/FDIS 10271: 2001 „Static Immersion Test". Zentrum für Zahn, Mundund Kieferheilkunde der Universität Tübingen, 2001.

150. Zwicker U. Titan und Titanlegierungen. Reine und angewandte Metallkunde in Einzeldarstellungen. Band 21, ISBN 3-540-05233-X, Springer-Verlag Berlin, Heidelberg, New York, 1974.

Intraoral Welding *of* Titanium Implants

"The splinting of dental implants alters the manner in which functional loads are distributed across the rehabilitative structure. Each implant, rather than acting independently, becomes an integral component of a unified mechanical system. By sharing stresses through mutual support, the implants function collectively to enhance the overall stability and biomechanical behavior of the implant-supported prosthesis."

"The welding process involves the targeted delivery of energy, both temporally and spatially concentrated, to the joint interface. This energy disrupts the stable equilibrium of atomic structures, allowing adjacent atoms to approach distances equal to or smaller than the lattice parameter of the crystalline structure. As a result, they reconfigure into a shared lattice, forming a new and stable crystalline network at the fusion site."

Join the Global Community Behind the Technique

Want more clinical cases, peer discussions, and practical insights?
Connect with implantologists worldwide in our official Facebook group: Welding Implants – Immediate Loading
→ Scan the QR code to join

Edition 3 is already in progress, be part of what's next!

Scan me!

About The Author

Grigore Lăzărescu, DDS, PhD, MBA

Dr. Grigore Lăzărescu is a specialist in oral rehabilitation, PhD in medical sciences, and Former Senior Lecturer at Titu Maiorescu University and Carol Davila University of Medicine and Pharmacy in Bucharest, Romania. He has over 20 years of experience in implant prosthodontics, with a focus on immediate loading and intraoral welding. An Honorary Member of the International Academy of Immediate Loading, he is known for promoting biomechanical precision and clinical pragmatism in full-arch rehabilitations.

978-973-0-42335-8